

The Response of Streams to Changes in Atmospheric Deposition of Sulfur and Nitrogen in the Adirondack Mountains

Final Report | Report Number 20-19 | July 2020

NYSERDA's Promise to New Yorkers:

NYSERDA provides resources, expertise, and objective information so New Yorkers can make confident, informed energy decisions.

Mission Statement:

Advance innovative energy solutions in ways that improve New York's economy and environment.

Vision Statement:

Serve as a catalyst – advancing energy innovation, technology, and investment; transforming New York's economy; and empowering people to choose clean and efficient energy as part of their everyday lives.

The Response of Streams to Changes in Atmospheric Deposition of Sulfur and Nitrogen in the Adirondack Mountains

Final Report

Prepared for:

New York State Energy Research and Development Authority

Diane Bertok
Project Manager

Prepared by:

Syracuse University

Syracuse, NY

C.T. Driscoll (Professor), S. Shao (Ph.D. Student)

with

E&S Environmental Chemistry, Inc.

T.J. Sullivan (Senior Research Scientist), T.C. McDonnell (Principal Scientist)

and

United States Geological Survey

B.P. Baldigo (Research Biologist), D.A. Burns (Research Hydrologist), G.B. Lawrence (Physical Scientist)

Notice

This report was prepared by E&S Environmental Chemistry, Inc., Syracuse University, and the United States Geological Survey in the course of performing work contracted for and sponsored by the New York State Energy Research and Development Authority (hereafter “NYSERDA”). The opinions expressed in this report do not necessarily reflect those of NYSEDA or the State of New York, and reference to any specific product, service, process, or method does not constitute an implied or expressed recommendation or endorsement of it. Further, NYSEDA, the State of New York, and the contracting organizations make no warranties or representations, expressed or implied, as to the fitness for particular purpose or merchantability of any product, apparatus, or service, or the usefulness, completeness, or accuracy of any processes, methods, or other information contained, described, disclosed, or referred to in this report. NYSEDA, the State of New York, and the contracting organizations make no representation that the use of any product, apparatus, process, method, or other information will not infringe privately owned rights and will assume no liability for any loss, injury, or damage resulting from, or occurring in connection with, the use of information contained, described, disclosed, or referred to in this report.

NYSERDA makes every effort to provide accurate information about copyright owners and related matters in the reports we publish. Contracting organizations are responsible for determining and satisfying copyright or other use restrictions regarding the content of reports that they write, in compliance with NYSEDA’s policies and federal law. If you are the copyright owner and believe a NYSEDA report has not properly attributed your work to you or has used it without permission, please email print@nyserda.ny.gov.

Information contained in this document, such as web page addresses, are current at the time of publication.

Abstract

Acidic deposition is the result of upwind sulfur (S) and nitrogen (N) emissions into the atmosphere from human activities. Environmental impacts from acidic deposition across forested landscapes include acidification of soil and drainage water, depletion of available soil nutrient bases, and impacts to and changes in forest and aquatic species composition and biodiversity. Acidic deposition can mobilize aluminum (Al) from soil-to-soil solution and subsequently to drainage water in forms that can be toxic to aquatic life. When exposed to decreasing levels of acidic deposition, which has been occurring in New York since the late 1970s, some soils and drainage waters have become gradually less acidic. Remaining questions relate to effects on stream resources, anticipated resource recovery under increasingly lower levels of deposition, and the levels of deposition (target loads, TLs) needed to reach a range of stream ecosystem recovery targets. Environmental scientists commonly estimate thresholds of air pollutant emissions and resulting atmospheric deposition at which adverse ecological effects are manifested. This analysis is often done using critical loads (CL) and/or TLs, using approaches that account for the spatial and temporal aspects of acidification and recovery. Exceedance represents the extent to which current levels of acidic deposition exceed the level expected to cause ecological harm. The research reported here is intended to help address S and N deposition TLs and ecosystem recovery of Adirondack streams, a resource that has been less thoroughly investigated than lakes. The overarching goal of this work is to highlight key considerations that will help inform decision-makers and ecosystem managers who are responsible for environmental policy in New York State and beyond. Salient aspects of stream TL modeling are discussed with an aim of informing not only scientists, but also policymakers, ecosystem managers, and nonscientists who are required to make decisions related to the effects of acidic deposition on natural ecosystems. Analyses reported herein quantify relations among chemical indicators and metrics of fish community health and biodiversity in streams of the Adirondack Park. This information is used to indicate levels of atmospheric deposition necessary to alleviate harmful effects on fish populations. Results of this investigation provide a framework that can be applied to better understand how modeled stream acid neutralizing capacity (ANC) values that are developed to support TL investigations can be adjusted to reflect high-flow ANC values that may be associated with toxic conditions. Since process models are often calibrated to a low-flow or average flow condition, the magnitude and spatial extent of TL exceedances increase substantially when episodic acidification is considered.

Keywords

Stream, acidification, sulfur, nitrogen, critical load, Adirondack Park, fish, hydrology

Acknowledgements

This research was conducted by E&S Environmental Chemistry, Inc., Syracuse University and the United States Geological Survey, under contract with the New York State Energy Research and Development Authority (NYSERDA). Any use of trade, firm, or product names is for descriptive purposes only and does not imply endorsement by the United States Government.

Table of Contents

Notice	ii
Abstract	iii
Keywords	iv
Acknowledgements	iv
List of Figures	vii
List of Tables	viii
Acronyms and Abbreviations	ix
Summary	S-1
1 Background	1
1.1 Acidic Deposition and its Effects.....	1
1.2 Influence of Variation in Discharge	4
1.3 Biological Response Functions	5
1.4 Regional Extrapolation	6
1.5 Target Loads.....	7
1.6 Goals and Objectives	7
2 Methods	9
2.1 Adirondack Region.....	9
2.2 Atmospheric Deposition and Meteorology.....	11
2.2.1 Wet and Dry Deposition	11
2.2.2 Meteorological Data.....	14
2.3 Soil and Stream Water Chemistry for Watershed Modeling and Spatial Extrapolation	14
2.4 Influences of Discharge on Stream Chemistry	17
2.5 Biological Responses	19
2.6 Model Applications	21
2.6.1 PnET-BGC Model Formulation.....	21
2.6.2 Scenarios	24
2.6.3 Model Evaluation Criteria.....	26
2.6.4 Sensitivity Analysis	27
2.7 Target Loads and Exceedance.....	27
2.8 Coupled Modeling, Hydrologic Analysis, and Biological Effects Assessment.....	28
2.9 Regionalization of Target Loads	30

3	Results.....	33
3.1	Ambient Stream Chemistry.....	33
3.2	Model Evaluation.....	33
3.3	Historical Acidification.....	37
3.4	Model Predictions of Future Stream and Soil Chemistry Under Different Deposition Scenarios	39
3.5	ANC Criterion Values and Target Loads	42
3.6	Biological Responses	48
3.7	Influence of Discharge on Stream Chemistry	57
3.8	Regionalization.....	59
4	Discussion.....	65
4.1	Stream Chemistry Simulations.....	65
4.2	Target Loads.....	66
4.3	Stream Discharge.....	68
4.4	Stream Biology.....	69
4.5	Comparison with Results for Adirondack Lakes	80
4.6	Integration of Biogeochemical, Hydrological, and Biological Models.....	82
4.7	Management Implications.....	89
5	References	91
	Appendix A. Regression Models Used to Reconstruct the Historical Wet Deposition at Huntington Wildlife Forest between 1900 and 1978	A-1
	Appendix B. Model Calibration Input Data	B-1
	Appendix C. The Role of Hydrologic Variation in WECASS stream Chemistry: ANC – Q Relations and Duration of Episodic Acidification	C-1
	Appendix D. Watershed Characteristics Used as Candidate Predictor Variables for Target Load Extrapolation	D-1
	Appendix E. Ambient Stream Chemistry from WECASS.....	E-1
	APPENDIX F. USGS Identification Numbers Needed for Data Retrieval from the National Water Information System (NWIS) Database	F-1
	Appendix G. Example Model Projections at Two Data-Intensive Sites	G-1
	Appendix H. Statistical Model Development for Predicting Target Loads	H-1
	Endnotes	EN-1

List of Figures

Figure 1. Map of Study Area	9
Figure 2. Estimate of Total Sulfur and Nitrogen Deposition from TDEP	11
Figure 3. Reconstruction of Wet Atmospheric Deposition of SO_4^{2-} , NO_3^- and NH_4^+ ($\text{meq m}^{-2} \text{ yr}^{-1}$).....	26
Figure 4. Schematic Depiction of Project Result Integration	29
Figure 5. Locations of Buck Creek and Archer Creek Monitoring Watersheds.....	31
Figure 6. Comparison of Model-Simulated versus Observed Stream Chemistry and Soil Base Saturation	35
Figure 7. Mean and Standard Deviation of Model-Predicted Selected Stream Chemistry and Soil Base Saturation	38
Figure 8. Projections of ANC of T24 (left) and Buck Creek (right).....	40
Figure 9. Target Loads (TLs) of SO_4^{2-} , NO_3^- , and NH_4^+ Deposition.....	42
Figure 10. Expectation for Modeled Streams to Attain ANC Criteria.....	45
Figure 11. Logistic Curves (Example 1) Describing the Probability of Observing Richness, Density, and Biomass in Fish Communities	50
Figure 12. Logistic Curves (Example 2) Describing the Probability of Observing Richness, Density, and Biomass in Fish Communities	51
Figure 13. Logistic Curves (Example 3) Describing the Probability of Observing Richness, Density, and Biomass in Fish Communities	52
Figure 14. Logistic Curves (Example 4) Describing the Probability of Observing Density and Biomass in Brook Trout Populations	54
Figure 15. Logistic Curves (Example 5) Describing the Probability of Observing Density and Biomass in Brook Trout Populations	55
Figure 16. Logistic Curves (Example 6) Describing the Probability of Observing Density and Biomass in Brook Trout Populations	56
Figure 17. Comparison of Modeled (PnET-BGC) and Statistical Predictions for Target Loads (TLs) Based on Current ANC and Geographic Location.....	60
Figure 18. Spatial Representation of Predicted TL (Example 1).....	61
Figure 19. Spatial Representation of Predicted TL (Example 2).....	62
Figure 20. Spatial Representation of Exceedance of TL (Example 1).....	63
Figure 21. Spatial Representation of Exceedance of TL (Example 2).....	64
Figure 22. Estimated Probabilities for Each of the 25 Model Streams	77
Figure 23. Linear and Nonlinear Relations between ANC Concentrations and Fish Communities/Brook Trout Population	78
Figure 24. Projected Conditions or Scenarios for Fish Communities and Brook Trout Population	79
Figure 25. Comparison of Lake and Stream TLs to Protect Aquatic Biota against Low ANC.....	81

List of Tables

Table 1. Physical Site Characteristics and Observed ANC.....	13
Table 2. Major Data Sources Used in This Study.....	15
Table 3. Locations and Drainage Areas of Six Stream Gauges.....	18
Table 4. Summary of the Model Inputs and Parameters Used in the PnET-BGC Model.....	23
Table 5. Model Scenarios for Changing SO_4^{2-} , NO_3^- , and NH_4^+ Deposition in the Future.....	25
Table 6. Comparisons of PnET-BGC Model Estimates	33
Table 7. Summary of Sensitivity Analysis of the PnET-BGC Simulated ANC (2050).....	36
Table 8. Summary Mean and Standard Deviation of Metrics of Model Performance	37
Table 9. Simulation Results for ANC ($\mu\text{eq L}^{-1}$).....	41
Table 10. Target Loads of $\text{SO}_4^{2-} + \text{NO}_3^- + \text{NH}_4^+$ Deposition	44
Table 11. Modeled Stream Recovery Classes for Target ANC = 20 $\mu\text{eq L}^{-1}$	46
Table 12. Modeled Stream Recovery Classes for Site-Specific Target ANC	47
Table 13. ANC Values Used in PnET-BGC Model Calibration and the Estimated ANC Values for Q_{85}	58
Table 14. Linear Regression Statistics for Predicting the TLs of Acidity in 2050 and 2150	67
Table 15. Calculated ANC Q_{27} ($\mu\text{eq L}^{-1}$) in 1850, Estimated ANC Q_{27} in 2015, and Predicted ANC Q_{27} in 2150.....	72
Table 16. Predicted Number of Fish Species for 24 Modeled Streams.....	83
Table 17. Predicted Fish Density (Number of Fish/0.1 ha) for 24 Modeled Streams	85
Table 18. Predicted Fish Biomass (g/0.1 ha) for the 24 Modeled Streams.....	86
Table 19. Predicted Brook Trout Density (Number of Brook Trout/0.1 ha) for the 24 Modeled Streams	87
Table 20. Predicted Brook Trout Biomass (g/0.1 ha) for 24 Modeled Streams.....	88

Acronyms and Abbreviations

AIC	Akaike Information Criterion
Al	aluminum
Al _i	inorganic monomeric aluminum
Al _m	total monomeric aluminum
Al _o	non-labile (organic) monomeric aluminum
ANC	acid neutralizing capacity
ASMP	Adirondack Sugar Maple Project
BCS	base cation surplus
BS	base saturation
C	carbon
Ca ²⁺	calcium
CAA	Clean Air Act
CASTNET	Clean Air Status and Trends Network
CL	critical load
Cl ⁻	chloride
Cm	centimeters
CO ₂	carbon dioxide
DIC	dissolved inorganic carbon
DOC	dissolved organic carbon
ECASS	East-Central Adirondack Stream Survey
EPA	United States Environmental Protection Agency
H ⁺	hydrogen ion
Ha	hectare
HBEF	Hubbard Brook Experimental Forest
HWF	Huntington Wildlife Forest
K ⁺	potassium
km ²	square kilo meters
L	liter
LHS-MC	Latin hypercube sampling - Monte Carlo
µeq L ⁻¹	microequivalents per liter
µmol L ⁻¹	micromoles per liter
Mg ²⁺	magnesium
N	nitrogen
Na ⁺	sodium
NADP	National Atmospheric Deposition Program
NCDC	National Climatic Data Center
NH ₄ ⁺	ammonium

NMAE	normalized mean absolute error
NME	normalized mean error
NO ₃	nitrate
NO _x	nitrogen oxide
NWIS	National Water Information System
NYSERDA	New York State Energy Research and Development Authority
PAR	photosynthetically active radiation
PnET-BGC	Photosynthesis and net Evapotranspiration Biogeochemical model
PnET-CN	pre-cursor model to PnET-BGC
PRISM	Parameter-elevation Regressions on Independent Slopes Model
Q _{percent}	discharge percentile
RCOO	estimate of the concentration of strongly acidic organic anions
S	sulfur
SO ₂	sulfur dioxide
SO ₄ ²⁻	sulfate
SO _x	sulfur oxide
SUNY-ESF	State University of New York College of Environmental Science and Forestry
TDEP	Total Deposition (model)
TL	target load
TMDL	total maximum daily load
USGS	United States Geological Survey
WASS	Western Adirondack Stream Survey
WECASS	Western Adirondack Stream Survey and East-Central Adirondack Stream Survey, collectively

Summary

Acidic deposition is the result of sulfur (S) and nitrogen (N) emissions into the atmosphere from human activities. It contributes to a range of environmental impacts across mostly montane forested landscapes, including acidification of soil and drainage water, depletion of available soil nutrient bases, and impacts to and changes in forest and aquatic species composition and biodiversity. Acidic deposition can mobilize aluminum (Al) from soil-to-soil solution and subsequently to drainage water in forms that can be toxic to aquatic life.

Acidification of soil and drainage water has environmental and economic consequences. Deleterious environmental effects are important to the Adirondack Park because part of the “forever wild” mission is to maintain natural conditions unaffected by human influence. Ecosystems show considerable variation in their inherent sensitivity to the effects of acidic deposition. When exposed to decreasing levels of acidic deposition, which has been occurring since the late 1970s, some soils and drainage water have become gradually less acidic. Recent decreases in acidic deposition have not yet resulted in soil recovery to preindustrial conditions, and despite encouraging signs (Lawrence et al. 2015a), the slow pace of soil recovery constrains the recovery of surface waters. Available evidence suggests that some aquatic ecosystem recovery is now occurring, especially in Adirondack lakes (Driscoll et al. 2016). Additional remaining questions relate to effects on stream resources, anticipated resource recovery under increasingly lower levels of deposition, and the levels of deposition (target loads, TLs) needed to reach a range of stream ecosystem recovery targets.

Environmental scientists commonly estimate thresholds of air pollutant emissions and resulting atmospheric deposition at which adverse ecological effects are manifested. This analysis is often done using critical loads (CL) and/or target loads, using approaches that account for the spatial and temporal aspects of acidification and recovery (Burns and Sullivan 2015). A CL is the amount of acidic deposition below which there is no ecological harm under future steady-state conditions, whereas the TL specifies the timeframe of the response. Exceedance represents the extent to which current levels of acidic deposition exceed the level expected to cause ecological harm. Exceedance relates ecosystem sensitivity to the measured pollutant deposition level.

The research reported here is intended to help address S and N deposition TLs and ecosystem recovery in Adirondack streams, a resource that has been less thoroughly investigated than lakes. The overarching goal of this work is to highlight key considerations that will help inform decision-makers and ecosystem managers who are responsible for environmental policy in New York State and beyond. In this report, salient aspects of stream modeling and a TL investigation are discussed with an aim of informing not only scientists, but also policymakers, ecosystem managers, and nonscientists who are required to make decisions related to the effects of acidic deposition on natural ecosystems.

Fish presence, absence, richness, and abundance are important aquatic metrics affected by surface water acidification. Fish mortality is dependent largely on the duration and intensity of high-flow conditions during hydrological episodes driven by snowmelt and rain storms that temporarily cause low pH and acid neutralizing capacity (ANC) and high inorganic monomeric Al (Al_i) concentrations in some surface waters (Baldigo et al. 2007). This response suggests that episodic acidification, as reflected by ANC values during high flow, is an important indicator when evaluating exceedance of aquatic TLs. Evaluating episodic acidification is especially important in flowing waters. Therefore, one objective of the analyses described in this report was to evaluate the extent of episodic acidification in Adirondack streams. This objective was accomplished by exploring the relations between stream discharge and ANC in the large stream chemistry data sets described by Lawrence et al. (2008a) and Lawrence et al. (2018a).

Improved understanding of the relations between surface water acid-base chemistry and biological response is also needed to determine specific TLs for N and S deposition that could help sustain or promote healthy fish and invertebrate populations, communities, and aquatic ecosystems (Greaver et al. 2012). Evidence suggests that Al_i concentrations largely drive toxicity and regulate the response of fish populations in acid-impacted streams of the western Adirondacks. If certain Al_i thresholds are exceeded for long enough periods, fish mortality and population losses can occur (Baldigo et al. 2007). The strong relations between Al_i and other acid-base variables, especially pH, ANC, and the base cation surplus (BCS), an index of acidification similar to ANC (Lawrence et al. 2007), indicates that mortality-threshold concentrations for pH and ANC can be estimated using their connection to Al_i .

Analyses reported herein quantify relations among chemical indicators and metrics of fish community health and biodiversity in streams of the Adirondack Park. This information is used to indicate levels of atmospheric deposition necessary to alleviate harmful effects on fish populations based on an assigned

ANC threshold of 20 microequivalents per liter ($\mu\text{eq L}^{-1}$) (Bulger et al. 1999, Fakhraei et al. 2014). These analyses provide equations and response curves that characterize how acidification currently affects local fish assemblages and can be applied to indicate how changes in Al_i , ANC, and pH are likely to contribute to future biological recovery.

Twenty-five small watersheds containing first or second order streams, mostly in the western portion of the Adirondack Park, were selected for site-specific biogeochemical modeling using the Photosynthesis and net Evapotranspiration Biogeochemical (PnET-BGC) model. Watersheds were selected that had the requisite soil and stream data necessary to calibrate the model and simulate stream and soil responses to changes in S and N deposition and that depicted a range of sensitivity to acidic deposition. Model sites were selected from among those sampled in previous Adirondack stream investigations. Model results were extrapolated from the 25 streams to a larger population of 401 streams that were part of two previous U.S. Geological Survey studies (Lawrence et al., 2008a; Lawrence et al., 2018a). These regional results provide additional context for the PnET-BGC model outcomes.

The PnET-BGC model was applied in this study to simulate past and likely future water chemistry and to calculate current and future TLs at the modeled streams. It is important to consider the flow conditions that are reflected by the ANC measurements used in scenario and TL model calibration, and how TL results may change when ANC values that reflect episodic acidification are utilized. Since the model was generally calibrated to samples representing moderately high to high-flow conditions, the modeled TLs are generally protective of the more acidic conditions aquatic biota may experience during the year. Fish-community surveys conducted in 47 headwater streams located mainly in the western Adirondack Mountains were used to support the assessment of impacts on aquatic biota. Brook trout were given special consideration because they are native to Adirondack streams and provide an important sport fishery.

PnET-BGC hindcast simulations were constructed for the 25 sites by running the model from 1850 to 2015, based on estimated historical deposition and meteorology. Model forecast simulations were continued through the year 2200, under several deposition control scenarios (for sulfate [SO_4^{2-}], nitrate [NO_3^-] and ammonium [NH_4^+] individually and in combination). These included the following:

- a “business-as-usual” scenario that held ambient deposition (average of 2013–2015) constant until the end of the simulation
- a “possible future” scenario that linearly ramped deposition from ambient values down to levels projected under the U.S. Environmental Protection Agency’s Clean Power Plan for the year 2020 and then held deposition constant until the end of the simulation

- a suite of “additional reduction” scenarios that linearly decreased deposition from the “possible future” (2020) level to the preindustrial deposition level (1850) at 25% intervals (25, 50, 75, and 100% reductions)
- an “increasing deposition” scenario that increased deposition linearly by 15% from ambient levels in 2016 to 2020 and then held deposition constant until the end of the simulation

Two ANC criteria were used as goals for recovery in this TLs analysis: a fixed ANC criterion of $20 \mu\text{eq L}^{-1}$, and a second based on the model-simulated, site-specific ANC estimated to have occurred under pre-industrial atmospheric deposition (~ 1850) at each modeled site. The fixed $20 \mu\text{eq L}^{-1}$ ANC was selected to represent likely protection of brook trout (*Salvelinus fontinalis*) health against elevated concentrations of Al_i . Models were also used to show whether sites could achieve values to within $20 \mu\text{eq L}^{-1}$ of pre-industrial ANC in response to reduced or eliminated acidic deposition. Endpoint years were set as 2050 and 2150 for determining TLs to attain a given stream ANC criterion in the short- and long-term future.

The Western Adirondack Stream Survey (WASS) and East-Central Adirondack Stream Survey (ECASS; collectively referred to as “WECASS”) were used as the basis for extrapolation of PnET-BGC model results. Model results were extrapolated to the individual WECASS sites and to 10-km grid cell summaries of the individual WECASS site results using statistical (regression) models. For the grid summaries, the minimum and median predicted TLs at all WECASS sites that occurred within a given grid cell were calculated and mapped along with maximum and median TL exceedance.

To develop a concise description of the biological effects associated with historical, ambient, and potential future atmospheric N and S deposition, results from the biogeochemical, hydrological, and biological study components were integrated to develop estimates of the expected number of species, density, and biomass of fish under preindustrial (1850), ambient (2015), and future (2050 and 2150) scenario summer baseflow (Q_{27} , 27th daily discharge percentile) conditions for each of the 25 PnET-BGC model sites. This analysis was achieved by using a linear regression model to adjust stream ANC simulated with PnET-BGC to the expected summer baseflow ANC for each stream site, defined here as the average daily discharge percentile at the time of fish sampling (Q_{27}). Adjusted ANC values were then used to derive the most likely (i.e., highest probability) number of species, density, and biomass of fish and the density and biomass of brook trout for each stream according to the biological logistic regression models.

PnET-BGC effectively simulated the hydrology and ambient chemistry of stream waters and soils in the Adirondack Park as demonstrated by good agreement between simulated and measured stream chemistry, such as SO_4^{2-} , calcium (Ca^{2+}) and ANC. Model hindcast scenarios suggested that stream concentrations of SO_4^{2-} were historically low (mean \pm one standard deviation; 12 ± 5 micromoles per liter [$\mu\text{mol L}^{-1}$]) during the preindustrial period (1850), increased to maximum concentrations of $62 \pm 21 \mu\text{mol L}^{-1}$ by approximately 1980 and then decreased to ambient (recent, but not necessarily current) concentrations of $35 \pm 11 \mu\text{mol L}^{-1}$ by 2015. The mean value of the model-simulated preindustrial stream ANC was $136 \pm 184 \mu\text{eq L}^{-1}$ among the modeled sites. Only one stream had simulated preindustrial ANC less than $20 \mu\text{eq L}^{-1}$, while eight of the 25 streams had simulated preindustrial ANC between 20 and $50 \mu\text{eq L}^{-1}$. Simulated stream ANC decreased to minimum values around the year 2000 ($75 \pm 158 \mu\text{eq L}^{-1}$), followed by a slight increasing trend. Model hindcasts suggested that, across the 25 modeled streams, acidic deposition resulted in decreases in ANC at a rate of $0.31 \mu\text{eq L}^{-1}\text{yr}^{-1}$ from 1850 to 2015 ($\Delta \text{ANC} = 51 \mu\text{eq L}^{-1}$ over 165 years). Hindcast simulations of soil chemistry suggested decreases in soil base saturation (BS) from preindustrial levels of $17.2\% \pm 6.9\%$ to minimum levels of $11.3\% \pm 6.1\%$ that occurred around 2010, with no significant recovery thereafter.

Model projections suggest that changes in acidic deposition would be effective in influencing future stream SO_4^{2-} and NO_3^- concentrations, ANC, and soil % BS at most acid-impacted watersheds. The 25 modeled streams were grouped into three recovery classes based on whether they (1) could achieve the ANC criterion without further acidic deposition load reductions; (2) could achieve the ANC criterion, but only with additional load reductions; or (3) were unable to attain the ANC criterion even if atmospheric deposition was decreased to preindustrial levels and then held at the preindustrial value until the year 2150. Results suggest that some streams may have had preindustrial ANC above $20 \mu\text{eq L}^{-1}$ yet are unable to recover to this level even if acidic deposition is eliminated in the future. This pattern indicates that full recovery of the acid buffering of streams may not be achievable, making these streams likely to remain low in ANC for the foreseeable future, even under low levels of future S and N deposition.

Baldigo et al. (2019a) developed equations to relate fish response metrics to stream chemistry using logistic (probabilistic) equations. Because the Al_i equation for ≥ 1 species explained the most deviance (33.0%), this model and a target of one or more species (essentially fish presence versus absence) appeared to be most effective in assessing community responses to improvements in water quality. One or more fish species is expected in 86% of streams and two or more species are expected in 39% of streams if baseflow Al_i concentrations decreased below about $1 \mu\text{mol L}^{-1}$. The Al_i equation

indicated that at least 98%, 48%, and 1% of study streams would have total densities of ≥ 100 fish per 0.1 hectare (ha) when concentrations of Al_i are undetectable, $1 \mu\text{mol L}^{-1}$, and $2 \mu\text{mol L}^{-1}$, respectively. The Al_i biomass equation indicated that at least 89%, 36%, and 4% of study streams would have total biomass ≥ 1500 grams (g) per 0.1 ha if concentrations of Al_i are undetectable, $1 \mu\text{mol L}^{-1}$, and $2 \mu\text{mol L}^{-1}$, respectively.

The strongest predictor of fisheries response to changes in acidic deposition is the concentration of Al_i , with clear benchmarks near 1.0 and $2.0 \mu\text{mol L}^{-1}$. These TLs and exceedances are influenced by flow conditions at the times of sample collection. A robust regional episodic acidification relationship was observed across streams of the Adirondack Park, which showed strong similarity in response to high flows in streams when baseflow ANC values were less than about $90 \mu\text{eq L}^{-1}$. For example, a hypothetical stream with a low-flow ANC value of $50 \mu\text{eq L}^{-1}$ would be estimated to decrease to $5 \mu\text{eq L}^{-1}$ under high-flow conditions, a value at which adverse effects on brook trout are expected.

An Al_i concentration of $2.0 \mu\text{mol L}^{-1}$ is an important acute threshold above which brook trout mortality increases sharply with exposures of as little as 2–4 days duration (Baldigo et al. 2007). This Al_i concentration threshold typically occurs when ANC values are about 0 to $20 \mu\text{eq L}^{-1}$ in Adirondack streams. Duration of exposure to toxic conditions is important in promulgating adverse effects on aquatic biota. High-flow periods lasting 10 days or more are most common during the spring snowmelt season of March to April as demonstrated at the intensively studied Buck Creek site in the Adirondack Park but can also occur at other times of the year. High-flow events of considerable duration are likely to cause extended periods of acidification accompanied by high Al_i concentration in many Adirondack streams. Here, high-flow conditions are defined as the 85th percentile of annual stream discharge conditions (i.e., Q_{85} - 85% of the daily flows are less than this value). During this study, the average discharge at the time of fish sampling was relatively low (Q_{27}); this benchmark was used for some of the fish response analyses reported herein. A decrease in ANC to $5 \mu\text{eq L}^{-1}$, and associated decrease in pH, would likely be accompanied by an increase in Al_i concentrations to above 1 or $2 \mu\text{mol L}^{-1}$. Even a stream with a low-flow ANC of $100 \mu\text{eq L}^{-1}$ is expected to decline to an ANC of $23 \mu\text{eq L}^{-1}$ at high flow, a value of potential concern depending on the persistence of that low ANC condition. In streams with low-flow ANC above $200 \mu\text{eq L}^{-1}$, the episodic decreases in ANC from high flow are typically large (i.e., $> 75 \mu\text{eq L}^{-1}$). However, this magnitude of ANC decrease is not expected to impact the health of aquatic biota because this high-flow ANC is not low enough to result in elevated concentrations of Al_i .

The stream chemistry values available for use in calibration of PnET-BGC were largely collected during moderate to moderately high-flow conditions. Because of this model calibration approach, differences in ANC between values used for model calibration and estimates of ANC at Q_{85} were generally minimal for the modeled sites. At 18 of the 25 PnET-BGC modeled streams, the difference between the model-calibrated ANC and the high-flow ANC was less than $25 \mu\text{eq L}^{-1}$. The use of stream chemistry collected under moderate to moderately high flows for model calibration enables simulation of the more stressful (to aquatic biota) chemical conditions.

Application of the TL regression models to the WECASS sites indicated that deposition TLs below $40 \text{ meq m}^{-2} \text{ yr}^{-1}$ (equivalent to $3 \text{ kg N ha}^{-1} \text{ yr}^{-1}$ and $3 \text{ kg S ha}^{-1} \text{ yr}^{-1}$) occur throughout the Adirondack region. Regional TLs for attaining site-specific ANC were generally lower than those for attaining a fixed $\text{ANC} = 20 \mu\text{eq L}^{-1}$ indicating that greater emissions decreases would be necessary to achieve recovery if best estimates of historic preindustrial stream ANC less than $20 \mu\text{eq L}^{-1}$ are considered. Higher deposition would be allowable (i.e., higher TL) to achieve resource recovery in 2150, as opposed to 2050. Target load exceedances followed similar patterns to TLs, with more exceedance where TL values were low.

Many streams, especially in the southwestern Adirondack Park, are currently in exceedance with respect to these TLs. This finding applies to the 25 streams modeled using PnET-BGC in this study, and to the broader group of streams found throughout the region to which the modeled site results were extrapolated.

The expected level of biological protection afforded by achieving the TL to attain ANC equal to the estimated preindustrial ANC minus $20 \mu\text{eq L}^{-1}$ by the year 2150 was determined in the same manner by adjusting conditions to represent the Q_{27} flow percentile. These results were then compared with expected biological conditions for the year 1850 to determine the level of biological protection each stream would achieve relative to preindustrial conditions if the TL of each stream were attained. This reflects improvement in chemical conditions to a level that will support biological recovery. The actual biological recovery will be limited by the ability of the species to re-populate a given stream.

Model simulations indicated that there are many low-order streams throughout the western Adirondack Park that exhibit low TLs of acidic deposition (less than $40 \text{ meq m}^{-2} \text{ yr}^{-1}$ to attain $\text{ANC} = 20 \mu\text{eq L}^{-1}$, or to attain ANC within $20 \mu\text{eq L}^{-1}$ of simulated preindustrial ANC). As a result, even with marked decreases in the levels of acidic deposition in the Adirondack region, many of these streams continue to exceed simulated TLs under continued S and N deposition at contemporary levels.

Modeled TLs using PnET-BGC were generally in close agreement with the TL values extrapolated to regional WECASS sites (R^2 for model fits at the 25 PnET-BGC sites = 0.53 to 0.89). These extrapolated TL values were generally lowest (below $20 \text{ meq m}^{-2} \text{ yr}^{-1}$) in the southwestern portion of the Adirondack Park. Such low TL values were widely distributed for TLs based on site-specific ANC target values (preindustrial ANC minus $20 \mu\text{eq L}^{-1}$), as compared with a fixed ANC target of $20 \mu\text{eq L}^{-1}$. Grid cell extrapolation results indicated widespread exceedance of TLs across the Adirondack Park.

The duration of episodic acidification, another concern regarding deleterious effects to biota, was evaluated in part through analysis of discharge data at Buck Creek, a small Adirondack stream with a long-term record. This analysis showed that consecutive multiday periods when discharge exceeds the 85th percentile are common in all years, and most years have at least one period of 10 or more consecutive days of high flow, typically during the March to April snowmelt season.

At 18 of the 25 streams where PnET-BGC modeling was applied, there was less than a $25 \mu\text{eq L}^{-1}$ difference between the model-calibrated ANC and the ANC reflective of high-flow conditions (Q_{85}). At the seven sites where this difference exceeded $25 \mu\text{eq L}^{-1}$, there was either a high-flow model-calibrated ANC of greater than $100 \mu\text{eq L}^{-1}$ or the model-calibrated ANC reflected low flow less than Q_{15} (15th percentile among daily discharge values for all days in the record). The relatively small difference between model-calibrated ANC and the ANC that reflects high-flow conditions in streams with low buffering (model-calibrated ANC < 100) indicated that model calibration was largely based on stream chemistry that reflected moderate to moderately high-stream flow. Effects on future model projections were not fully evaluated because the extent to which ANC changes with discharge ($\Delta\text{ANC}/\Delta Q$) is likely to change in the future as streams recover in response to decreased acidic deposition.

About half of the PnET-BGC modeled streams were projected to have lost one or more fish species since preindustrial times based on models of fish-community metrics and ANC estimates that were adjusted to summer baseflow discharge percentiles (Q_{27}). None of the future scenarios were able to fully recover the number of fish species believed to have been present in all modeled streams prior to year 1850. A 100% reduction in N and S deposition beyond the U.S. Environmental Protection Agency Clean Power Plan would allow brook trout density and community richness, density, and biomass in modeled streams to recover most closely to preindustrial conditions when compared to all other emission scenarios.

Simulated TLs for 25 streams in this study were broadly similar to lake TLs modeled by Fakhraei et al. (2014) for lakes classified by New York State as impaired under Section 303(d) of the Clean Air Act. In both cases, the simulated TLs of about 30% of the modeled water bodies were either less than $10 \text{ meq m}^{-2} \text{ yr}^{-1}$ or non-attainable via reductions in acidic deposition. This result confirms that lakes classified by the State as impaired, and therefore subject to Total Maximum Daily Load (TMDL) analysis, and streams selected for modeling in this study included many highly acid-sensitive surface waters. The data sets differed in that the modeled streams and the WECASS streams also included large numbers (about 30–40%) of water bodies that were of low acid-sensitivity. These generally insensitive streams were mostly located in the eastern portion of the Adirondack region.

The results of this investigation provide a framework that can be applied to better understand how modeled ANC values that are developed to support TL investigations can be adjusted to reflect high-flow ANC values that may be associated with toxic conditions. Since process models are often calibrated to a low-flow or average-flow condition, the magnitude and spatial extent of TL exceedances increase substantially when episodic acidification is considered.

1 Background

1.1 Acidic Deposition and Its Effects

Acidic deposition includes many forms of sulfur (S) and nitrogen (N) that are released to the atmosphere from combustion of fossil fuels. The term “acid rain” is specific to wet precipitation (i.e., rain and snow). Dry acidic deposition includes gaseous compounds and solid particles that are deposited directly onto topographic landscape features and vegetation. Acidic deposition causes a range of effects across the largely montane forested landscape, including acidification of soil and drainage water; toxicity to fish and other aquatic biota; depletion of available soil nutrient base cations, such as calcium (Ca) and magnesium (Mg^{2+}); reduced growth and regeneration of various plant species; increased susceptibility of foliage to winter injury; and changes in species composition and biodiversity. Such effects have been thoroughly studied in the Adirondack Mountain region of New York State (cf., Driscoll et al. 2001, Sullivan et al. 2006a, Lawrence et al. 2008a, Fakhraei et al. 2014, Sullivan et al. 2014, Sutherland et al. 2015).

Deposition of S and N increased substantially in the eastern United States throughout the 20th century due to human-caused emission sources (Husar et al. 1991, Galloway and Cowling 2002). For more than a century, air pollution has affected sensitive aquatic and terrestrial resources and caused substantial damage at some locations, especially in the southwestern Adirondack Mountain region in New York State (Sullivan 2015). Acidification of soil and drainage water in the Adirondack Park has been caused primarily by atmospheric deposition of acid derived from sulfur dioxide emissions. Nitrogen oxide gases are also contributors in the process of acidification but to a lesser extent. Nitrogen deposition is becoming proportionally more important with large recent reductions in S emissions and deposition (Fakhraei et al. 2014, Sullivan 2015). Emissions of S and N into the atmosphere at locations upwind from the Adirondack Park increased several-fold during the late 19th and the 20th centuries to levels high enough to impair sensitive terrestrial and aquatic ecosystems. Federal and state rules and legislation have reduced S and N emissions and deposition prior to and since the turn of the 21st century, and some ecosystem recovery (both chemical and biological change) has been documented for lakes (Driscoll et al. 2007, Sullivan 2015, Sutherland et al. 2015, Driscoll et al. 2016). Recent decreases in acidic deposition, however, have not resulted in complete soil recovery to preindustrial conditions, and this constrains surface water recovery. Some evidence of partial soil recovery in this region was reported by Lawrence et al. (2012).

Reductions in sulfur dioxide (SO₂) and nitrogen oxides (NO_x) emissions have occurred across the eastern U.S. since the 1970s in response to provisions of the Clean Air Act (CAA), including substantial emissions reductions since the 1990s in accordance with Title IV of the 1990 CAA Amendments (Burns et al., 2011). These emissions reductions have led to large decreases in atmospheric deposition of S and N in the Adirondack Mountain region. For example, the National Trends Network site at Huntington Wildlife Forest (HWF) in the central Adirondack region reported a 78% decrease in wet deposition of inorganic S from 1979 to 2016 and a 36% decrease in wet deposition of inorganic N over the same period.¹ Dry deposition of S and N has also decreased substantially (Schwede and Lear 2014). Recent decreases in acidic deposition have led to changes in surface water chemistry that have included decreases in SO₄²⁻, NO₃⁻, and Al_i concentrations, and increases in pH and ANC values (Lawrence et al. 2011, Driscoll et al. 2016, Sullivan et al. 2018). Recovery of surface water chemistry to date, however, can best be described as limited and primarily a result of three factors. First, long-term depletion of soil exchangeable base cations due to decades of acidic deposition has limited the ability of the soil to offset declines in S and N deposition (Johnson et al. 2008). Second, declines in S and N deposition are increasingly buffered by internal soil sources of SO₄²⁻ and NO₃⁻ to surface waters (Mitchell et al. 2011). Third, increases in dissolved organic carbon (DOC) concentrations in many Adirondack surface waters have been noted during this recovery period, and the strong acid fraction of this DOC has likely slowed the rate of recovery in pH and ANC (Lawrence et al. 2011, Driscoll et al. 2016).

Acidification of soil and drainage water caused by atmospheric deposition of S and N has had environmental and economic consequences (Beier et al. 2017). Both S and N acidify base-poor soils and reduce base nutrient availability. An increased N supply can increase primary production, alter species composition, and affect biodiversity (Bobbink et al. 2010). Ecosystem effects of increasing N supply include changes in N and carbon (C) cycling and ecological responses (Neff et al. 2002, Gilliam et al. 2018). These deleterious effects are important to the Adirondack Park due to its “forever wild” mission to maintain natural conditions that allow for the enjoyment of nature by future generations.²

Acidic deposition not only acidifies sensitive soils, resulting in depletion of nutrient base cations, but also mobilizes aluminum (Al) from soil-to-soil solution and subsequently to drainage water in chemical forms that are toxic to aquatic life and plant roots. Some plant species are highly susceptible to stress from soil and soil solution acidification (U.S. EPA 2008), most notably sugar maple (*Acer saccharum*; Sullivan et al. 2013) and red spruce (*Picea rubens*; Schaberg et al. 2000).

The mobility of atmospherically deposited strong acid anions such as sulfate (SO_4^{2-}) and nitrate (NO_3^-) in the soil and in water is dependent on flow paths and other watershed characteristics. Neutralization of acid inputs largely occur by the release of base cations to drainage water through the processes of weathering and ion exchange (van Breemen et al. 1983). Sulfate and NO_3^- leach to surface waters and their charge is largely balanced by base cations (Ca^{2+} , Mg^{2+} , potassium [K^+], and sodium [Na^+]) and acidic cations (hydrogen ion [H^+] and inorganic monomeric Al [Al_i]). Base cation loss from the soil caused by acidic deposition occurs in combination with cation loss caused by the natural leaching of organic and carbonic acids (Hemond 1994). Thus, acidic deposition enhances natural base cation loss from the soil rooting zone (Cronan et al. 1978), promotes transport of Al_i to surface waters, and affects the health of a variety of plant and animal species, especially those that require substantial supplies of Ca^{2+} and/or Mg^{2+} or prefer higher pH values. Thus, acidic deposition can contribute to changes in species distributions and abundance in both the terrestrial and aquatic communities (Sullivan 2015).

Aquatic effects of S and N deposition in the Adirondack Mountains have been well studied over the past three decades (cf., Driscoll et al. 2001, Driscoll et al. 2003, Sullivan et al. 2006b, Jenkins et al. 2007, Lawrence et al. 2008b, Baldigo et al. 2009, Sullivan 2015). Investigations have included long-term monitoring, process studies, and mathematical modeling of ecosystem responses and target loads (TLs), focused largely on lakes and soils. Scientists have considerable understanding of the effects of atmospheric deposition on sensitive lake and soil resources in the Adirondack Mountains. Additional key questions relate to effects of acidic deposition on stream resources, anticipated stream recovery under increasingly lower levels of deposition, and TLs needed to achieve a range of stream ecosystem recovery levels. The New York State Energy Research and Development Authority (NYSERDA) funds much of the research in this region intended to address these and related issues.

Surface water acidification is a concern, in part, because Al_i concentrations increase as pH and ANC decrease (Driscoll 1985). This increase in Al_i is especially pronounced as pH decreases to less than 5.2 to 5.3 and as ANC decreases to less than 20 to 30 $\mu\text{eq L}^{-1}$, with some variation in these values as a function of DOC concentrations (Lawrence et al. 2007). Elevated Al_i concentrations (higher than about 2 $\mu\text{mol L}^{-1}$) in surface waters are associated with toxicity to several types of aquatic organisms, including fish, algae, and invertebrates (Gensemer and Playle 1999). In the Adirondack region and elsewhere in eastern North America, the surface waters with the lowest pH and ANC values, and typically the highest Al_i concentrations, have often shown the greatest magnitude of recovery over the past few decades as acidic deposition has decreased (Lawrence et al. 2011, Driscoll et al. 2016). This pattern is encouraging because it suggests an improvement in water chemistry habitat for aquatic

biota that are sensitive to Al toxicity. Of concern, however, is episodic acidification as reflected by declines in pH and ANC values that may persist for days to weeks, and which is especially acute in Adirondack streams during spring snowmelt (Baldigo et al. 2007). Episodic acidification has been challenging to evaluate because many surface water monitoring programs collect samples at fixed time intervals that often exclude periods when episodic acidification is expected to be most pronounced. A survey of streams in the western Adirondack Park estimated that more than half of the streams were episodically acidic, which raises concerns about toxicity to aquatic biota (Lawrence et al. 2008b).

1.2 Influence of Variation in Discharge

Target load investigations that focus on aquatic acidification, such as the study described herein, typically evaluate atmospheric deposition of S and/or N relative to a broad indicator of acid-base conditions, often ANC (Sullivan et al. 2012, Zhou et al. 2015). Models such as the Photosynthesis and net Evapotranspiration Biogeochemical (PnET-BGC) model are applied in such investigations by calibrating parameters to fit ANC and other surface water variable values at a time step that typically varies from monthly to annual (Sullivan et al. 2012, Fakhraei et al. 2014, Zhou et al. 2015). Such models can also be calibrated to seasonal high-flow conditions or to some other standardized flow regime. This might better reflect ANC under high-flow conditions, when values may be 20 to 50 $\mu\text{eq L}^{-1}$ or more lower than the annual average value (Wigington et al. 1996).

Studies of fish held in situ in cages have shown that fish mortality is dependent on the duration and intensity of episodic acidification, which is driven by low pH/ANC values, decreased base cation concentrations, high Al_i concentrations, and sometimes increased DOC concentrations (Baldigo et al. 2007, McDonnell et al. 2018a). This response suggests that episodic acidification, as reflected by ANC values during high flow, is an important indicator when evaluating exceedance of aquatic TLs, that is, the extent to which the deposition loading exceeds the TL. However, exceedance under high flow has not been evaluated in previous TL investigations. An important distinction can be made between lakes and streams in this regard. Episodic acidification in lakes tends to affect primarily the shallowest depths of the lakes, providing ample water volume for mobile biota such as fish to find refugia in deeper waters to avoid toxic conditions (Gubala et al. 1991). However, streams do not provide such readily accessible refugia except in downstream (higher order) locations or well-buffered reaches, which may be difficult for fish to access during large runoff events when acidic conditions and high flows can prevail throughout a stream network. As a result, evaluating episodic acidification is especially important in flowing waters. Therefore, to achieve the objectives of this study, an evaluation was needed of the extent of episodic acidification in Adirondack streams. This is important because high flow decreases ANC and pH,

and elevates Al_i , leading to fish mortality. This response is more prevalent in streams than lakes. Episodic acidification was considered by exploring relations between stream discharge and ANC in the large Western Adirondack Stream Survey (WASS) and East-Central Adirondack Stream Survey (ECASS; collectively referred to as “WECASS”), using the WASS data set described in Lawrence et al. (2011), and the ECASS data set described in Lawrence et al. (2018a). These data represent stream chemistry collected repeatedly at more than 500 streams over a range of flow conditions and ANC values sufficient to define a regional response at high flow.

1.3 Biological Response Functions

Improved understanding of the relations between surface water acid-base chemistry and biological response is needed to determine specific TLs for N and S deposition that could lead to unimpaired fish and invertebrate populations, communities, and aquatic ecosystems in Adirondack streams (U.S. EPA 2009). However, the relations among emission rates and deposition loads of N and S, surface water acid-base chemistry, and the health of terrestrial and aquatic species and their assemblages (populations and communities) are complex, regionally variable, and challenging to characterize (Greaver et al. 2012). Nevertheless, several relations between acid-base constituents and metrics describing the condition of fish communities in general, and more specifically brook trout (*Salvelinus fontinalis*) populations, provide strong evidence that Al_i concentrations affect fish populations in poorly buffered streams of the western Adirondack Park.

The objective of the biological analyses reported herein is to redefine and quantify relations among chemical indicators and fishery metrics in Adirondack streams and to use these relations to inform TL calculations and ultimately the U.S. Environmental Protection Agency (EPA) Risk and Exposure Assessment (REA) for Secondary National Ambient Air Quality Standards for nitrogen oxides and sulfur oxides (SO_x ; cf., U.S. EPA 2009, 2017). These equations and associated response curves may be used not only to characterize how acidification currently affects local fish assemblages, but also to forecast and assess how changes in chemical indicators, such as Al_i , ANC, and pH, will likely affect biological recovery. The focus of this analysis is on the indicators that best reflect the health of aquatic ecosystems in headwater streams.

Numerous studies, mostly in the Adirondack Park (Driscoll et al. 1980, Baker et al. 1996, van Sickle et al. 1996, Baldigo et al. 2007, Driscoll et al. 2007, Lawrence et al. 2008b, Lawrence et al. 2013), indicate that acidic surface water conditions often result when concentrations of strong acid anions exceed concentrations of base cations. This condition is associated with higher Al_i concentrations

(Lawrence et al. 2008b). Prior studies that characterized the condition of fish assemblages and toxicity of streams in the western Adirondack Park indicated that Al_i thresholds for immature brook trout survival were in the range of 1 to 4 $\mu\text{mol L}^{-1}$, or generally $\sim 2 \mu\text{mol L}^{-1}$, and that time-weighted medians, or Al_i concentration-duration factors, were strong predictors of brook trout mortality (Simonin et al. 1993, van Sickle et al. 1996, Baldigo et al. 2007). The strong relations between Al_i and other acid-base variables, especially pH and ANC in stream waters (Lawrence et al. 2007) suggests that mortality-threshold concentrations for pH and ANC can be estimated using their relationships with Al_i , which increases under high flow.

Recovery of surface water chemistry to a specified value of an index measurement such as $ANC = 20 \mu\text{eq L}^{-1}$ does not guarantee biological recovery. The species of interest must have a means of dispersal to reach a previously acidified habitat that is now chemically suitable for reproduction and survival. Fish may not be able to easily reach a lake that has recovered water quality because of physical barriers such as dams or waterfalls that may limit migration in connecting waters. Also, contemporary environmental conditions may be quite different than those that existed at an earlier time when a given species was present in a water body. For example, the climate in the Adirondack Park has changed substantially from that of 50 to 100 years ago (Stager et al. 2009), and additional climatic changes are expected in the 21st century. These climate-driven changes, including warmer water temperature, are likely to favor some species over others, and could challenge cold-water species such as brook trout. Additionally, any species occupying a habitat where it has previously been eradicated may have to compete with a different mix of species than was present historically. Invasive plants, mollusks, and fish that were not evident 50 years ago are present in many Adirondack lakes today (Strayer 2010). Renewed competition, especially from non-native species, may limit the re-establishment of native species in their former habitats.

1.4 Regional Extrapolation

Site-specific results provide limited information for management and policy purposes if not accompanied by analysis of the broader regional context. For this reason, efforts were made to extrapolate the results of modeled watersheds to the larger population of Adirondack streams. Regional extrapolation focuses on the extent to which water bodies across a broad spatial scale reflect a specified condition. Extrapolation of modeling results from a finite number of streams ($n=25$ in this study) to the regional landscape provides broader context for model outcomes.

1.5 Target Loads

Anthropogenic activities, including those that emit S and N into the atmosphere, adversely impact natural ecosystems in New York State and elsewhere. Environmental policy should be based on recognition of such impacts, with consideration of costs and benefits of atmospheric emissions controls. For this to occur, environmental scientists must measure levels of pollutant emissions into the atmosphere, and consequent deposition from the atmosphere to the ground surface, where adverse ecological effects are manifested. This may be done using CLs and TLs (Burns and Sullivan 2015). The CL/TL approach can account for the spatial and temporal elements of acidification and recovery. A CL is the amount of acid deposition (usually expressed on an annual basis) below which there is no known ecological harm under future steady-state conditions based on current scientific knowledge (Nilsson and Grennfelt 1988). The TL is similar to a CL, although a TL is conducted for a particular time frame by which the specified level of protection will be attained. Critical load and TL concepts and calculations can provide a range of benefits to resource managers and other interested parties, including the following:

- facilitating science-based communication with stakeholders and managers
- determining whether air quality (ambient and/or future) will meet or exceed thresholds for ecosystem damage or recovery
- integrating air quality with land management and effects of natural and human-caused disturbances
- understanding deposition thresholds that trigger impairment
- informing effects to allow determination of appropriate air quality standards at federal and state levels
- improving resource management
- quantifying protection afforded by various levels of emissions controls
- providing a framework for decision-making

1.6 Goals and Objectives

The goals of this study were to conduct an analysis of the environmental effects of acidic deposition on streams in the Adirondack Park and highlight key considerations that will help inform decision-makers and ecosystem managers who are responsible for environmental policy in New York State and beyond. Streams in this park have been less thoroughly investigated than lakes. The primary objective was to quantify the past, ambient (recent or current, depending on data availability), and future acidification of streams in the Adirondack Park, as affected by acidic atmospheric deposition. Future changes

were assessed based on multiple emissions/deposition scenarios. This analysis was accomplished by establishing relationships between stream chemistry and discharge and between stream chemistry and biological conditions. Target loads were used to determine thresholds of biological harm under normalized flow conditions.

2 Methods

2.1 Adirondack Region

The Adirondack Park (Figure 1) is an ideal location for exploring model scenario projections of resource recovery and TLs of acidic deposition as tools for managing natural resources and formulating environmental policy in New York State. This park is one of the largest protected areas in the eastern U.S., has experienced pronounced temporal and spatial gradients in acidic deposition, and shows highly variable surface water chemistry. There is a broad mix of public and private land use in the park, including protected wilderness areas. The legacy of past and current acidic deposition in the region interacts with the effects of other ecological stressors, including climate change and associated pressures caused or exacerbated by changing patterns in temperature, precipitation, and snowpack dynamics (Arseneau et al. 2016).

Figure 1. Map of Study Area



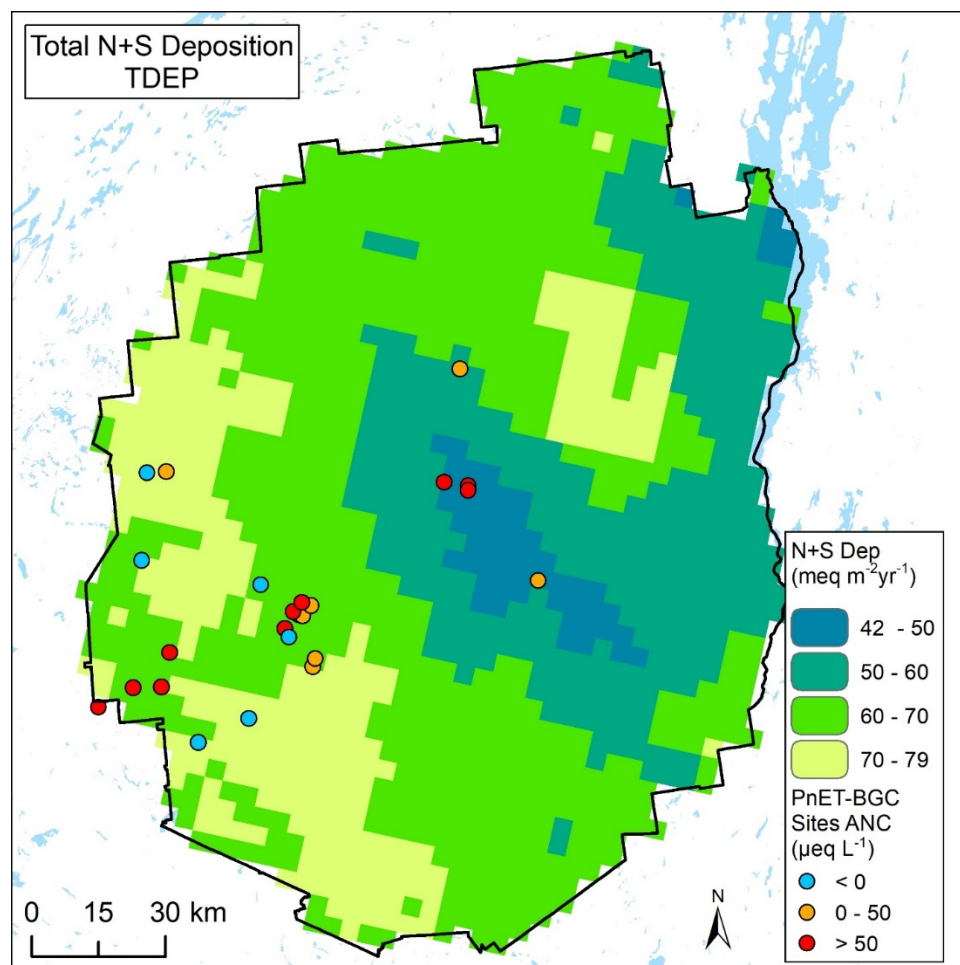
The Adirondack Park hosts a large diversity of plant and animal life, and supports wildlife, timber production, and clean water supplies. These resources provide the foundation for tourism and fishing economies and attract millions of visitors each year (Brown and Connelly 1986, Thorndike 1999) who participate in seasonal recreation and enjoy the aesthetics of summer boating, autumn foliage colors, and winter snowscapes.

The Adirondack Park is a 2.4-million ha forested area with about 2800 lakes (>2000 m² surface area). The Adirondack Park contains an extensive network of streams that drain relatively high-elevation areas, abundant wetlands, and diverse forests (Driscoll et al. 1991). Several landscape factors contribute to the high sensitivity of some Adirondack resources to acidification damage, including thin deposits of glacial till, slow weathering of bedrock and glacial deposits, shallow and naturally acidic soils, and steep slopes.

The area has received high inputs of acidic deposition, with a spatial pattern of decreasing deposition from the southwest to the northeast (Figure 2; Ito et al. 2002). Bedrock geology of the region is composed primarily of gneiss and metasedimentary rock. Soils are largely Spodosols derived from glacial till. The growing season extends from late May to early September. Snow depths at the time of peak accumulation typically range from about 0.5 to 1.5 meters (m). Snowmelt typically occurs in late March to early April, resulting in elevated stream flow (Lawrence et al. 2004). Dominant vegetation is northern hardwood forest, consisting largely of yellow birch (*Betula alleghaniensis* Britton), American beech (*Fagus grandifolia* Ehrh.) and sugar maple. The region also has about 10% cover by coniferous trees, including red spruce, balsam fir (*Abies balsamea* L. Mill.), and eastern hemlock (*Tsuga canadensis*). Many forests in the region have undergone cutting, and/or experienced substantial blow downs, fires, and various forest pests (Driscoll et al. 1991).

Figure 2. Estimate of Total Sulfur and Nitrogen Deposition from TDEP

The figure includes location of the 25 Adirondack Park streams to which PnET-BGC modeling was applied in this study.



2.2 Atmospheric Deposition and Meteorology

2.2.1 Wet and Dry Deposition

The Arbutus Lake watershed in the Huntington Wildlife Forest (HWF) in the central Adirondack Park ($43^{\circ} 58' \text{ N}$, $74^{\circ} 13' \text{ W}$) was used because of its lengthy record to estimate wet deposition to the watersheds of the study streams. Recent wet deposition of the major solutes (Na^+ , Mg^{2+} , K^+ , Ca^{2+} , chloride $[\text{Cl}^-]$, NO_3^- , SO_4^{2-} , and ammonium $[\text{NH}_4^+]$) to the Arbutus watershed over the period 1978–2015 were obtained from the National Atmospheric Deposition Program.³ Estimates of atmospheric wet deposition were needed for 1900 to 1978 during which measured deposition was unavailable. These estimates were developed from linear regression of measured concentrations of wet deposition at HWF (NADP NY20) for the years 1979–2015 with national emissions from the

U.S. Environmental Protection Agency (appendix A), and emissions estimates for 1900 to 1978⁴ were then applied to estimate wet deposition for this period (see appendix A). To extrapolate wet deposition data at HWF to other Adirondack stream sites modeled in this study, it was assumed that the time series of wet deposition for the other sites was proportional to values at the HWF (Table 1). The spatial models developed by Fakhraei et al. (2014), based on data from NADP and the New York State Department of Environmental Conservation, were used to develop deposition time series for all other modeled stream sites.

PnET-BGC dry deposition inputs for S and oxidized N were based on estimates of dry to wet deposition ratios, taken from the regional regression model developed by Ollinger et al. (1993) and modified by Chen and Driscoll (2004) to include effects of forest composition. The forest composition for each study watershed was determined through a Geographic Information Systems (GIS) data layer obtained from the National Land Cover Database.⁵ The dry to wet deposition ratios for base cations, NH_4^+ , and Cl^- were derived from throughfall measurements at the HWF (Shepard et al. 1989). Since consistent temporal and spatial patterns were not observed in dry to wet ratios of base cations, NH_4^+ , and Cl^- among CASTNET (EPA Clean Air Status and Trends Network) and nearby NADP deposition monitoring sites in the northeastern U.S. (Chen and Driscoll 2004), dry-to-wet deposition ratios were assumed to be constant for base cations, NH_4^+ , and Cl^- at each site throughout the simulation period.

Table 1. Physical Site Characteristics and Observed ANC

Table includes the 25 study streams that were used for model simulations using the PnET-BGC model. The deposition ratio to Huntington Wildlife Forest (HWF) was estimated by using the spatial models developed by Fakhraei et al. (2014).

USGS Sites	Latitude (decimal degree)	Longitude (decimal degree)	Elevation^a (m)	ANC ($\mu\text{eq L}^{-1}$)	Deposition Ratio to HWF
North_Buck	43.743562	-74.712254	652.3	-42.0	1.02
35014	43.486256	-75.002906	494.8	-35.2	1.21
27026	43.698481	-74.749378	597.8	-27.1	1.06
T24	43.533806	-74.861833	708.7	-24.3	1.03
22019	43.854408	-75.161067	444.0	-16.2	1.22
12003	44.030897	-75.146819	469.1	-3.8	1.18
WF	43.804667	-74.828361	623.3	-3.7	1.06
South_Buck	43.741597	-74.710970	611.1	9.5	1.05
13008	44.033656	-75.092789	523.9	3.8	1.13
24002	43.762253	-74.686622	590.9	4.2	1.05
28011	43.655078	-74.676514	577.7	8.2	1.08
28014	43.639069	-74.683419	652.6	14.8	1.02
NW	43.810000	-74.050778	448.7	12.4	1.02
Buck Creek	43.743947	-74.722194	546.1	16.6	1.09
AMP	44.240250	-74.265361	525.3	42.1	0.96
27019	43.715700	-74.760600	603.8	112.4	1.07
Archer	43.993611	-74.245278	497.1	111.1	1.00
30009	43.598219	-75.105869	477.0	118.2	1.23
26008	43.667211	-75.081928	513.1	115.9	1.19
30019	43.596681	-75.183794	407.2	119.7	1.28
29012	43.556864	-75.280742	331.3	158.3	1.35
28030	43.750047	-74.737983	549.3	226.2	1.09
N1	44.009611	-74.313500	581.0	238.0	0.96
24001	43.768447	-74.713675	546.7	262.2	1.09
S14	44.000000	-74.250000	609.9	784.9	0.93

^a Elevation at the base of the watershed, with the exception of Archer, where the elevation of a nearby NADP site (NY20) was used. Datum is NAD83, except NAD27 for Buck Creek

2.2.2 Meteorological Data

Air temperature, precipitation, and photosynthetically active radiation (PAR) for the Arbutus watershed were derived from measurements taken at the HWF from 1940 to 2015 and provided by the State University of New York College of Environmental Science and Forestry (SUNY-ESF).⁶ For the years between 1895 and 1939, monthly data from the Parameter-elevation Regressions on Independent Slopes Model⁷ (PRISM) were used to reconstruct maximum and minimum temperature and precipitation estimates. Average values for the period 1895–1939 were used to represent historical meteorological data for the Arbutus watershed.

To extrapolate the meteorological data from the Arbutus watershed to other sites, spatial models of meteorological patterns developed by Fakhraei et al. (2014) were applied using data from the National Climatic Data Center (NCDC). Photosynthetically active radiation at other stream sites was scaled from the Arbutus watershed, using values derived from the regression models developed by Aber and Freuder (2000).

2.3 Soil and Stream Water Chemistry for Watershed Modeling and Spatial Extrapolation

Watersheds selected for dynamic biogeochemical modeling in this project had previously been characterized in terms of both soil and stream chemistry data for model calibration/confirmation. Sufficient soil and stream chemistry data for modeling with PnET-BGC were available in 25 watersheds (< 1km² area, Table 2). The necessary soils data were pooled from several Adirondack soil sampling efforts dating back to 1997. Each soil pit was excavated with a shovel to expose a pit face from which soil samples were collected from the upper B horizon (approximately the top 10 cm) for chemical analysis. Soil chemistry from the upper B horizon was used in this analysis because it closely relates to stream chemistry and forest tree species composition (Lawrence et al., 2018b).

Table 2. Major Data Sources Used in This Study

Database	Source	Major Information Provided
Adirondack Lakes Survey (ALS)	http://www.adirondacklakessurvey.org/historic.php (accessed March 10, 2016)	Watershed characteristics for 11 sites
Adirondack Park Agency (APA)	https://apa.ny.gov/ (accessed March 10, 2016)	Land cover and land disturbance
National Atmospheric Deposition Program (NADP)	http://nadp.slh.wisc.edu/ (accessed January 13, 2016)	Precipitation and wet deposition
National Land Cover Database	https://www.mrlc.gov/data/nlcd-2006-land-cover-conus (accessed May 15, 2016)	Forest composition for 25 sites
U.S. Geological Survey Water Data for the Nation	https://doi.org/10.5066/F7P55KJN (accessed January 15, 2018)	All stream chemistry
U.S. Geological Survey data release	https://doi.org/10.5066/P9YAWRON	All soil chemistry
Precipitation-elevation Regressions on Independent Slopes Model (PRISM)	http://prism.oregonstate.edu/ (accessed January 13, 2016)	Climate data
State University of New York College of Environmental Science and Forestry (SUNY-ESF)	https://www.esf.edu/hss/em/huntington/archive.html (accessed January 13, 2016)	Meteorology, hydrology and stream chemistry data for two sites

Soil data for the Buck Creek watersheds, which provided the most intensive data on soil chemistry of the study watersheds, were averaged from samplings conducted in tributary watersheds during 1997 and 2009-2010 in North Buck, and 1998 and 2014 in South Buck. Detailed information on these watersheds, which have been monitored since 1998, are available in Lawrence et al. (2004), Lawrence et al. (2011), and Lawrence et al. (2018b). Soil samples from the upper 10 cm of the B horizon were collected along seven transects laid out perpendicular to the fall line in each watershed, distributed from upper to lower elevations. In North Buck, samples were collected at 27 locations along these transects during both samplings. In South Buck, samples were collected along these transects at 30 locations in 1998, and 27 locations in 2014.

Eight first-order watersheds where soils were sampled for chemical characterization as part of the WASS were also used for the watershed modeling reported here. The streams in these watersheds varied from chronically acidic ($\text{ANC} < 0 \mu\text{eq L}^{-1}$) to well-buffered ($\text{ANC} > 200 \mu\text{eq L}^{-1}$). In each watershed, soil samples were collected in 2004 from August-October at three locations for each of five plots (15 total sampling locations per watershed). The locations of the five plots were chosen to represent landscape variability within each watershed, including a range of elevations from upper to lower parts of the watershed. Soil samples were collected from the upper 10 cm of the B horizons from the faces of small pits. Samples from each plot were combined and mixed by horizon before analysis, resulting in five measurements per watershed. Further details on WASS soil sampling is available in Lawrence et al. (2008a).

Sixteen watersheds in the Adirondack Sugar Maple Project (ASMP) were selected for modeling simulations in the current investigation. These watersheds were selected to span the full range of soil Ca availability within the Adirondack region. In the ASMP study design, an upper B horizon soil sample was collected in each of two or three plots (20 m by 50 m) that had been established in each watershed. Four of the study watersheds were sampled in both the WASS and the ASMP surveys so the total number of watersheds included from these two studies was 20. In each of the four overlapping watersheds, soil data were available from seven to eight locations. An additional watershed within the Honnedaga Lake drainage (T24) was also included, which provided detailed soil chemistry within each of five plots in the watershed. The 21 WASS, ASMP and Honnedaga watersheds, plus the three Buck watersheds and Archer Creek watershed resulted in a total of 25 modeled watersheds. Soil data from the WASS, ASMP, and Buck Creek watersheds are available along with further information on sampling design, collection methods, and chemical analysis in Lawrence et al. (2020). The 25 watersheds represented a greater than 100-fold range in soil Ca^{2+} concentrations in the upper B horizon (cf., Lawrence et al. 2008a, Page and Mitchell 2008, Lawrence et al. 2020).

The 25 watersheds are listed with coordinates, elevation, ANC and relative deposition estimates in Table 1. The streams draining the 25 watersheds encompass a wide range of pH, ANC, and concentrations of Ali. Monthly, or more frequent stream water chemistry data were available for Archer Creek from 1996–2015, Buck Creek from 2001–2015 (ANC and pH records extended from 1991–2015), the tributaries of Buck Creek from 1998–2015, and watershed T24 at Honnedaga Lake

from 2011–2015. For the remainder of the stream sites, water chemistry data were available from the WASS (collected 2004–05) or the ASMP (collected in 2009–2011). Among the 25 streams, seven had ANC values less than $0 \mu\text{eq L}^{-1}$, eight had ANC values between 0 and $50 \mu\text{eq L}^{-1}$, and 10 had ANC values greater than $50 \mu\text{eq L}^{-1}$ based on sampling during the snowmelt period (Figure 2).

To extend the information obtained from the modeled watersheds throughout the Adirondack region, the WASS, ECASS, and WASS resampling was used to provide chemical data for over 400 streams. Details of sampling and chemical analysis for these sampling programs are provided in appendix B along with a summary description of ambient stream chemistry for these streams. All stream chemistry data from the three Buck Creek watersheds, Honnedaga (T24), WASS, ECASS, and WASS resampling are available through the U.S. Geological Survey, National Water Information System database (U.S. Geological Survey, 2018), all data sources utilized in this report are described in Table 2.

2.4 Influences of Discharge on Stream Chemistry

Assessing the role of streamflow (discharge) on regional stream chemistry is important because surface water ANC, pH, and Al_i concentrations vary with streamflow. Therefore, model parameters that are calibrated to a specific stream chemistry data set will be affected by streamflow at the time of sample collection. If the calibration data set does not adequately consider stream chemistry at the highest flows, then modeled results may not adequately represent episodic acidification, which affects aquatic biota. To evaluate model calibration data relative to episodic acidification, estimates or measurements of streamflow at the time of sample collection are necessary for the modeled sites. Site-specific measurements of stream discharge of adequate length (10 or more years) were available at three of the sampled streams, Buck Creek and the North and South Buck Creek tributaries, which have gauges that record stage for conversion to estimates of discharge at 15-minute intervals. Discharge estimates were made for each sample at all streams (including all modeled streams) that were not gauged by relating the discharge from one of six nearby gauges maintained by the U.S. Geological Survey (USGS) in the region (Table 3) to that of the sampled stream. Because of their small size and proximity to the Buck Creek gauge, the North and South Buck Creek tributary gauges were not used to estimate flow in other streams. Flow percentiles were calculated at each gauge based on daily mean discharge values for water years 2003 through 2015, representing the full range of time that included all samples analyzed in this investigation. The gauge closest to each stream site was selected to represent the flow percentile at the location without a gauge following a similar approach as described in Lawrence et al. (2015b). In most cases, a gauge was within 35 km of a sampled stream site. At stream sites represented by Buck Creek, the flow percentile for the date of collection was assigned to each sample. Because the other five stream

gauges used in this analysis have watersheds with drainage areas that ranged from two to three orders of magnitude larger than Buck Creek and the WECASS streams, the flow percentile on the day following collection was assigned to each of these samples. This estimate of a one-day lag at the larger streams was tested and confirmed by exploring correlations between daily mean discharge at Buck Creek with those of each of the five gauges at lags of zero, one, two, three, and four days. The one-day lag consistently yielded the correlation coefficients that were an average of 0.07 greater than those without a lag.

Table 3. Locations and Drainage Areas of Six Stream Gauges

The gauges were used to estimate flow percentiles for each stream sample analyzed in the investigation.

Site Name	USGS Site ID	Drainage Area (km ²)	Latitude (decimal degrees)	Longitude (decimal degrees)
Buck Creek near Inlet	04253296	3.3	43.743947	-74.722194
Grass River at Chase Mills	04265432	1548.8	44.846667	-75.078056
Hudson River near Newcomb	01312000	497.3	43.966667	-74.131667
Independence River at Donnatsburg	04256000	229.7	43.746806	-75.333444
Little AuSable River near Valcour	04273800	175.6	44.594167	-73.496111
West Canada Creek Near Wilmurt	01343060	616.4	43.366111	-74.957778

Prior to performing analyses of the relation between ANC and discharge among samples collected at a given stream, data from some of the sites and samples collected were not included in the interpretation due to the following reasons. First, any stream site which had an ANC greater than 400 $\mu\text{eq L}^{-1}$ for any sample collected was not included because such streams are considered insensitive to both chronic and episodic acidification and are highly likely to maintain an ANC of greater than 100 $\mu\text{eq L}^{-1}$, even during the highest flow conditions (Davies et al. 1999). Second, any sample at a given stream for which the discharge difference (ΔQ) among any two samples was less than 10% were eliminated based on the assumption that differences of less than this amount could not be reliably estimated at an site without a gauge. Finally, stream sites where ANC at low flow (ANC_{max}) was based on a discharge percentile (Q_{percent}) value greater than 50% were not considered because these data did not represent low-flow ANC values for the stream. These data screening steps resulted in a data set of 309 WECASS streams that was used for hydrological analyses.

The extent of episodic acidification was defined as the magnitude of the decrease in ANC as a function of the increase in stream discharge relative to the sample with the lowest discharge at each site:

Equation 1 $\Delta\text{ANC}/\Delta\text{Q} = (\text{ANC}_i - \text{ANC}_{\text{max}})/(\text{Q}_i - \text{Q}_{\text{min}})$

where ANC_i is the value for a given sample, ANC_{max} is the value at the lowest discharge among the samples collected at a given site, Q_i is the discharge for each sample, and Q_{min} is the discharge for the sample collected under the lowest discharge at each site. Results and discussion associated with the development of the $\Delta\text{ANC}/\Delta\text{Q}$ relation are included in appendix C.

PnET-BGC was applied to simulate past and likely future water chemistry and to calculate current and future TL exceedances at the 25 modeled streams described above. To evaluate how stream discharge may have affected these modeling results, a $\text{Q}_{\text{percent}}$ value was assigned to each of the stream samples that was used to calculate the representative ANC values that were then applied in PnET-BGC model calibration for each of the 25 sites. The $\text{Q}_{\text{percent}}$ values were averaged among the samples used to calculate each representative ANC calibration value. To explore how the model assessment of TL exceedances may have been affected by episodic acidification, the ANC for each of the model $\text{Q}_{\text{percent}}$ values was adjusted to a high-flow value of Q_{85} and compared with the model calibration ANC value. These $\text{Q}_{\text{percent}}$ values were adjusted by using the site-specific $\Delta\text{ANC}/\Delta\text{Q}$ value at the 15 WASS-ECASS sites and the Honnedaga site, T24. At four additional streams where model calibration was based on only one sample, a regional $\Delta\text{ANC}/\Delta\text{Q}$ slope was applied to adjust the calibration ANC values. The five remaining sites included those in the Buck Creek and Archer Creek watersheds that have been the subject of numerous stream chemistry investigations and have been sampled many times over more than 10 years (Lawrence et al. 2007, Christopher et al. 2008, Lawrence et al. 2011, Kang and Mitchell 2013). These five sites were sampled sufficiently to develop least squares linear regressions between $\text{Q}_{\text{percent}}$ and ANC, and these highly significant relations ($p < 0.001$) were used to estimate the ANC at a Q_{85} value.

2.5 Biological Responses

Relations between stream chemistry and biology were investigated to inform TL analyses and selection of critical criteria values. Additional stream chemistry data were needed to establish relationships between indicators of stream acidity and biological response. Water chemistry samples were collected over multiple years for the biological assessment reported here at hundreds of locations in the Adirondack Park. Fish-community surveys were conducted in 47 headwater (1st and 2nd order) streams located mainly in the western Adirondack Mountains under baseflow conditions during summer months (July and August) of 2014, 2015, and 2016 to provide a broad range in Al_i concentrations and potential

toxicity. Fish assemblages at six of the 47 sites were sampled during each year to assess annual variability and to increase the total number of observations (surveys) to 59. Except for Durgin Brook, all sites were located in the Black and Oswegatchie River basins in the western Adirondack Park. Information on site selection, topography, forest cover, soils, climate, and precipitation in the study area is summarized elsewhere (Baldigo et al. 2007, Baldigo et al. 2019a).

At least one 1-liter (L) grab sample was collected from each stream during the summer 2014–2016 fish surveys and transported for analysis to the USGS New York Water Science Center Laboratory in Troy, NY. All water samples for the fish study were analyzed for pH, ANC, Ca^{2+} , Mg^{2+} , Na^+ , K^+ , SO_4^{2-} , NO_3^- , Cl^- , DOC, silicon (Si), NH_4^+ , total monomeric Al (Al_m), and non-labile (organic) monomeric Al (Al_o) according to EPA approved methods and are available through the U.S. Geological Survey, National Water Information System database (U.S. Geological Survey, 2018). Al_i concentrations were estimated as the Al_m concentration minus the Al_o concentration. Negative Al_i values were assigned a value of zero ($0 \mu\text{mol L}^{-1}$). Values of Base Cation Surplus (BCS), were calculated by the difference between summed concentrations of base cations (Ca^{2+} , Mg^{2+} , Na^+ , and K^+) and strongly acidic anions (SO_4^{2-} , NO_3^- , Cl^- , and RCOO_s^-), where RCOO_s^- is an estimate of the concentration of strongly acidic organic anions Lawrence et al. (2007).

Sample reaches for fish-community surveys generally ranged from 20–35 mean channel widths in length (up to 100 m) and often encompassed one to two complete geomorphic channel-unit sequences (Simonson et al. 1994, Fitzpatrick et al. 1998, Meador et al. 2003). Fish were collected from seine-blocked reaches during three to four sample passes using a backpack electroshocker and three to five netters. Fish collected during each pass were identified to species, and length and weight for all fish were recorded. The numbers of fish captured during each pass were used to estimate population size and biomass (and 95% confidence intervals - CIs) per unit area for the fish community and for each population using the Moran-Zippin method of proportional reduction (Zippin 1958, Van Deventer and Platts 1985).

All chemistry data were merged with fish metrics from each of the 59 surveys by site and date, and then used to generate, summarize, and rank the efficacy of numerous chemical and biological metric response equations. First, the relations between key fishery metrics and Al_i , pH, and ANC concentrations were examined to assess the strength and form of any apparent relations. Second, the raw values for biological metrics from each observation (site year⁻¹) were transformed to binary data (0 and 1) within 10–16 response levels or classes encompassing the full range of original data. Third, the relations between binary values

in each of the metric response levels and selected chemical constituents were assessed using logistic regression analysis in STATGRAPHICS Centurion software (StatPoint 2010). The logistic equations (and their associated response surfaces) define the probabilities for occurrences of particular outcomes. Thus, statistically significant ($p \leq 0.05$) relationships specify the likelihood of observing various occurrences (i.e., response levels) for fish metrics across gradients of chemical constituents (or watershed factors), based on the 59 fish surveys completed in streams of the western Adirondack Park between 2014 and 2016. All logistic equations follow the same format, where the probability that any dependent variable, $F(y)$ (e.g., community biomass) equals or exceeds a given biological response level (e.g., > 1000 g per 0.1 ha) over the range of any independent variable (x) (e.g., Al_i). For example,

Equation 2 $F(y) = e^{(\beta_0 + \beta_1 x)} / (1 + e^{(\beta_0 + \beta_1 x)}), \text{ or simply } = 1 / (1 + e^{-(\beta_0 + \beta_1 x)}),$

where e is the natural logarithm base, β_0 is the intercept from a linear regression (i.e., the value when the predictor is equal to zero), and β_1 is the logistic regression coefficient. Important logistic equations were plotted to illustrate the range of the statistically significant (and non-significant) relations.

2.6 Model Applications

2.6.1 PnET-BGC Model Formulation

Scenarios of changing levels of acidic deposition and TLs were simulated using PnET-BGC, an integrated forest vegetation-soil-water biogeochemical model widely used to assess the effects of air pollution, climate change, and land disturbances on forest and aquatic ecosystems (Gbondo-Tugbawa et al. 2001, Pourmokhtarian et al. 2017). This model was formulated by linking two sub-models: PnET-CN (Aber et al. 1997) and BGC (Gbondo-Tugbawa et al. 2001). The biogeochemical processes in the model include tree photosynthesis, growth and productivity, litter production and decay, mineralization of soil organic matter and associated elements, immobilization of N, nitrification, interactions of major elements in vegetation and organic matter, abiotic soil processes, solution speciation, and surface water processes (Gbondo-Tugbawa et al. 2001). The model operates on a monthly time step and is generally applied at the small watershed scale (approximately 10 to 1,000 ha). The Gaines–Thomas formulation is applied to describe cation exchange reactions within the soil. The exchangeable cations considered in the model include Ca^{2+} , Mg^{2+} , Na^+ , H^+ , Al^{3+} , K^+ and NH_4^+ . A pH-dependent adsorption isotherm is used to describe the SO_4^{2-} and dissolved organic matter adsorption process. Speciation of Al_m is calculated in the model,

including both organic and inorganic forms. Organic acids are described using a triprotic analogue (Org3-; Driscoll et al. 1994) and the total amount of organic acid is estimated as a fraction (using the site density) of DOC (Fakhraei and Driscoll 2015). PnET-BGC simulates ANC as an analog to measured ANC by Gran plot analysis (Gran 1952) by considering the contributions of dissolved inorganic carbon (DIC), organic anions, and Al complexes (Driscoll et al. 1994, Fakhraei and Driscoll 2015).

PnET-BGC includes a carbon dioxide (CO₂) uptake algorithm that considers the effects of increases in atmospheric CO₂ concentration on forest ecosystem processes (Pourmokhtarian et al. 2012). The hydrologic algorithms used in PnET-BGC were summarized by Aber and Federer (1992) and Chen and Driscoll (2005a). A more detailed description of the model, including a detailed uncertainty analysis of parameter values, is available in Gbondo-Tugbawa et al. (2001), Pourmokhtarian et al. (2017), and Fakhraei et al. (2016).

PnET-BGC was first tested against vegetation, soil, and water biogeochemistry data from the Hubbard Brook Experimental Forest (HBEF) in New Hampshire (Gbondo-Tugbawa et al. 2001) and then extended successfully to the Adirondack (Zhai et al. 2008, Fakhraei et al. 2014) and Catskill regions (Chen and Driscoll 2004) of New York State, northern New England (Chen and Driscoll 2005b), and the southern Appalachian Mountain region (Fakhraei et al. 2016). The model has been used to project the response of acid-sensitive forest ecosystems to future controls on atmospheric S and N emissions at the HBEF, the Adirondack Park, northern New England, and the Great Smoky Mountains (Gbondo-Tugbawa and Driscoll 2003, Chen and Driscoll 2005b, Wu and Driscoll 2009, Fakhraei et al. 2014, Zhou et al. 2015, Fakhraei et al. 2016).

PnET-BGC hindcast and forecast simulations were constructed for the 25 stream watershed sites for which PnET-BGC was calibrated and applied for this study. Sensitivity and uncertainty analyses of the PnET-BGC model calculations were based on the application of three sensitivity and uncertainty analysis methods (first-order sensitivity index, Morris one-factor-at-a-time, and Latin hypercube sampling associated with a Monte Carlo [LHS-MC] technique). The Morris technique was applied on the input factors used to quantify interaction effects of input factors on model output. An LHS-MC analysis describes uncertainty in model outputs. Using this technique, ±10% uncertainty in the input factors was propagated to the model output. R version 3.0.1 (R Core Team 2013) was used to implement the sensitivity and uncertainty analysis functions. Model inputs and parameter values are given in Table 4.

Table 4. Summary of the Model Inputs and Parameters Used in the PnET-BGC Model

Model Inputs	Notation	Unit
Precipitation	PPT	cm month ⁻¹
Maximum monthly air temperature	Tmax	°C
Minimum monthly air temperature	Tmin	°C
Daily solar radiation	PAR	μmol m ⁻² s ⁻¹
Mean monthly atmospheric CO ₂ concentration	CO2c	ppm
SO ₄ ²⁻ wet atmospheric deposition	Wet _{SO4}	g S m ⁻² month ⁻¹
NO ₃ ⁻ wet atmospheric deposition	Wet _{NO3}	g N m ⁻² month ⁻¹
NH ₄ ⁺ wet atmospheric deposition	Wet _{NH4}	g N m ⁻² month ⁻¹
Na ⁺ wet atmospheric deposition	Wet _{Na}	g m ⁻² month ⁻¹
Mg ²⁺ wet atmospheric deposition	Wet _{Mg}	g m ⁻² month ⁻¹
K ⁺ wet atmospheric deposition	Wet _K	g m ⁻² month ⁻¹
Al ³⁺ wet atmospheric deposition	Wet _{Al}	g m ⁻² month ⁻¹
F ⁻ wet atmospheric deposition	Wet _F	g m ⁻² month ⁻¹
Cl ⁻ wet atmospheric deposition	Wet _{Cl}	g m ⁻² month ⁻¹
SO ₄ ²⁻ dry to wet atmospheric deposition ratio	DWR _{SO4}	
NO ₃ ⁻ dry to wet atmospheric deposition ratio	DWR _{NO3}	
NH ₄ ⁺ dry to wet atmospheric deposition ratio	DWR _{NH4}	
Na ⁺ dry to wet atmospheric deposition ratio	DWR _{Na}	
Mg ²⁺ dry to wet atmospheric deposition ratio	DWR _{Mg}	
K ⁺ dry to wet atmospheric deposition ratio	DWR _K	
Al ³⁺ dry to wet atmospheric deposition ratio	DWR _{Al}	
F ⁻ dry to wet atmospheric deposition ratio	DWR _F	
Cl ⁻ dry to wet atmospheric deposition ratio	DWR _{Cl}	
Site Characteristics and Biogeochemistry Parameters		
Water holding capacity	WHC	cm
Nitrogen sink	Nsink	%
Soil mass per unit area	SoilMass	kg m ⁻²
SO ₄ ²⁻ adsorption coefficient	K _{XSO4}	
DOC adsorption coefficient	K _{XDOC}	
Cation exchange capacity	CEC	mol kg ⁻¹
DOC site density	m	(mol site) (mol C) ⁻¹
DOC partitioning coefficient	DOCPart	
Fast flow fraction	Fast flow frac	%
Ca weathering rate	Weathering Ca	g m ⁻² month ⁻¹
Na weathering rate	Weathering Na	g m ⁻² month ⁻¹
Mg weathering rate	Weathering Mg	g m ⁻² month ⁻¹
Al weathering rate	Weathering Al	g m ⁻² month ⁻¹
K weathering rate	Weathering K	g m ⁻² month ⁻¹
Cl weathering rate	Weathering Cl	g m ⁻² month ⁻¹

Table 4 continued

Model Inputs	Notation	Unit
S weathering rate	Weathering S	$\text{g m}^{-2} \text{ month}^{-1}$
P weathering rate	Weathering P	$\text{g m}^{-2} \text{ month}^{-1}$
F weathering rate	Weathering F	$\text{g m}^{-2} \text{ month}^{-1}$
Selectivity coefficient of Mg^{2+} against H^+	$K_{x2\text{Mg}}$	
Selectivity coefficient of Ca^{2+} against H^+	$K_{x2\text{Ca}}$	
Selectivity coefficient of K^+ against H^+	$K_{x\text{K}}$	
Selectivity coefficient of Al^{3+} against H^+	$K_{x3\text{Al}}$	
Selectivity coefficient of Na^+ against H^+	$K_{x\text{Na}}$	
First organic acid dissociation constant	pKa1	
Second organic acid dissociation constant	pKa2	
Third organic acid dissociation constant	pKa3	
Aluminum solubility constant	$K_{\text{Al}(\text{OH})_3}$	
First organic acid and Al binding constant	pKAl1	
Second organic acid and Al binding constant	pKAl2	
Third organic acid and Al binding constant	pKAl3	
First apparent soil acidity constant	$K_{x\text{OH}2}$	
Second apparent soil acidity constant	$K_{x\text{O}}$	

2.6.2 Scenarios

Monthly values of atmospheric deposition of all major elements and meteorological data (precipitation, minimum and maximum temperature, solar radiation) were input for the entire simulation period. Forest vegetation type, and soil physical and chemical characteristics were held constant over time (Table B-1). Known major land disturbance events, including forest cutting and climatic events, were considered in model simulations. Stream chemistry and stream flow data were used for hydrological and chemical calibration of the model. The sources of inputs used for model calibration are summarized in Table 2. Simulations were initiated in the year 1000, allowing for a spin-up period to achieve steady state (e.g., net ecosystem production [NEP] of the simulated forested watershed remains close to zero; Fakhraei et al., 2014) before anthropogenic disturbances were applied in the model after 1850. The model simulations were run under constant preindustrial meteorology and deposition and no land disturbance until 1850 to achieve steady state. The model was run from 1850 to 2015 based on reconstructed historical deposition and meteorology data, using the vegetation, soil, and hydrologic parameters discussed previously to assess impacts on stream chemistry caused by past and ambient acidic deposition. The model simulations of stream chemistry were compared with measured values over this period to evaluate model performance.

Model simulations were continued through the year 2200 to observe the effects associated with several deposition control scenarios (for SO_4^{2-} , NO_3^- , and NH_4^+ individually and in combination). These included (Table 5):

- Scenario 1: a “business-as-usual” scenario that held ambient deposition (average of 2013–2015) constant until the end of the simulation.
- Scenario 2: a “possible future” scenario that linearly ramped deposition from ambient values down to levels projected under the U.S. Environmental Protection Agency Clean Power Plan for the year 2020 (deposition reductions $\text{SO}_4^{2-} = 24\%$, $\text{NO}_3^- = 31\%$ and $\text{NH}_4^+ = 29\%$; Driscoll et al. 2015) and then held deposition constant until the end of the simulations (Fakhraei et al. 2016).
- Scenarios 3–6: a suite of “additional reduction” scenarios that linearly decreased deposition from the “possible future” (2020) level to the preindustrial deposition level (1850) at 25% intervals (25, 50, 75, and 100% reductions, respectively). Simulated changes in deposition were ramped down linearly from 2021 to 2030 and then held constant until the end of the simulation.
- Scenario 7: an “increasing deposition” scenario that increased deposition 15% from ambient levels was linearly applied for the period from 2016 to 2020 and then held constant until the end of the simulation (Figure 3).

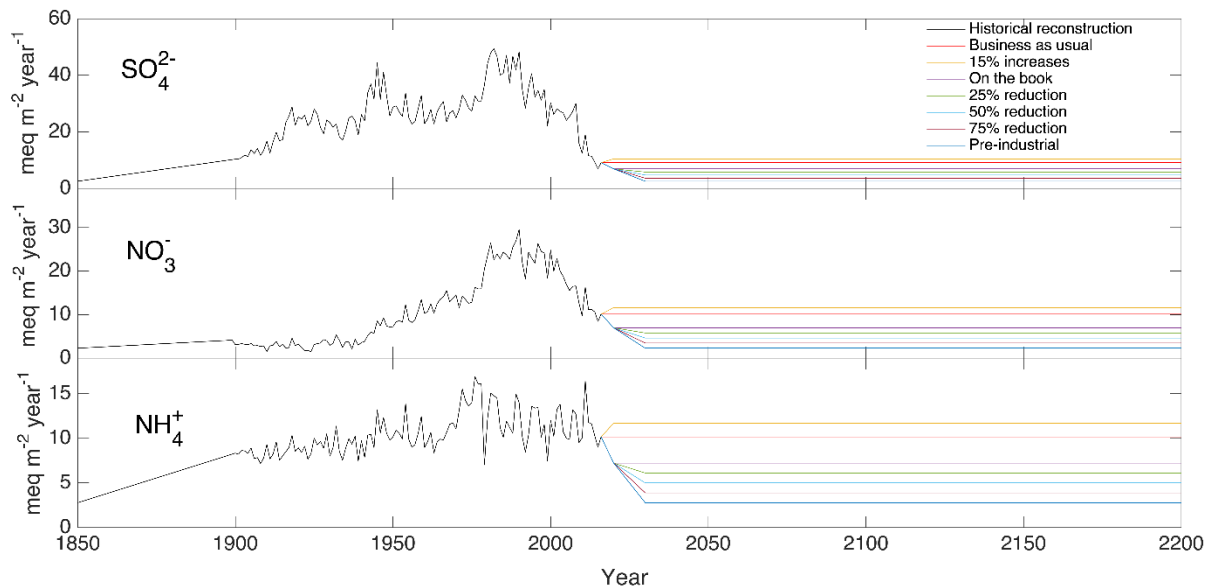
Table 5. Model Scenarios for Changing SO_4^{2-} , NO_3^- , and NH_4^+ Deposition in the Future

Scenario Number	Description
1	Business as usual (average of 2013-2015)
2	Possible deposition future (Clean Power Plan)
3	Additional deposition reduction 25%
4	Additional deposition reduction 50%
5	Additional deposition reduction 75%
6	Additional deposition reduction 100%
7	Increased deposition 15%

To determine and evaluate the most effective approach to achieve further recovery of Adirondack stream ANC, the scenarios were applied to the model projections of ambient stream ANC as (1) decreases in atmospheric deposition of SO_4^{2-} alone; (2) equal percentage decreases in SO_4^{2-} and NO_3^- deposition; and (3) equal decreases in deposition of SO_4^{2-} , NO_3^- , and NH_4^+ simultaneously. Additional reductions in oxidized N and S could result from further emissions controls of these sources. However, reductions in NH_4^+ emissions may be less likely. ANC response surfaces were developed for the two specified endpoint years (2050 and 2150) in this TL analysis. These ANC response surfaces were obtained using the model simulated stream ANC under the different future deposition scenarios.

Figure 3. Reconstruction of Wet Atmospheric Deposition of SO_4^{2-} , NO_3^- and NH_4^+ ($\text{meq m}^{-2} \text{ yr}^{-1}$)

The data were collected at Huntington Wildlife Forest in the Adirondacks during the period 1850-2200. Future projections (present-2200) are shown under the “business-as-usual” scenario, the “possible future” scenario (EPA Clean Power Plan), a 15% increase scenario, and four reductions applied to the “possible future” scenario, including a 100% reduction in anthropogenic emissions (return to preindustrial levels).



2.6.3 Model Evaluation Criteria

Two statistical criteria were used to assess model performance: normalized mean error (NME) and normalized mean absolute error (NMAE; Janssen and Heuberger 1995). The NME provides a comparison of model simulated values to observed values on an average basis. A negative value of NME indicates underestimation and a positive value indicates overestimation by the model simulation. The NMAE indicates the absolute discrepancy between overall average model predictions and observations. The NMAE is used to evaluate the performance of the model in depicting measured trends in streamwater chemistry. An NMAE value of zero is considered optimal and indicates full agreement between model simulation and observed data. NME and NMAE are defined as follows:

Equation 3
$$NME = \frac{\bar{s} - \bar{o}}{\bar{o}}$$

Equation 4
$$NMAE = \frac{\sum_{t=1}^n (|s_t - o_t|)}{n\bar{o}}$$

where \bar{s} and \bar{o} are the average of model simulated values and observed values, s_t is the model simulated value at time t , o_t is the observed value at time t , and n is the number of observations.

2.6.4 Sensitivity Analysis

A model sensitivity analysis was conducted by examining the relative change in model output divided by the relative change in parameter values to evaluate the relative sensitivity of model simulations to a given change in a model input or parameter. The sensitivity index of a parameter Y_i is defined as (Jørgensen and Bendoricchio 2001):

Equation 5
$$S_{Parameter, Y_i} = \frac{\partial X/X}{\partial Y_i/Y_i}$$

where ∂X is the relative change in the model output X , and ∂Y_i is the relative change in the model input factor Y_i . The higher the value of $S_{Parameter, Y_i}$, the more sensitive the model is to the parameter of interest. Stream ANC was selected as an output of interest since it is an integrating indicator of the sensitivity of the watershed to acidic deposition. Sensitivity analyses were conducted on 21 model parameters and inputs. The analysis was conducted primarily by examining the change in model output under preindustrial (1850) and future (2050) conditions in response to a change in a model parameter or input of interest. Simulations were conducted for each site to estimate the degree of sensitivity by applying a 15% and 2 °C change (i.e., increase or decrease) in model parameters and inputs, and temperature, respectively. The most sensitive parameters were identified by comparing the median values of calculated $S_{Parameter, Y_i}$ values for the modeled streams.

2.7 Target Loads and Exceedance

An important objective of this study was to estimate the TLs of acidity for the 25 streams with monitored stream and soil chemistry data. To calculate the stream-specific TLs, target ANC criteria were specified for future endpoint years. Since the chemical and biological recovery of stream ecosystems from acidification occurs over periods that can range from decades to centuries (Josephson et al. 2014), endpoint years of 2050 and 2150 were selected to allow partial to near full chemical recovery of the streams to occur. Two approaches were used to set ANC criteria for calculating TL values. First, a fixed ANC criterion of 20 $\mu\text{eq L}^{-1}$ was specified to allow for at least partial biological recovery for all study streams (U.S. EPA 2009). In the second approach, the ANC criterion was determined as the ANC value 20 $\mu\text{eq L}^{-1}$ less than the 1850 ANC value estimated by hindcast simulations (Fakhraei et al. 2016) of each modeled stream. This site-specific ANC criterion was used because the model outputs suggested that chemical recovery to pre-industrial levels is not possible for the modeled streams, even if acidic deposition is reduced to zero and then maintained at that level over the period of model simulation (until 2200).

The extent of TL exceedance was determined by subtracting the TL from average (2014–2015) ambient deposition available from the Total Deposition (TDEP) model of Schwede and Lear (2014)⁸ with positive values indicating exceedance (i.e., ambient deposition is above the TL) and negative values indicating that the site is currently not in exceedance (i.e., ambient deposition is below the TL). The TDEP approach represents an interagency federal effort to estimate total wet plus dry S and N deposition since 2000 across the conterminous U.S. Target load exceedances were calculated for both fixed and site-specific ANC criteria.

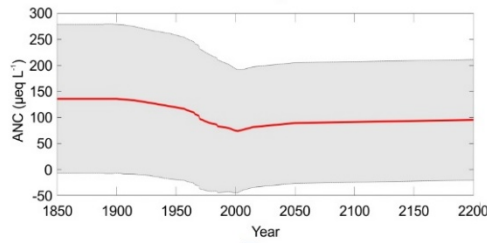
2.8 Coupled Modeling, Hydrologic Analysis, and Biological Effects Assessment

Results were integrated across the biogeochemical modeling, hydrological analysis, and biological effects components of this project. The general approach is outlined in Figure 4. The PnET-BGC biogeochemical model was applied to each watershed site based on observed stream chemistry under the flow conditions that prevailed at the time of water sampling. At each site, modeled historical (1850), ambient (2015), and future (2150) stream ANC for all scenarios was then adjusted based on the ANC/flow relationship to reflect the expected ANC under summer baseflow conditions. Summer base flow was designated as the 27th percentile among all daily flows at each stream (Q_{27}) during water years 2003–2015, the average flow condition at the time of data collection for development of fish response functions. The ANC criterion for establishing site-specific TLs were also adjusted to summer base flow conditions. These flow adjustments to modeled ANC were made using the $\Delta\text{ANC}/\Delta Q$ relations described in appendix C. Finally, relationships between summer baseflow (Q_{27}) ANC and various fish response metrics were applied to estimate fish conditions under scenarios of past, ambient, and future conditions and attainment of site-specific TLs. The fish response metrics included community richness, density, and biomass, and also the density and biomass of brook trout populations. Through this process, expected fish responses were estimated for each modeled stream at multiple periods of simulation under changing levels of acidic deposition, standardized to consider differences in flow condition at the times of sampling.

Figure 4. Schematic Depiction of Project Result Integration

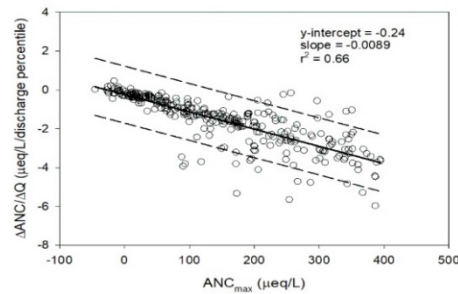
Step 1

PnET-BGC simulated stream ANC under *moderate to high flow conditions* at the 25 PnET-BGC model sites



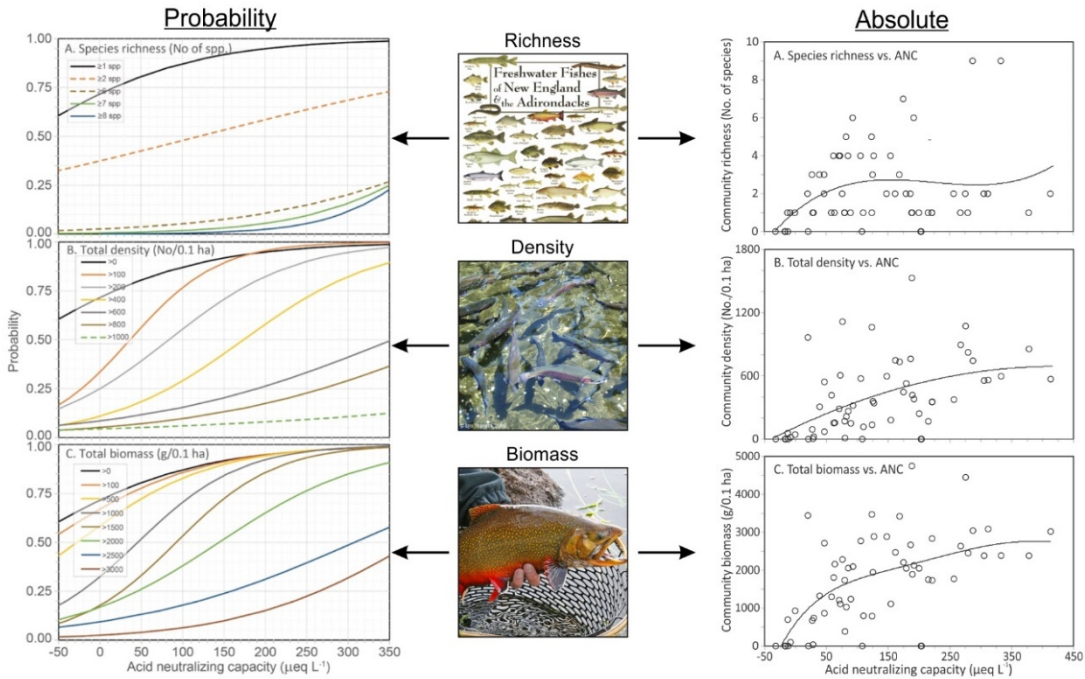
Step 2

Linear regression to adjust PnET-BGC modeled ANC under *moderate to high flow conditions* to expected ANC under *summer baseflow conditions (Q₂₇)*



Step 3

Apply equations developed from measured ANC during *summer baseflow conditions (Q₂₇)* and fish surveys to estimate either the probability for different levels, or the absolute values, of the expected historical, ambient (present-day), and future fish metrics for all 25 PnET-BGC models stream sites

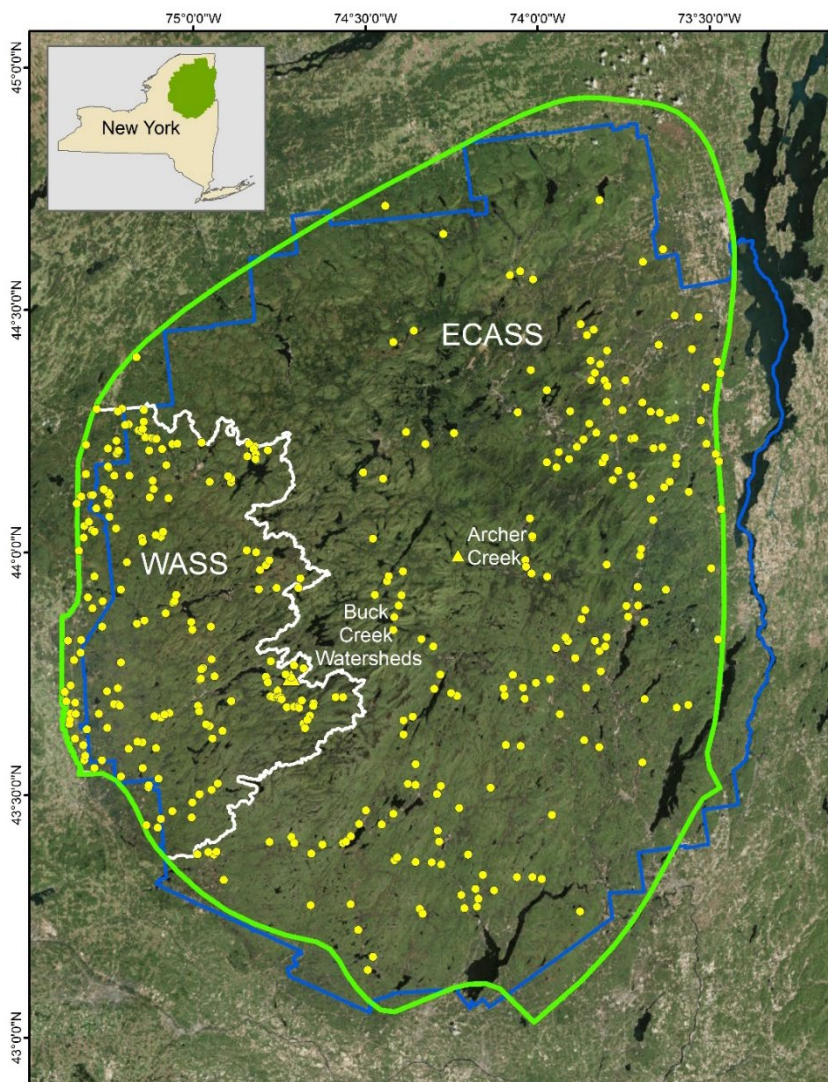


2.9 Regionalization of Target Loads

Results for the 25 modeled sites were extrapolated across the wider Adirondack region. The best spatial coverage of stream chemistry for Adirondack Mountain streams is provided by WECASS. These surveys were used as the basis for extrapolation of modeling results (Figure 5). Therefore, the primary spatial frameworks for regionalization of TLs generated by PnET-BGC consisted of the individual WECASS sample locations and 10-km grid cell summaries of the individual WECASS sites. For the grid summaries, the minimum and median predicted TLs at all WECASS sites that occurred within a grid cell were calculated and mapped.

Figure 5. Locations of Buck Creek and Archer Creek Monitoring Watersheds

The watersheds are indicated by triangles, and streams sampled in the ECASS (East-Central Adirondack Stream Survey), and WASS (Western Adirondack Stream Survey), indicated by circles. WASS study area is outlined in white. The green line encompasses the Adirondack ecoregion; the blue line encompasses the Adirondack State Park.



Individual linear regression models were developed to predict each of the four different TLs, based on two ANC criteria ($ANC = 20 \mu\text{eq L}^{-1}$ and site-specific ANC that varied by stream) and two endpoint years (2050 and 2150). Available stream chemistry sampled between the months of March and May were extracted from the WECASS database and averaged to represent ambient (2004–2011) stream chemistry during the spring snowmelt season at 401 sites throughout the Adirondack region. In addition to landscape predictor variables, measured stream chemistry at these WECASS sites was used to predict

TLs determined using PnET-BGC. Nineteen candidate predictor variables representing watershed conditions describing current ANC, current BCS, current N and S deposition (average of 2014 and 2015), long-term average N and S deposition (1955-2015), latitude, longitude, elevation, slope, forest type (deciduous/coniferous), soil texture, soil organic carbon (C), soil pH, and root zone depth provided the basis for model selection (see appendix D). All possible models including up to four predictors were evaluated and the Akaike Information Criterion (AIC) was used to rank the models. The selected predictor variables from the top five models (based on lowest AIC), for predicting each of the four types of TLs were tabulated and the three most commonly selected predictors among these models were chosen to use as the basis for developing final regression models for all four types of TLs.

Regionalized TL and exceedance were expressed and mapped two ways. In the first approach, TL and associated exceedance values were estimated at each of the WECASS sites and mapped as point symbols. In the second approach, the study region was divided into 10-km x 10-km grid squares. The TL was represented at each grid cell as either the median or the minimum value and the TL exceedance was represented as the median or the maximum value among WECASS sites located within the grid cell. Target load exceedances were determined by subtracting the estimated TL from total S + N deposition provided by TDEP (Schwede and Lear 2014).⁹

3 Results

3.1 Ambient Stream Chemistry

Chemistry varied from ANC values ranging from $-67 \mu\text{eq L}^{-1}$ to greater than $1000 \mu\text{eq L}^{-1}$ among the streams sampled in the WECASS surveys, both spatially and seasonally. Stream chemistry results are reported elsewhere (Lawrence et al. 2008a, Lawrence et al. 2018a) and are briefly summarized in appendices B and E. USGS National Water Information System (NWIS) identification numbers for stream sites considered in this analysis are provided in appendix F.

3.2 Model Evaluation

PnET-BGC model performance was evaluated based on statistical metrics that indicate the extent to which simulation results agreed with measured values (Table 6, Figure 6). Model performance varied among sites and stream solutes, partly due to differences in sampling intensity and duration. Archer Creek, Buck Creek and the tributaries of Buck Creek showed the best model performances, attributable to the relatively long records of monthly observations.

Table 6. Comparisons of PnET-BGC Model Estimates

Comparisons between preindustrial (Year 1850) chemistry and estimates for Year 2000 and ambient (Year 2015) chemistry (units in $\mu\text{eq L}^{-1}$) for 25 modeled sites.

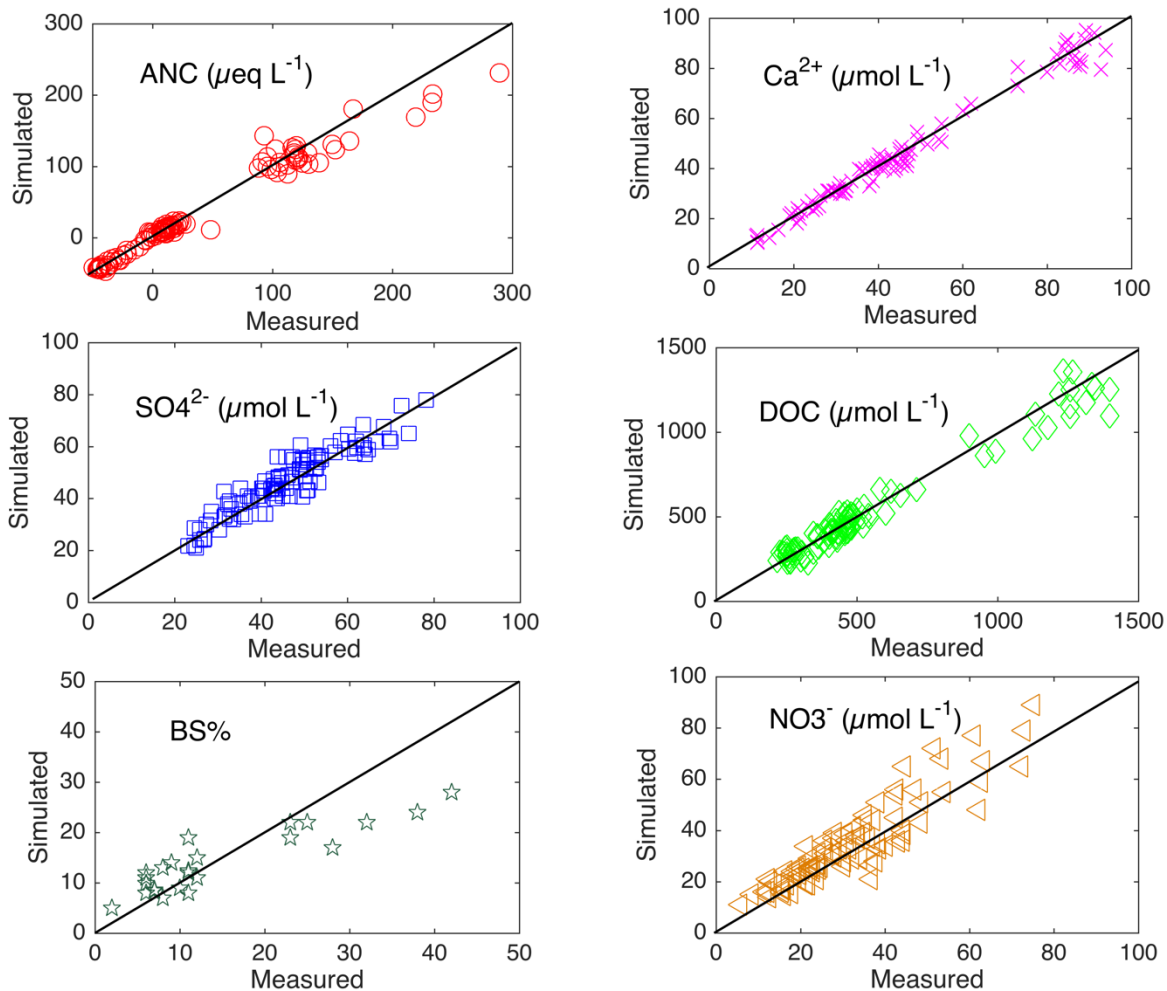
Site	Simulated Preindustrial (Year 1850) Chemistry			Simulated Year 2000 Chemistry			Simulated Ambient (Year 2015) Chemistry		
	SO ₄ ²⁻	NO ₃ ⁻	ANC	SO ₄ ²⁻	NO ₃ ⁻	ANC	SO ₄ ²⁻	NO ₃ ⁻	ANC
North Buck	31.6	6.8	22.8	114.4	24.4	-44.3	67.5	18.6	-42.1
35014	17.5	6.2	10.0	62.1	67.1	-45.8	42.6	70.2	-34.1
27026	15.1	7.5	25.5	81.5	64.7	-31.2	46.4	65.2	-27.8
T24	14.8	3.9	28.7	75.1	18.4	-31.2	53.4	16.8	-22.8
22019	25.5	3.8	23.4	94.1	36.1	-23.5	62.2	13.8	-16.4
12003	20.5	3.9	28.2	75.5	17.8	-14.5	47.6	21.4	-2.3
WF	8.8	7.8	25.9	71.8	45.2	-15.8	53.7	36.8	-3.7
South Buck	24.4	4.8	53.2	93.4	35.2	7.8	72.4	48.5	9.6
13008	30.4	4.2	38.4	112.8	56.3	2.1	81.6	33.8	4.0
24002	16.1	8.9	37.3	85.4	76.3	-6.8	52.3	58.7	2.8
28011	19.2	4.6	52.6	70.7	43.7	4.8	42.6	46.4	7.6

Table 6 continued

Site	Simulated Preindustrial (Year 1850) Chemistry			Simulated Year 2000 Chemistry			Simulated Ambient (Year 2015) Chemistry		
	SO ₄ ²⁻	NO ₃ ⁻	ANC	SO ₄ ²⁻	NO ₃ ⁻	ANC	SO ₄ ²⁻	NO ₃ ⁻	ANC
28014	9.0	7.2	51.8	71.6	58.2	8.7	65.3	33.9	14.8
NW	11.3	3.3	56.5	73.7	19.5	-2.1	67.3	11.8	11.5
Buck Creek	22.9	5.7	56.3	111.7	42.7	12.2	94.4	23.6	19.7
AMP	31.7	4.5	93.1	119.6	29.4	30.8	94.2	30.7	37.5
27019	31.2	6.5	160.6	113.3	57.9	96.4	92.2	31.5	115.7
Archer	42.7	4.8	148.8	112.5	38.8	102.1	85.1	27.9	110.7
30009	36.5	6.1	155.8	127.7	42.9	113.5	74.9	21.1	114.8
26008	33.6	4.1	163.2	102.6	30.8	108.5	62.4	11.5	112.2
30019	10.4	7.3	163.8	63.8	18.5	108.8	45.2	20.5	113.4
29012	27.2	4.0	218.3	116.4	18.1	147.3	77.8	11.2	154.1
28030	7.8	4.2	271.6	74.2	60.7	216.2	49.1	31.2	230.1
N1	20.4	5.5	285.1	102.9	40.7	212.2	70.9	32.2	230.1
24001	30.9	7.9	336.8	137.7	64.8	201.2	105.3	54.8	221.4
S14	41.3	5.2	894.1	145.2	40.5	720.4	128.2	58.5	738.7

Figure 6. Comparison of Model-Simulated versus Observed Stream Chemistry and Soil Base Saturation

Comparison includes 24 modeled streams (all except S14) with very high values of ANC, BS, and Ca^{2+} . The measured values are displayed as mean annual values.



The results of the first-order sensitivity analysis of model simulated ANC associated with 16 model parameters and inputs for all 25 streams is shown in Table 7. The different physical characteristics of the study sites and the complex interactions among various components of the model could contribute to the magnitude of variation in ANC change in the simulations. Overall, the sensitivity analysis indicated that the model is most sensitive to variation in precipitation quantity ($S_{\text{ANC}} = 1.09$ which indicates $1.09 \mu\text{eq L}^{-1}$ decrease in ANC in response to 15% increase in precipitation), Ca^{2+} and Na^+ weathering rates, maximum monthly air temperature, SO_4^{2-} wet deposition, and DOC site density. The sensitivity analysis results provided a guide to focus on these important inputs and parameters for model calibration and improved the overall model projections.

Table 7. Summary of Sensitivity Analysis of the PnET-BGC Simulated ANC (2050)

The summary responds to the variation in 16 input factors used in the model. Average values of the first order sensitivity index for 25 modeled streams are sorted by absolute value.

PARAMETERS	NOTATION	UNIT	S _{ANC}
Precipitation	PPT	cm month ⁻¹	1.09
Ca ²⁺ weathering rate	Weathering Ca	g m ⁻² month ⁻¹	0.93
Na ⁺ weathering rate	Weathering Na	g m ⁻² month ⁻¹	0.67
Maximum monthly air temperature	Tmax	°C	0.61
SO ₄ ²⁻ wet deposition	WetSO4	g S m ⁻² month ⁻¹	0.52
DOC site density		(mol site) (mol C) ⁻¹	0.52
K ⁺ weathering rate	Weathering K	g m ⁻² month ⁻¹	0.31
DOC partitioning coefficient	DOCPart		0.16
Mg ²⁺ weathering rate	Weathering Mg	g m ⁻² month ⁻¹	0.11
Cl ⁻ weathering rate	Weathering Cl	g m ⁻² month ⁻¹	0.10
Minimum monthly air temperature	Tmin	°C	0.10
Nitrogen sink	Nsink	%	0.08
Water holding capacity	WHC	cm	0.06
Soil mass per unit area	SoilMass	kg m ⁻²	0.06
NO ₃ ⁻ wet deposition	WetNO3	g S m ⁻² month ⁻¹	0.04
Cation exchange capacity	CEC	mol kg ⁻¹	0.02

The PnET-BGC model effectively simulated the hydrology and ambient chemistry of stream waters and soils in the Adirondack Park. The model-simulated annual stream discharge (652 ± 133 mm) for Archer Creek was close to the measured values (705 ± 135 mm; NME = -0.07, NMAE = 0.10). Mean NME and NMAE values also indicated good agreement between measured and model simulated SO₄²⁻ across all the sites (NME = 0.04 ± 0.05 ; NMAE = 0.08 ± 0.05 ; Table 8). Simulated stream Ca²⁺ and ANC agreed well with observations, except for one well-buffered site (S14). Low ANC sites ($< 100 \mu\text{eq L}^{-1}$), which are the major focus of this study, showed good agreement between measured and modeled stream Ca²⁺ and ANC (Ca²⁺: NME = -0.02 ± 0.03 and NMAE = 0.06 ± 0.05 ; ANC: NME = -0.08 ± 0.11 and NMAE = 0.13 ± 0.06). The simulated DOC concentrations also agreed well with measured data at lower concentrations ($< 600 \mu\text{mol L}^{-1}$), but somewhat underestimated DOC at higher values. Modeled stream NO₃⁻ showed relatively larger discrepancies when compared with observed values than did other stream chemical variables (Figure 6). These relatively large discrepancies can be attributed to the simplification of the complex N cycle in forested watersheds depicted by PnET-BGC (e.g., assumption that denitrification loss is low) and/or the challenges in characterizing historical land disturbances and

meteorological conditions in model simulations. Furthermore, the total of 3–5 samples were collected from some streams likely do not represent the annual volume weighted NO_3^- concentrations. Model simulated soil % BS, except at higher values, generally agreed with the measured values ($\text{NME} = -0.26 \pm 0.15$), especially at % BS < 25% (Figure 6).

Table 8. Summary Mean and Standard Deviation of Metrics of Model Performance

Focused on the simulation of Ca^{2+} , SO_4^{2-} , NO_3^- , ANC, and DOC concentrations for 24 modeled Adirondack streams and soil base saturation of their watersheds. Site S14 was not included in this summary because it is a well-buffered stream and has very high values of ANC, %BS, and Ca^{2+} .

Stream Constituent	NME ^a		NMAE ^b	
	Mean	SD	Mean	SD
Ca²⁺	-0.13	0.12	0.16	0.11
SO₄²⁻	0.04	0.05	0.08	0.05
NO₃⁻	0.18	0.14	0.35	0.24
ANC	-0.11	0.17	0.18	0.15
DOC	-0.15	0.11	0.17	0.10
% BS	-0.26	0.15	0.26	0.15

^a NME—normalized mean error

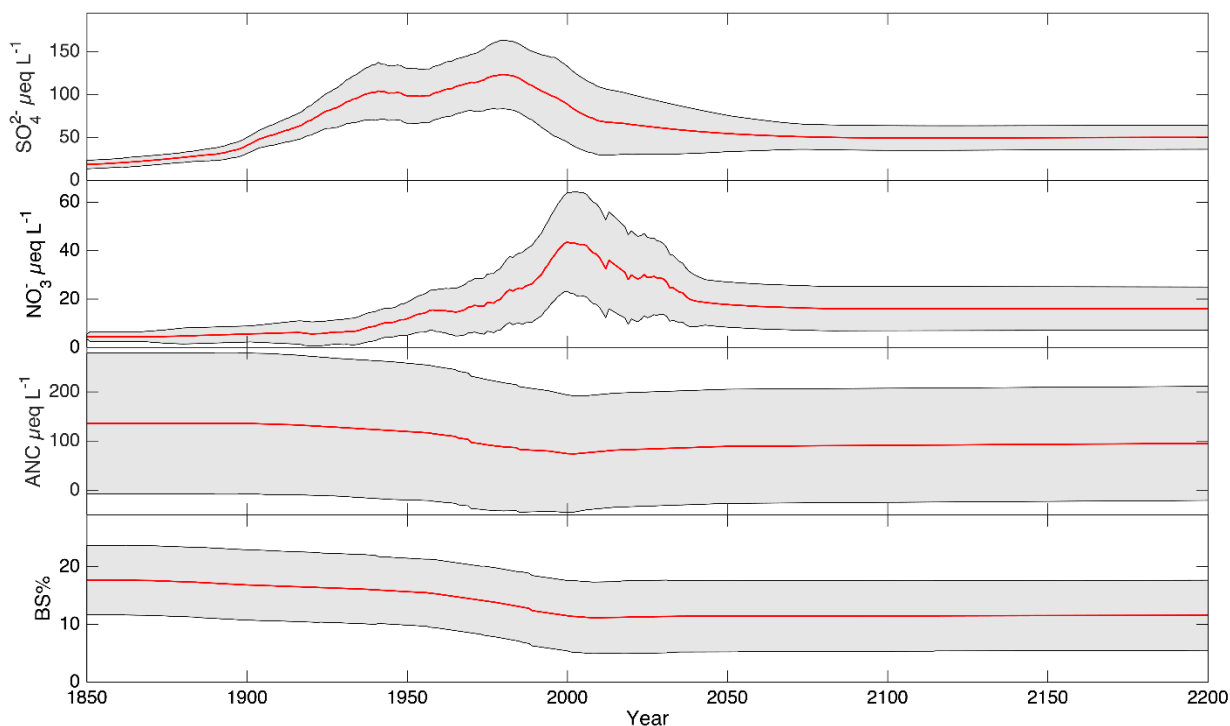
^b NMAE—normalized mean absolute error

3.3 Historical Acidification

Model simulations were conducted to evaluate time series of annual volume-weighted concentrations of stream SO_4^{2-} , NO_3^- and ANC and soil % BS from 1850 to 2200 for the 25 model sites (Figure 7). The model hindcast scenarios suggested that stream SO_4^{2-} concentrations may have been historically low (mean \pm one standard deviation; $12 \pm 5 \mu\text{mol L}^{-1}$) during the preindustrial period (1850), increasing to maximum concentrations of $62 \pm 21 \mu\text{mol L}^{-1}$ by approximately 1980 and then followed by decreasing trends to ambient concentrations in about 2015 ($35 \pm 11 \mu\text{mol L}^{-1}$). Long-term temporal patterns in stream NO_3^- concentrations were similar to temporal patterns of stream SO_4^{2-} concentrations, although peak NO_3^- values occurred about 10 years after peak SO_4^{2-} concentrations. The model-simulated preindustrial NO_3^- concentrations were low for all 25 modeled streams ($5.5 \pm 1.6 \mu\text{mol L}^{-1}$) and did not show significant increasing trends until the 1930s, peaking around the 2000s at $42 \pm 18 \mu\text{mol L}^{-1}$.

Figure 7. Mean and Standard Deviation of Model-Predicted Selected Stream Chemistry and Soil Base Saturation

The data are based on the 25 simulated Adirondack streams during the period 1850–2200. Stream chemistry includes SO_4^{2-} , NO_3^- and ANC. Future projections are shown under the “business-as-usual” scenario.



The mean value of the model simulated preindustrial stream ANC was $136 \pm 184 \mu\text{eq L}^{-1}$ among the modeled sites. Only one stream (35014: $\text{ANC} = 10.0 \mu\text{eq L}^{-1}$) had simulated preindustrial ANC less than $20 \mu\text{eq L}^{-1}$, and one had a very high value (S14: $\text{ANC} = 894.1 \mu\text{eq L}^{-1}$). Eight streams had simulated preindustrial ANC between 20 and $50 \mu\text{eq L}^{-1}$. The remaining 16 streams had model simulated preindustrial ANC greater than $50 \mu\text{eq L}^{-1}$ (Table 6). Coinciding with increases in concentrations of simulated stream SO_4^{2-} and NO_3^- , the simulated stream ANC decreased to minimum values around the year 2000 ($75 \pm 158 \mu\text{eq L}^{-1}$), followed by a slight increasing trend in recent years. Model hindcasts suggested that, across the 25 modeled streams, acidic deposition resulted in decreases in ANC of about $50 \mu\text{eq L}^{-1}$ on average since 1850.

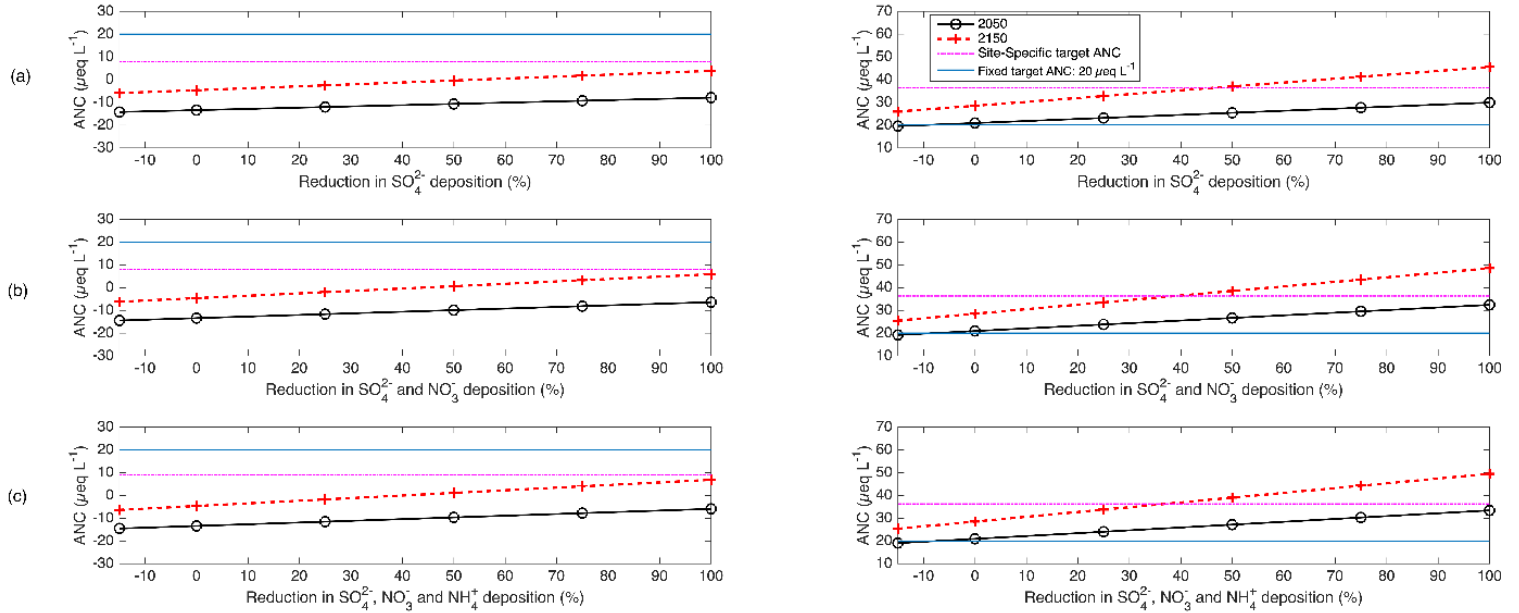
Historical increases in acidic atmospheric deposition to the modeled watersheds not only acidified the streams, but also acidified the soil. Hindcast simulations of soil chemistry suggest decreases in soil % BS from preindustrial levels of $17.2\% \pm 6.9\%$ to the minimum levels of $11.3\% \pm 6.1\%$ in about 2010, with no significant recovery thereafter. This marked decrease in soil base saturation was likely the result of soil exchangeable cation depletion resulting from sustained historical anthropogenic N and S deposition and strong acid anion leaching.

3.4 Model Predictions of Future Stream and Soil Chemistry Under Different Deposition Scenarios

Model projections suggested that changes in acidic deposition influenced future stream SO_4^{2-} and NO_3^- concentrations and ANC and soil % BS at most affected watersheds in the Adirondack Park. Examples are given in appendix G. ANC response surfaces (examples shown in Figure 8) for each stream were developed by depicting different ANC values with their corresponding reduction levels (-15, 0, 25, 50, 75 and 100%) for the three deposition scenarios (SO_4^{2-} alone; SO_4^{2-} and NO_3^- ; and SO_4^{2-} , NO_3^- , and NH_4^+). Model projections suggested that, to achieve the same level of recovery in stream ANC, the scenarios that considered decreases in atmospheric SO_4^{2-} , NO_3^- , and NH_4^+ deposition combined required less percentage reduction than either decreases in SO_4^{2-} plus NO_3^- deposition or decreases in SO_4^{2-} deposition alone (Figure 8).

Figure 8. Projections of ANC of T24 (left) and Buck Creek (right)

The projections are in response to different load reduction scenarios: (a) SO_4^{2-} load reduction, (b) SO_4^{2-} and NO_3^- load reduction, and (c) SO_4^{2-} , NO_3^- , and NH_4^+ load reduction for different target years (2050 and 2200) in relation to ANC targets of $20 \mu\text{eq L}^{-1}$ and preindustrial ANC ($-20 \mu\text{eq L}^{-1}$).



Results of the ANC simulations for the two endpoint years (2050 and 2150) are given in Table 9. ANC simulation results varied with scenario and endpoint year. Differences among scenarios were generally small for the streams having lower ANC.

Table 9. Simulation Results for ANC ($\mu\text{eq L}^{-1}$)

Results are from 25 modeled sites under different scenarios of reductions in SO_4^{2-} , $\text{NO}_3^- + \text{NH}_4^+$ deposition (see Table 5) for 2050 and 2150. Model results are compared with measured ambient ANC.

Site	Ambient ANC	Year 2050 ANC Simulation							Year 2150 ANC Simulation						
		Scenario Number ^a							Scenario Number ^a						
		1	2	3	4	5	6	7	1	2	3	4	5	6	7
North Buck	-42.1	-29.4	-28.6	-27.1	-25.5	-23.1	-20.5	-37.7	-26.1	-25.7	-23.6	-21.1	-19.3	-16.7	-32.8
35014	-34.1	-33.1	-32.8	-32.4	-31.5	-30.8	-30.1	-36.7	-28.1	-27.4	-27.0	-26.4	-25.7	-25.1	-38.4
27026	-27.8	-24.7	-24.0	-22.4	-20.1	-17.4	-15.7	-30.1	-22.1	-21.1	-20.3	-18.7	-16.6	-15.1	-32.5
T24	-22.8	-14.5	-13.2	-11.6	-9.7	-7.8	-5.9	-15.6	-4.7	-3.7	-1.8	1.1	4.0	6.9	-6.4
22019	-16.4	-13.5	-12.2	-10.8	-8.1	-6.1	-3.0	-18.9	-11.1	-6.2	-5.1	-2.8	1.1	3.5	-20.5
12003	-2.3	4.8	5.1	6.0	7.1	8.7	10.5	4.1	6.3	7.0	8.2	11.5	15.7	20.9	4.9
WF	-3.7	2.1	3.7	4.6	6.3	7.9	9.5	-1.9	4.1	4.7	5.9	7.5	8.9	10.6	-2.2
South Buck	9.6	13.4	14.4	15.9	18.4	21.0	23.4	10.9	18.1	19.3	20.9	23.6	26.9	28.8	13.4
13008	4.0	7.4	8.2	10.5	15.0	19.5	24.0	6.3	11.1	13.5	16.2	19.3	22.3	25.4	8.8
24002	2.8	6.4	7.5	8.7	11.5	16.3	21.1	5.1	8.3	10.5	14.5	18.5	22.4	26.4	7.3
28011	7.6	14.8	15.3	16.3	17.1	18.4	19.9	10.3	22.2	27.0	32.6	41.1	46.9	51.2	14.0
28014	14.8	16.9	18.8	20.2	24.4	32.6	41.8	13.9	18.4	20.7	26.4	37.0	46.5	50.1	12.6
NW	11.5	18.4	20.3	24.1	29.5	36.9	44.7	16.4	25.1	28.2	33.4	37.4	44.9	52.4	17.1
Buck Creek	19.7	20.5	21.4	24.0	27.2	30.3	33.4	19.0	28.1	30.2	33.8	39.0	42.3	49.5	25.4
AMP	37.5	46.8	51.3	53.5	58.9	64.1	70.5	43.8	54.7	60.5	64.9	72.6	80.9	91.2	41.5
27019	115.7	119.8	121.3	123.8	128.4	131.0	134.1	114.1	124.8	125.7	127.1	130.4	134.7	137.8	115.4
Archer	110.7	116.5	117.3	118.8	120.1	122.4	124.1	107.3	119.9	120.9	122.1	124.8	127.2	129.5	105.4
30009	114.8	121.3	124.3	129.1	135.5	142.8	148.7	115.6	128.7	129.9	133.7	139.6	145.4	151.4	110.7
26008	112.2	120.7	125.4	130.1	138.7	145.7	153.6	112.8	125.4	133.1	135.5	142.8	150.3	158.8	114.9
30019	113.4	123.3	128.9	133.9	144.5	153.1	161.4	121.1	133.2	136.1	140.2	147.8	154.1	162.5	117.4
29012	154.1	161.4	163.3	165.9	170.5	176.1	181.1	153.1	169.5	171.2	175.3	181.6	187.8	194.1	156.2
28030	230.1	233.5	236.6	240.9	246.1	253.1	260.7	228.1	240.3	244.5	246.7	253.4	259.7	264.1	225.1
N1	230.1	246.3	256.3	259.2	262.9	269.9	275.1	241.2	258.7	262.2	265.6	271.1	276.5	281.7	238.4
24001	221.4	282.1	283.9	286.1	290.9	297.1	301.9	276.6	316.8	317.8	320.1	323.5	328.9	333.5	310.1
S14	738.7	791.1	795.5	800.1	804.9	808.7	815.5	780.2	798.4	799.7	802.1	807.9	812.4	816.8	788.1

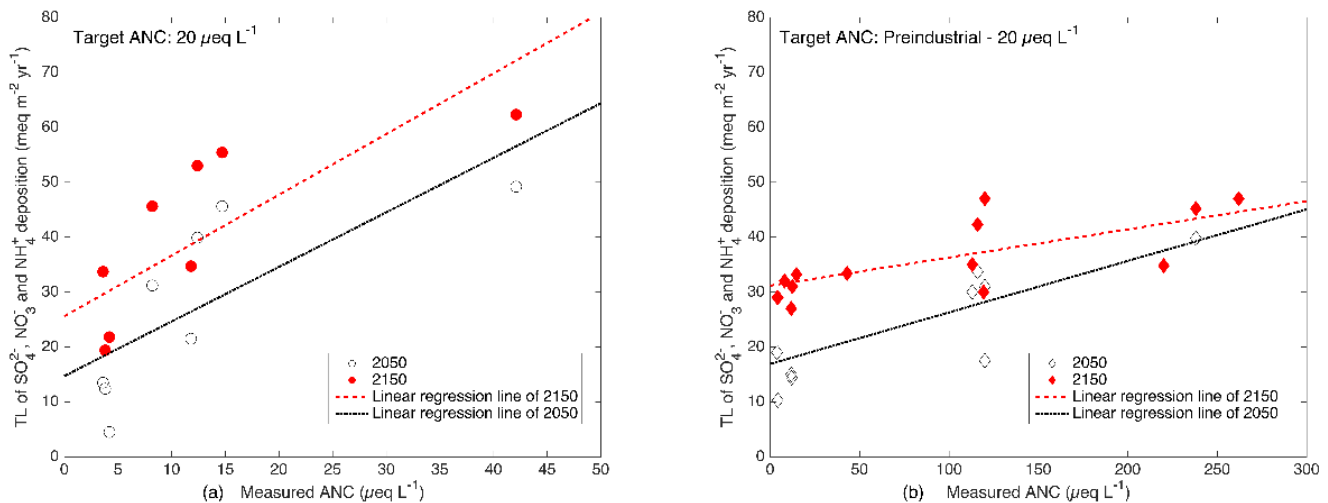
^a Scenario numbers are defined in Table 5.

3.5 ANC Criterion Values and Target Loads

Two types of ANC criteria were used as goals for stream recovery in the TLs analysis: a single fixed ANC criterion used for all sites and one based on the model simulated site-specific ANC (Table 10). A fixed $20 \mu\text{eq L}^{-1}$ ANC was selected to represent likely protection of brook trout health against elevated concentrations of Al_i . Simulations suggested that Adirondack streams may have had a range of preindustrial ANC values of 10 to $894 \mu\text{eq L}^{-1}$. The data further suggested that only one of the 25 modeled Adirondack streams had a preindustrial stream ANC below $20 \mu\text{eq L}^{-1}$. Others may have had preindustrial ANC above $20 \mu\text{eq L}^{-1}$ but have since acidified and are unable to recover to this level even if acidic deposition is eliminated in the future. In general, TL values were lower at sites that had lower ANC (Figure 9).

Figure 9. Target Loads (TLs) of SO_4^{2-} , NO_3^- , and NH_4^+ Deposition

The (left) TLs of SO_4^{2-} , NO_3^- , and NH_4^+ deposition ($\text{meq m}^{-2} \text{yr}^{-1}$) needed to achieve the ANC criterion of $20 \mu\text{eq L}^{-1}$ plotted against the mean of observed ANC for the years 2004-2005 for Adirondack streams (eight for year 2050 and nine for year 2150) that were able to reach $\text{ANC} = 20 \mu\text{eq L}^{-1}$ and (right) the TLs of the same deposition constituents needed to increase ANC to within 20meq L^{-1} of preindustrial ANC by the year 2150 (11 for year 2050 and 16 for year 2150).



The 25 modeled streams were grouped into three recovery classes based on whether they: (1) could achieve the ANC criterion without further load reductions; (2) could achieve the ANC criterion, but only with additional load reductions; or (3) were unable to attain the ANC criterion even if atmospheric deposition was decreased to preindustrial levels and then held there until the year 2200 (Table 10). For example, relatively insensitive streams like Archer Creek do not require any additional decrease in acidic deposition to achieve an ANC criterion of $20 \mu\text{eq L}^{-1}$. Overall, 13 and 14 streams of the 25 simulated did

not require additional decreases in acidic deposition to achieve the ANC criterion of $20 \mu\text{eq L}^{-1}$ by the years 2050 and 2150, respectively (Figure 10). However, model projections suggested that the highly sensitive stream T24 will not be able to achieve the ANC criterion of $20 \mu\text{eq L}^{-1}$ by 2150 even with a 100% reduction in SO_4^{2-} , NO_3^- , and NH_4^+ deposition (Tables 11 and 12). Note that seven and six streams in this study, like T24, could not attain the ANC criterion of $20 \mu\text{eq L}^{-1}$ by the years 2050 and 2150, respectively. These highly acid-sensitive and impacted watersheds are characterized by low rates of base cation supply from weathering. Many also experience elevated inputs of naturally occurring organic acids. Finally, some streams are recoverable with additional reductions in acidic deposition. For example, the south tributary of Buck Creek cannot achieve the ANC criterion of $20 \mu\text{eq L}^{-1}$ by the year 2150 without additional decreases in SO_4^{2-} , NO_3^- , and NH_4^+ deposition. However, recovery to the ANC criterion of $20 \mu\text{eq L}^{-1}$ by the year 2150 was simulated for this stream with an 18% reduction in SO_4^{2-} , NO_3^- , and NH_4^+ deposition (Table 10).

Table 10. Target Loads of SO₄²⁻ + NO₃⁻ + NH₄⁺ Deposition

Target loads of SO₄²⁻ + NO₃⁻ + NH₄⁺ deposition to reach ANC targets by 2050 and 2150 based upon PnET-BGC model simulations for 25 Adirondack study streams. ANC values are in µeq L⁻¹ and deposition values are in meq m⁻² yr⁻¹.

Sites	Preindustrial ANC (µeq L ⁻¹)	Measured ANC	Ambient Deposition	TL to Reach ANC Criterion of 20		TL to Reach Site Specific ANC Criterion	
				2050	2150	2050	2150
North Buck	22.8	-38.3	39.9	N/A ^a	N/A	N/A	N/A
35014	10.1	-35.2	47.3	N/A	N/A	N/A	N/A
27026	25.5	-27.1	41.4	N/A	N/A	N/A	N/A
T24	28.7	-25.3	40.3	N/A	N/A	N/A	N/A
22019	23.4	-16.2	47.7	N/A	N/A	N/A	18.1
12003	28.2	-6.4	46.1	N/A	8.8	22.6	34.6
WF	25.9	-3.7	41.4	N/A	N/A	21.1	36.5
South Buck	53.2	3.6	41.1	13.5	33.7	N/A	N/A
13008	38.4	3.8	44.2	12.4	19.4	19.0	29.2
24002	37.3	4.2	41.1	4.5	21.8	10.3	28.7
28011	52.6	8.2	42.2	31.2	45.6	N/A	32.1
28014	51.8	11.8	39.9	28.6	34.7	15.2	27.1
NW	56.5	12.4	39.9	45.1	53.0	14.4	31.1
Buck Creek	56.3	14.7	42.6	41.3	55.4	N/A	33.2
AMP	93.1	42.1	37.5	49.2	62.3	N/A	33.4
27019	160.6	95.7	41.8	WB ^b	WB	N/A	N/A
Archer	148.8	113.0	39.1	WB	WB	29.3	35.2
30009	155.8	116.5	48.1	WB	WB	33.7	42.5
26008	163.2	119.3	42.6	WB	WB	17.5	29.8
30019	163.8	119.8	50.0	WB	WB	31.1	WB
29012	218.3	164.1	52.8	WB	WB	WB	WB
28030	271.6	219.3	42.6	WB	WB	WB	34.8
N1	285.1	238.0	37.5	WB	WB	39.8	45.2
24001	336.8	262.2	42.6	WB	WB	WB	46.9
S14	894.1	619.4	36.4	WB	WB	WB	WB

^a N/A indicates that there is no applicable TL because past base cation depletion is not sufficiently reversible in the model to achieve recovery to preindustrial conditions.

^b WB indicates that the TL is not a useful statistic because the site is so well buffered.

Figure 10. Expectation for Modeled Streams to Attain ANC Criteria

Number of modeled streams (out of 25) expected to attain the ANC criterion of $20 \mu\text{eq L}^{-1}$ (left panel) and the pre-industrial minus 20 ANC $20 \mu\text{eq L}^{-1}$ criterion (right panel) by the years 2050 and 2150 as a result of decreasing ambient atmospheric SO_4^{2-} , NO_3^- , and NH_4^+ deposition.

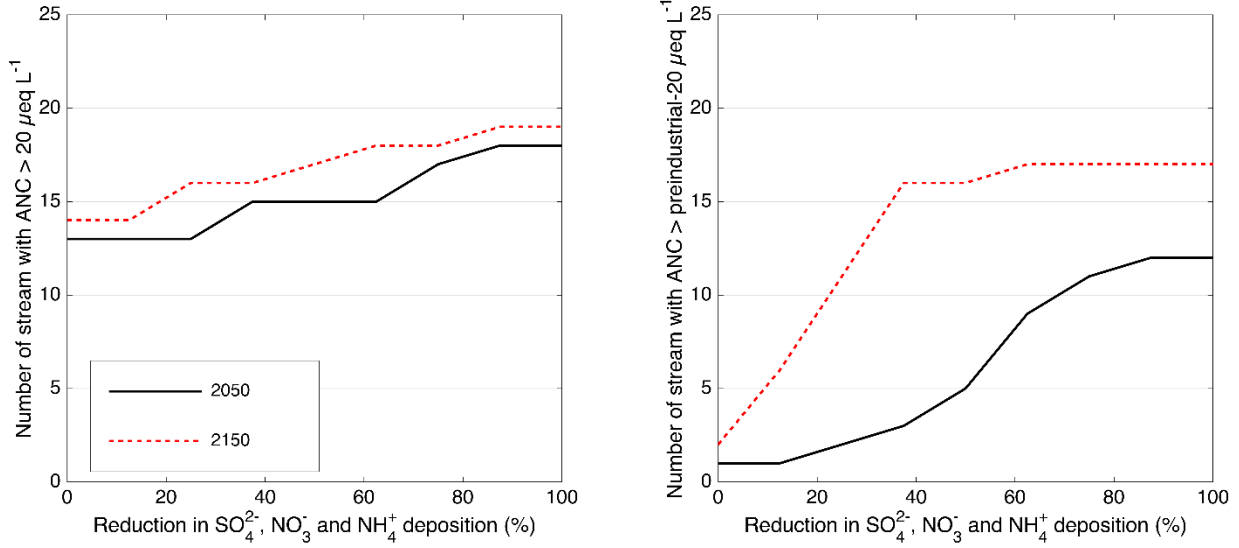


Table 11. Modeled Stream Recovery Classes for Target ANC = 20 µeq L⁻¹

Site <u>Target ANC = 20 µeq L⁻¹</u>	Site could achieve ANC criterion without additional deposition reduction		Site could achieve ANC criterion only with additional deposition reduction		Site unable to achieve ANC criterion under decreases in deposition to preindustrial levels	
	Year 2050	Year 2150	Year 2050	Year 2150	Year 2050	Year 2150
North Buck					X	X
35014					X	X
27026					X	X
T24					X	X
22019					X	X
12003				X	X	
WF					X	X
South Buck			X	X		
13008			X	X		
24002			X	X		
28011		X	X			
28014			X	X		
NW	X	X				
Buck Creek	X	X				
AMP	X	X				
27019	X	X				
Archer	X	X				
30009	X	X				
26008	X	X				
30019	X	X				
29012	X	X				
28030	X	X				
N1	X	X				
24001	X	X				
S14	X	X				

Table 12. Modeled Stream Recovery Classes for Site-Specific Target ANC

Site Target ANC = Site-Specific	Site could achieve ANC criterion without additional further deposition reduction		Site could achieve ANC criterion only with additional further deposition reduction		Site unable to achieve ANC criterion under decreases in deposition to preindustrial level	
	Year 2050	Year 2150	Year 2050	Year 2150	Year 2050	Year 2150
North Buck					X	X
35014					X	X
27026					X	X
T24					X	X
22019				X	X	
12003			X	X		
WF			X	X		
South Buck					X	X
13008			X	X		
24002			X	X		
28011				X	X	
28014			X	X		
NW			X	X		
Buck Creek				X	X	
AMP				X	X	
27019					X	X
Archer			X	X		
30009			X	X		
26008			X	X		
30019			X	X		
29012					X	X
28030				X	X	
N1	X	X				
24001		X	X			
S14					X	X

3.6 Biological Responses

Contemporaneous stream chemistry and fish-survey data collected during the period 2014–2016 and used in this analysis are described in detail by Baldigo et al. (2019a) and George and Baldigo (2018). The original response equations and figures for total fish community richness, density, and biomass, and for density and biomass of brook trout populations, which are summarized herein, were taken from Baldigo et al. (2019b). Significant logistic equations describing the probability of observing one, two, three...eight or more fish species in all surveys indicated that ANC (Figure 11A), pH (Figure 12A), and Al_i (Figure 13A) explained from 6.7 to 33.0% of the deviance in the data by the various models (Baldigo et al. 2019b). The equations for richness ≥ 1 and ≥ 2 species were suitable for predicting the response of fish communities to changes in stream acid-base chemistry given that streams with Al_i concentrations < 1 and $< 2 \mu\text{mol L}^{-1}$ had an average of two species (Baldigo et al. 2019a). Because the Al_i equation for ≥ 1 species explained 33.0% of the deviance, and the equation for ≥ 2 species explained 9.6% of the deviance, the first would be most effective in assessing community responses to changes in stream acidity.

Significant logistic equations describing the probability of observing fish densities $> \text{zero}$, > 100 , > 200 ... > 1000 fish per 0.1 ha in communities from all surveys showed that ANC (Figure 11B), pH (Figure 12B), and Al_i (Figure 13B) explained from 8.1 to 35.7% of the deviance in the data from the various models (Baldigo et al. 2019b). The ANC, pH, and Al_i response curves and corresponding equations for total density > 400 fish per 0.1 ha would be suitable for predicting the response of fish communities to changes in acid-base chemistry of streams, given that streams with Al_i concentrations $< 1.0 \mu\text{mol L}^{-1}$ had an average density of 444.2 fish per 0.1 ha and those with Al_i concentrations $< 2.0 \mu\text{mol L}^{-1}$ had an average density of 391.8 fish per 0.1 ha (Baldigo et al. 2019a). The ANC equation for > 400 fish per 0.1 ha accounted for 21.9% of the deviance, whereas the Al_i equation for > 400 fish per 0.1 ha only accounted for 8.1% of the deviance (Baldigo et al. 2019b). The Al_i equation for > 100 fish per 0.1 ha accounted for the most (35.7%) deviance and was, therefore, slightly preferred over the other two response curves. All three density-response curves would be effective in assessing expected community responses to changes in stream acidity.

Significant logistic equations describing the probability of observing biomass >zero, >100, >200...>3000 g per 0.1 ha in communities from all surveys indicated that ANC (Figure 11C), pH (Figure 12C), and Al_i (Figure 13C) explained from 8.5 to 33.0% of the deviance in data as represented by various models (Baldigo et al. 2019b). The ANC, pH, and Al_i response curves and corresponding equations for total biomass >1500 g per 0.1 ha would be suitable for predicting the response of fish communities to changes in acid-base chemistry of streams given that streams with Al_i concentrations <1 $\mu\text{mol L}^{-1}$ had average biomass of 1924.4 g per 0.1 ha and those with Al_i concentrations <2 $\mu\text{mol L}^{-1}$ had an average biomass of 1742.2 g per 0.1 ha (Baldigo et al. 2019a). The ANC equation for >1500 fish per 0.1 ha accounted for 29.2% of the deviance, whereas the Al_i equation for >1500 fish per 0.1 ha accounted for 19.1% of the deviance (Baldigo et al. 2019b). Thus, both biomass-response curves would be effective in assessing community responses to changes in stream acidity.

Figure 11. Logistic Curves (Example 1) Describing the Probability of Observing Richness, Density, and Biomass in Fish Communities

The logistic curves describe the probability of observing (A) richness from one to eight or more fish species, (B) density of more than zero to 1000 fish per 0.1 ha, and (C) biomass of more than zero to 3000 g per 0.1 ha in fish communities as a function of summer baseflow ANC in 47 headwater streams of the western Adirondack Mountains sampled during 2014–2016 (from Baldigo et al. 2019b). The dashed lines denote logistic equations that are not significant at 95% confidence ($P > 0.05$).

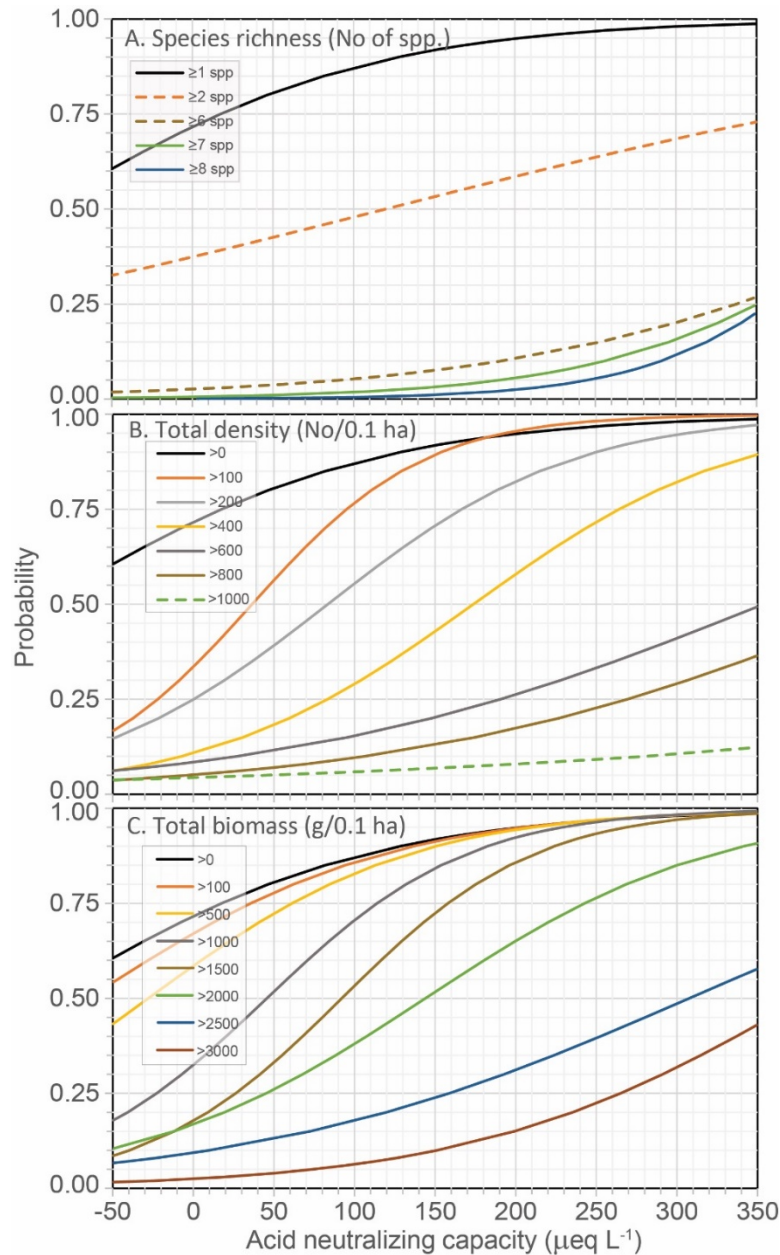


Figure 12. Logistic Curves (Example 2) Describing the Probability of Observing Richness, Density, and Biomass in Fish Communities

The logistic curves describe the probability of observing (A) richness from one to eight or more species, (B) density of more than zero to 800 fish per 0.1 ha, and (C) biomass of more than zero to 3000 g per 0.1 ha in fish communities as a function of summer baseflow pH in 47 headwater streams of the western Adirondack Mountains sampled during 2014–2016 (from Baldigo et al. 2019b). The dashed lines denote logistic equations that are not significant at 95% confidence ($P > 0.05$).

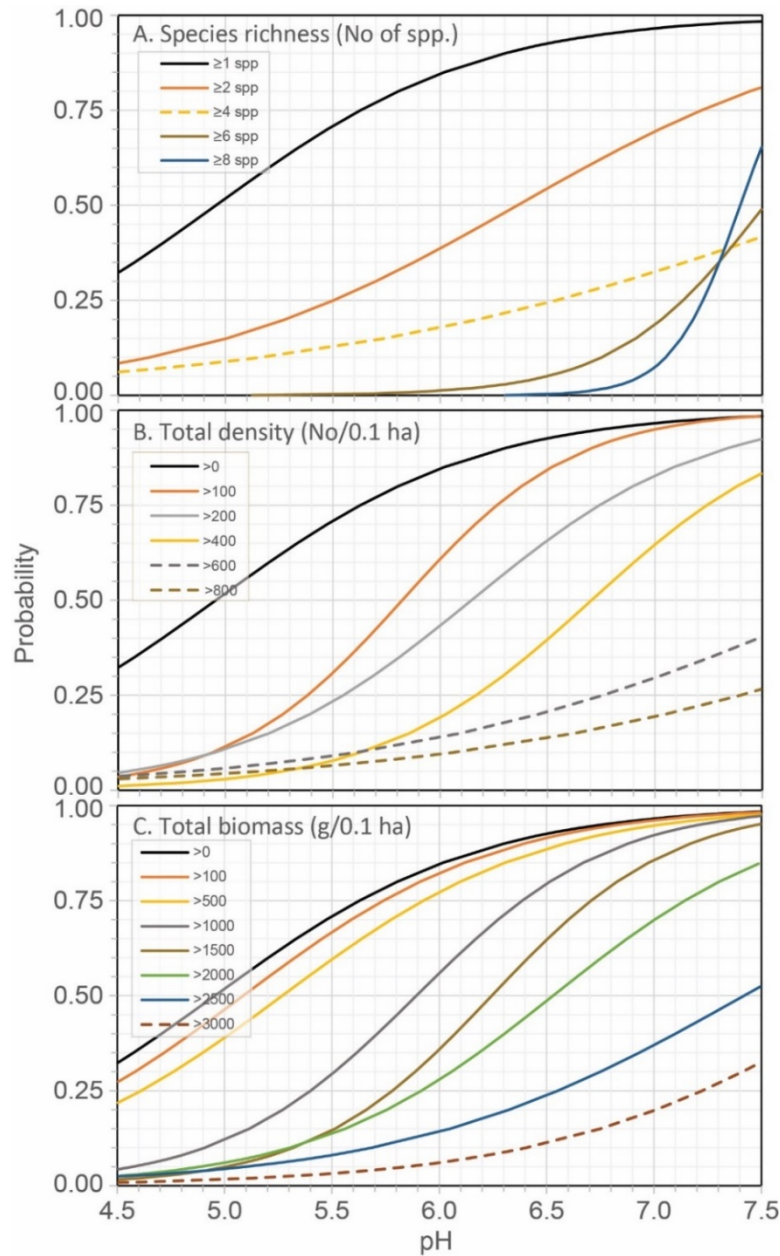
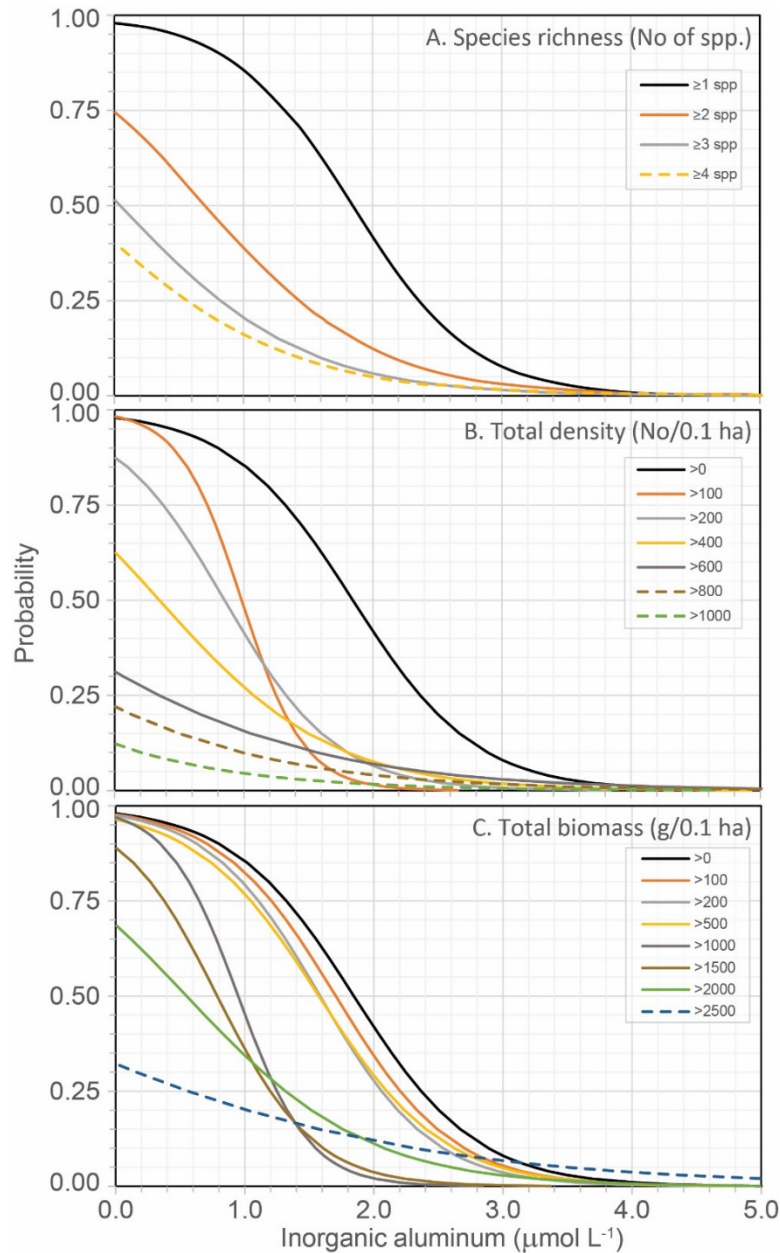


Figure 13. Logistic Curves (Example 3) Describing the Probability of Observing Richness, Density, and Biomass in Fish Communities

The logistic curves describe the probability of observing (A) richness from one to four or more species, (B) density of more than zero to 1000 fish per 0.1 ha, and (C) biomass of more than zero to 2500 per 0.1 ha in fish communities as a function of summer baseflow Ali in 47 headwater streams of the western Adirondack Mountains sampled during 2014–2016 (from Baldigo et al. 2019b). The dashed lines denote logistic equations that are not significant at 95% confidence ($P > 0.05$).



Significant logistic equations describing the probability of observing densities of brook trout populations >zero, >100, >200...>1000 fish per 0.1 ha in all surveys indicated that ANC (Figure 14A), pH (Figure 15A), and Al_i (Figure 16A) explained 6.7 to 28.5% of the deviance in data from various models (Baldigo et al. 2019b). The ANC, pH, and Al_i response curves and corresponding equations for brook trout density >200 fish per 0.1 ha would be suitable for predicting fish responses to changes in acid-base chemistry, given that streams with Al_i concentrations $<1 \mu\text{mol L}^{-1}$ had an average density of 280.8 fish per 0.1 ha and those with Al_i concentrations $<2 \mu\text{mol L}^{-1}$ had an average density of 244.6 fish per 0.1 ha (Baldigo et al. 2019a). The ANC equation for >200 fish per 0.1 ha accounted for 20.7% of the deviance, whereas the Al_i equation for >100 fish per 0.1 ha accounted 28.5% of the deviance (Baldigo et al. 2019b). The Al_i equation for >0 fish per 0.1 ha accounted for 26.3% of the deviance, and the pH equation for >100 fish per 0.1 ha accounted for 28.5% of the deviance. Thus, the Al_i and pH equations could predict population responses slightly better than ANC. All four brook trout density-response curves would be effective in assessing population responses to changes in stream acidity.

Significant logistic equations describing the probability of observing biomass of brook trout populations >zero, >100, >200...>1000 g per 0.1 ha in all surveys indicated that ANC (Figure 14B), pH (Figure 15B), and Al_i (Figure 16B) explained from 9.3 to 26.3% of the deviance in data from the various models (Baldigo et al. 2019b). The ANC, pH, and Al_i response curves and equations for brook trout biomass >1000 g per 0.1 ha would be most suitable for predicting their response to changes in acid-base chemistry given that streams with Al_i concentrations $<1 \mu\text{mol L}^{-1}$ had average biomass of 1384.0 g per 0.1 ha and those with Al_i concentrations $<2 \mu\text{mol L}^{-1}$ had average biomass of 1236.6 g per 0.1 ha (Baldigo et al. 2019a). The Al_i brook trout biomass equation for >1000 g per 0.1 ha accounted for 16.6% of the deviance, whereas the Al_i equation for >0 g per 0.1 ha accounted 26.3% of the deviance (Baldigo et al. 2019b). The ANC and pH equations for >1000 g per 0.1 ha accounted for 11.7 and 13.7% of the deviance, respectively. Thus, these equations could predict population responses (to densities >1000 g per 0.1 ha) nearly as well as Al_i . All four brook trout biomass-response curves would be effective in assessing population responses to changes in stream acidity.

Figure 14. Logistic Curves (Example 4) Describing the Probability of Observing Density and Biomass in Brook Trout Populations

The logistic curves describe the probability of observing (A) density of zero to 1000 or more brook trout per 0.1 ha and (B) biomass of more than zero to 2500 g per 0.1 ha in brook trout populations as a function of summer baseflow ANC in 47 headwater streams of the western Adirondack Mountains of New York sampled during 2014–2016 (from Baldigo et al. 2019b). The dashed lines denote logistic equations that are not significant at 95% confidence ($P > 0.05$).

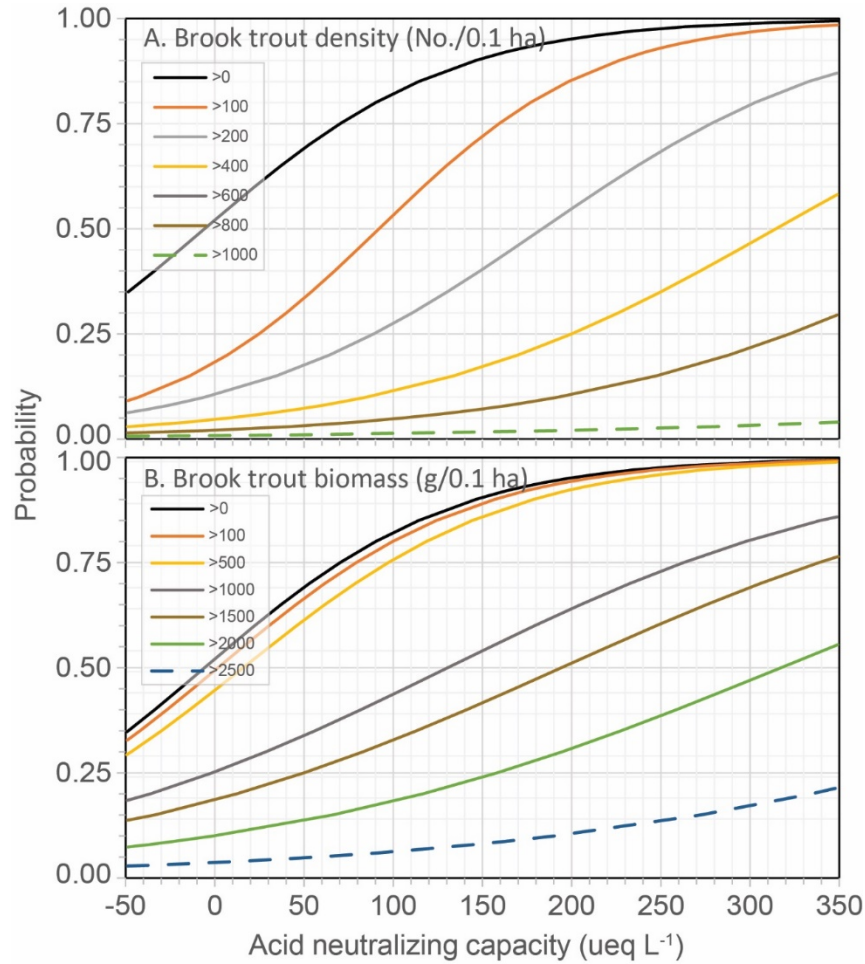


Figure 15. Logistic Curves (Example 5) Describing the Probability of Observing Density and Biomass in Brook Trout Populations

The logistic curves describe the probability of observing (A) density of zero to 800 or more brook trout per 0.1 ha and (B) biomass of more than zero to 2500 g per 0.1 ha in brook trout populations as a function of summer baseflow pH in 47 headwater streams of the western Adirondack Mountains sampled during 2014–2016 (from Baldigo et al. 2019b). The dashed lines denote logistic equations that are not significant at 95% confidence ($P > 0.05$).

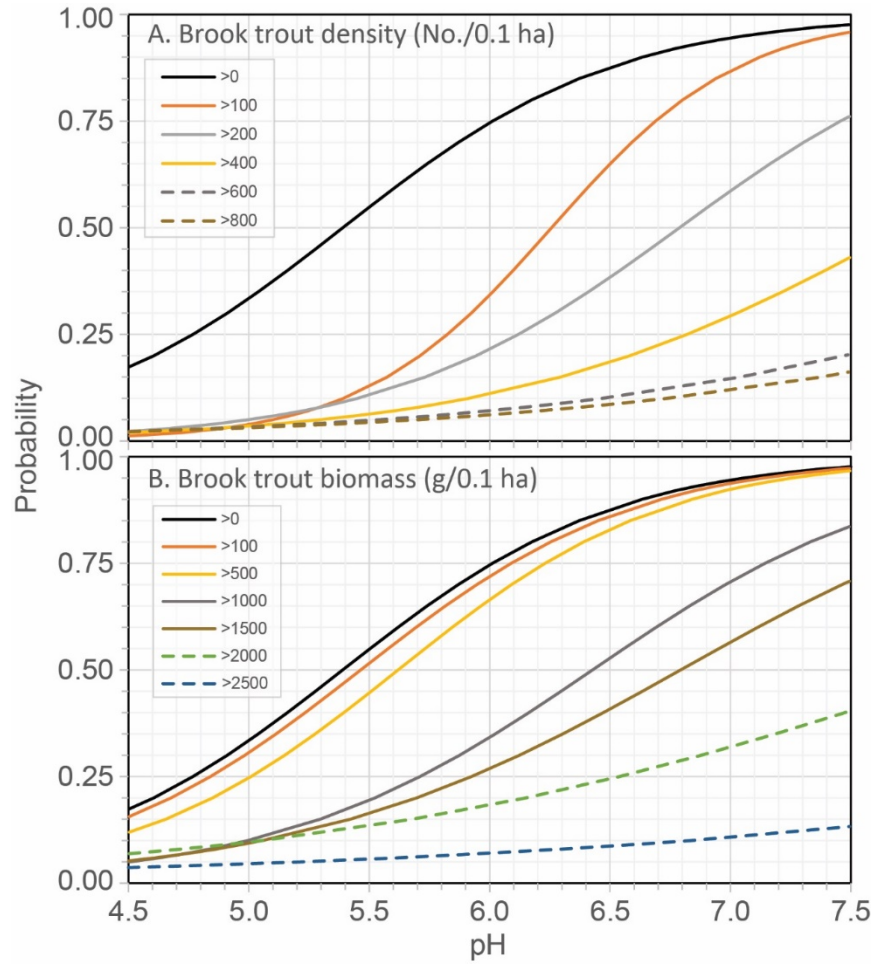
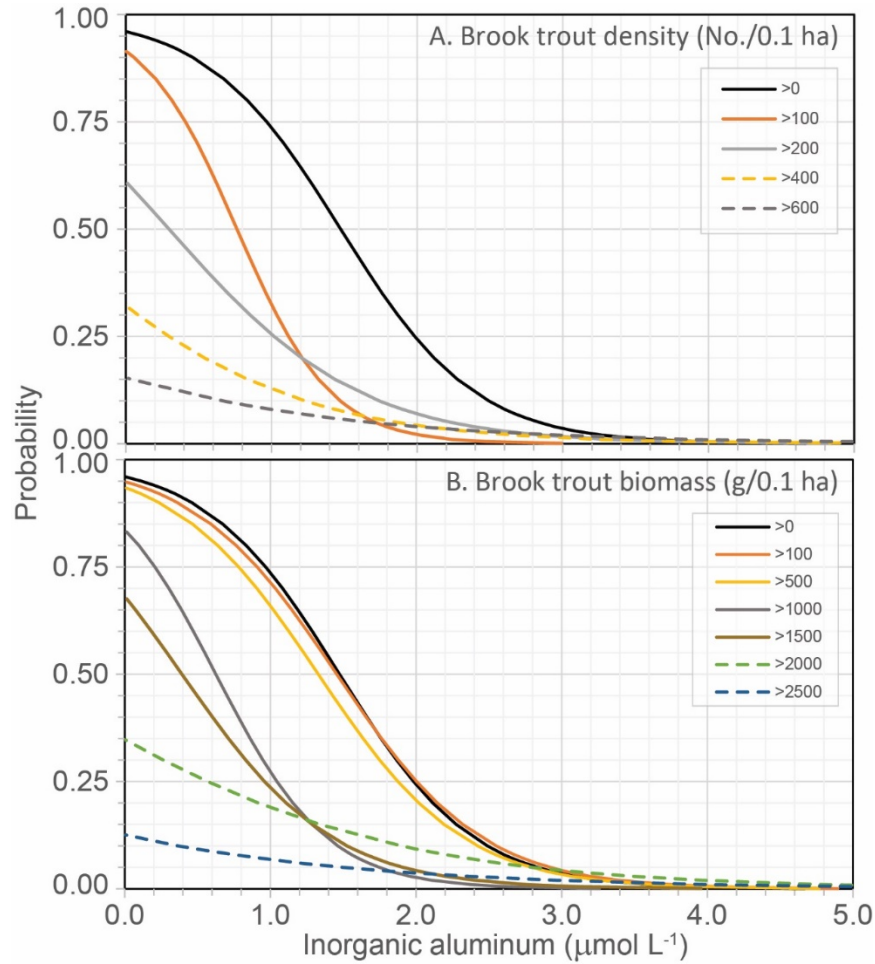


Figure 16. Logistic Curves (Example 6) Describing the Probability of Observing Density and Biomass in Brook Trout Populations

The logistic curves describe the probability of observing (A) density of zero to 600 or more fish per 0.1 ha and (B) biomass of more than zero to 2500 g per 0.1 ha in brook trout populations as a function of summer baseflow Al_i in 47 headwater streams of the western Adirondack Mountains sampled during 2014–2016 (from Baldigo et al. 2019b). The dashed lines denote logistic equations that are not significant at 95% confidence ($P > 0.05$).



3.7 Influence of Discharge on Stream Chemistry

Estimates of Q_{percent} for the set of ANC values used in PnET-BGC model calibration are provided in Table 13. These values for the 25 modeled streams were greater than 50% with only four exceptions, indicating that model calibration was generally performed for samples collected during moderate to moderately high-flow conditions. At four sites, a low-flow ANC value was used in calibration. Because of this intended bias towards model calibration with relatively high-flow stream chemistry at most sites, there were few large differences in ANC between calibration values and estimates of ANC at high flow (Q_{85}) for each modeled site. At 18 of the 25 PnET-BGC modeled streams, the difference between the model-calibrated ANC and the high-flow ANC was less than $25 \mu\text{eq L}^{-1}$. At the seven streams where these differences in ANC were greater than $25 \mu\text{eq L}^{-1}$, there were two principal driving factors. First, because the change in ANC with discharge increases as ANC increases, five sites where model-calibrated ANC values were greater than $100 \mu\text{eq L}^{-1}$ also had ANC differences at high flow of greater than $25 \mu\text{eq L}^{-1}$. Second, three sites where model-calibrated Q_{percent} values were less than 15% also had ANC differences that exceeded $25 \mu\text{eq L}^{-1}$, highlighting the strong differences that may arise between ANC values that reflect episodic acidification and modeled ANC when calibration is performed with samples that reflect low-flow ANC values. We believe that this is the first stream assessment that has pointed to the importance of considering the flow conditions that are reflected by the ANC measurements used in scenario and TL model calibration, and how results may change when ANC values that reflect episodic acidification are considered.

Table 13. ANC Values Used in PnET-BGC Model Calibration and the Estimated ANC Values for Q₈₅

Comparison of the ANC values used in PnET-BGC model calibration and the estimated ANC values for Q₈₅ for each of the 25 modeled streams. Model Site IDs correspond with IDs shown in the Descriptive Text column of the table in appendix F.

Model Site ID	USGS Site ID	Q_{percent}	ANC ($\mu\text{eq L}^{-1}$)	ANC for Q₈₅ ($\mu\text{eq L}^{-1}$)	Difference ($\mu\text{eq L}^{-1}$)
North Buck Creek	04253295	63.4	-42.0	-46.8	-4.8
35014	432910075001001	79.2	-35.2	-36.2	-1.0
27026	434154074445701	74.5	-27.1	-27.0	+0.1
T24	0134277112	55.1	-24.3	-42.0	-17.7
22019	435115075093901	75.4	-16.2	-19.7	-3.5
12003	440151075084801	62.4	-3.8	-9.7	-5.9
WF	434816074494201	10.4	-3.7	-19.2	-15.5
South Buck Creek	04253294	63.4	9.5	-2.2	-11.7
13008	440201075053401	73.0	3.8	-1.7	-5.5
24002	434544074411101	71.7	4.2	-6.4	-10.6
28011	433918074403501	74.5	8.2	-9.7	-1.5
28014	433820074410001	83.6	14.8	14.2	-0.6
NW	434836074030201	3.6	12.4	-16.1	-28.5
Buck Creek	04253296	63.4	16.6	4.9	-11.7
AMP	441424074155501	11.5	42.1	-3.1	-45.2
27019	434256074453801	83.0	112.4	103.3	-9.1
Archer Creek	435937074144301	57.0	111.1	97.7	-13.4
30009	433553075062101	82.0	118.2	109.9	-8.3
26008	434001075045401	83.6	115.9	113.2	-2.7
30019	433548075110101	63.8	119.7	55.3	-64.4
29012	433324075165001	83.0	158.3	151.6	-6.7
28030	434500074441601	63.4	226.2	176.7	-49.5
N1	440034074184801	11.5	238.0	64.7	-173.3
24001	434606074424901	71.7	262.2	209.7	-52.5
S14	NA	54.1	784.9	712.1	-72.8

3.8 Regionalization

Regionalization of simulation results was accomplished using linear regression, whereby the TLs generated by PnET-BGC were estimated from watershed and stream condition variables. Each of the five linear regression models with lowest AIC for predicting the four types of TLs were essentially equivalent based on AIC (i.e., $\Delta AIC < 2$). The three predictors most commonly selected across all models ($n = 20$) were current ANC, latitude, and longitude. Although other predictors, such as current deposition, elevation, and soil percent silt, were also often selected (see appendix H), the final set of predictor variables was constrained to three due to the relatively small sample size. The regression models used for extrapolating TLs from the PnET-BGC model sites to the broader landscape were specified as follows:

Equation 6

$$TL_{ANC=20, \text{Year } 2050} = 2470.74 + 0.635 * \text{Current ANC} - 16.365 * \text{Latitude} + 23.233 * \text{Longitude}$$

Equation 7

$$TL_{ANC=20, \text{Year } 2150} = 2634.44 + 0.901 * \text{Current ANC} - 22.836 * \text{Latitude} + 21.526 * \text{Longitude}$$

Equation 8

$$TL_{ANC\text{site-specific}, \text{Year } 2050} = -1025.86 + 0.152 * \text{Current ANC} + 8.726 * \text{Latitude} - 8.715 * \text{Longitude}$$

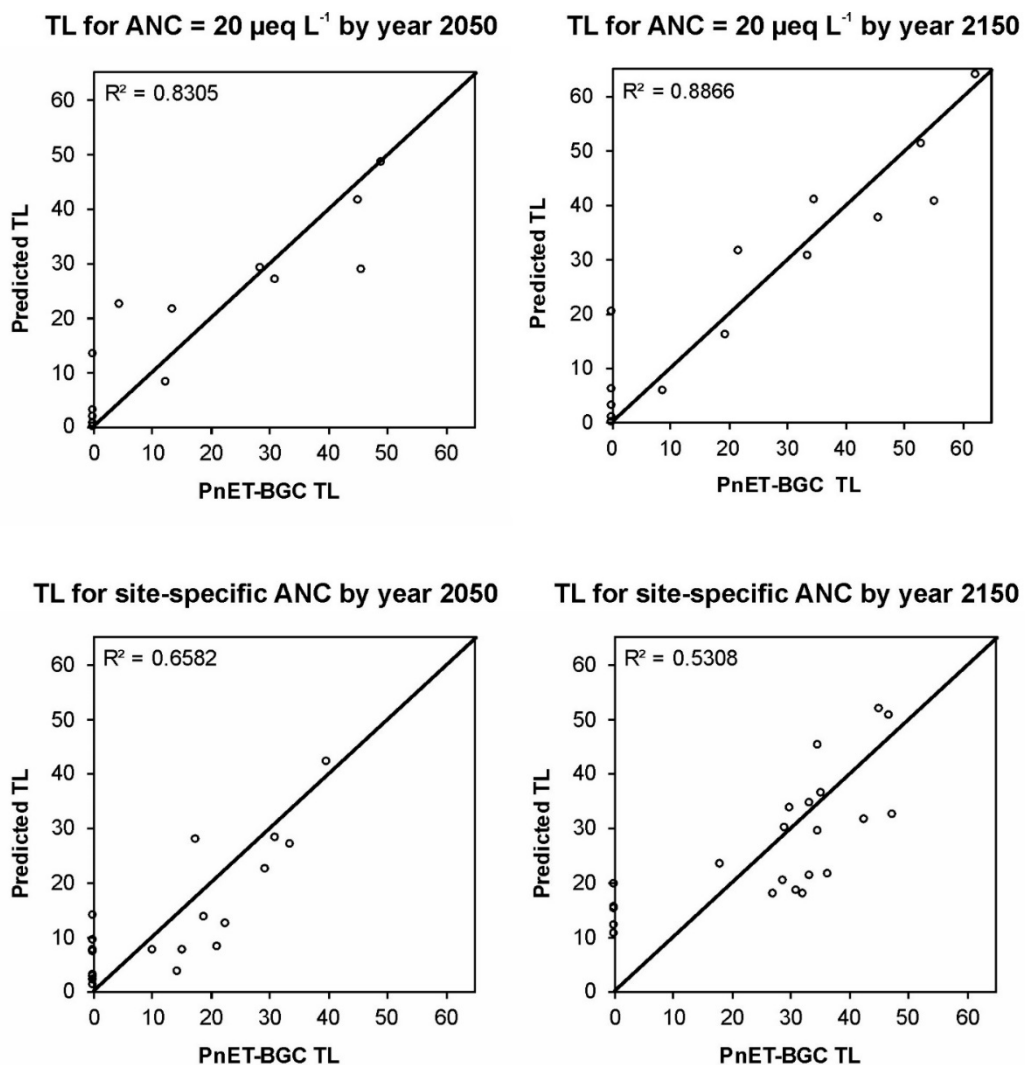
Equation 9

$$TL_{ANC\text{site-specific}, \text{Year } 2150} = -1615.34 + 0.115 * \text{Current ANC} + 26.771 * \text{Latitude} - 6.206 * \text{Longitude}$$

Regression models were more successful for predicting TLs for achieving $ANC = 20 \mu\text{eq L}^{-1}$ than for the site-specific TLs (Figure 17; appendix H). More than 80% of the variation was explained for the TL models intended to attain the fixed ANC criterion, as opposed to 65% and 53% for the TLs to attain site-specific ANC by year 2050 and 2150, respectively.

Figure 17. Comparison of Modeled (PnET-BGC) and Statistical Predictions for Target Loads (TLs) Based on Current ANC and Geographic Location

TL units are $\text{meq m}^{-2} \text{yr}^{-1}$. Negative predictions were set to zero on these plots.



Application of the TL regression models to the WECASS sites indicated that TLs below 40 $\text{meq m}^{-2} \text{yr}^{-1}$ (a low deposition value which is equivalent to 3 $\text{kg N ha}^{-1} \text{yr}^{-1}$ and 3 $\text{kg S ha}^{-1} \text{yr}^{-1}$) occur throughout the Adirondack region (Figures 18 and 19). Regional TLs for attaining site-specific ANC were generally lower and resource recovery was slower than those for attaining ANC = 20 $\mu\text{eq L}^{-1}$. Target load exceedance followed similar patterns to TL (Figures 20 and 21).

Figure 18. Spatial Representation of Predicted TL (Example 1)

Spatial representation for the Adirondack Park of predicted Target Load (TL) for attaining ANC = 20 $\mu\text{eq L}^{-1}$ (left) and site-specific ANC (right) at WECASS sites by year 2050 (top panels); grid cell extrapolation of TL results (middle and bottom panels). The site-specific scenarios (right side of graphic) were based on achieving PnET-BGC estimates of preindustrial ANC minus 20 $\mu\text{eq L}^{-1}$.

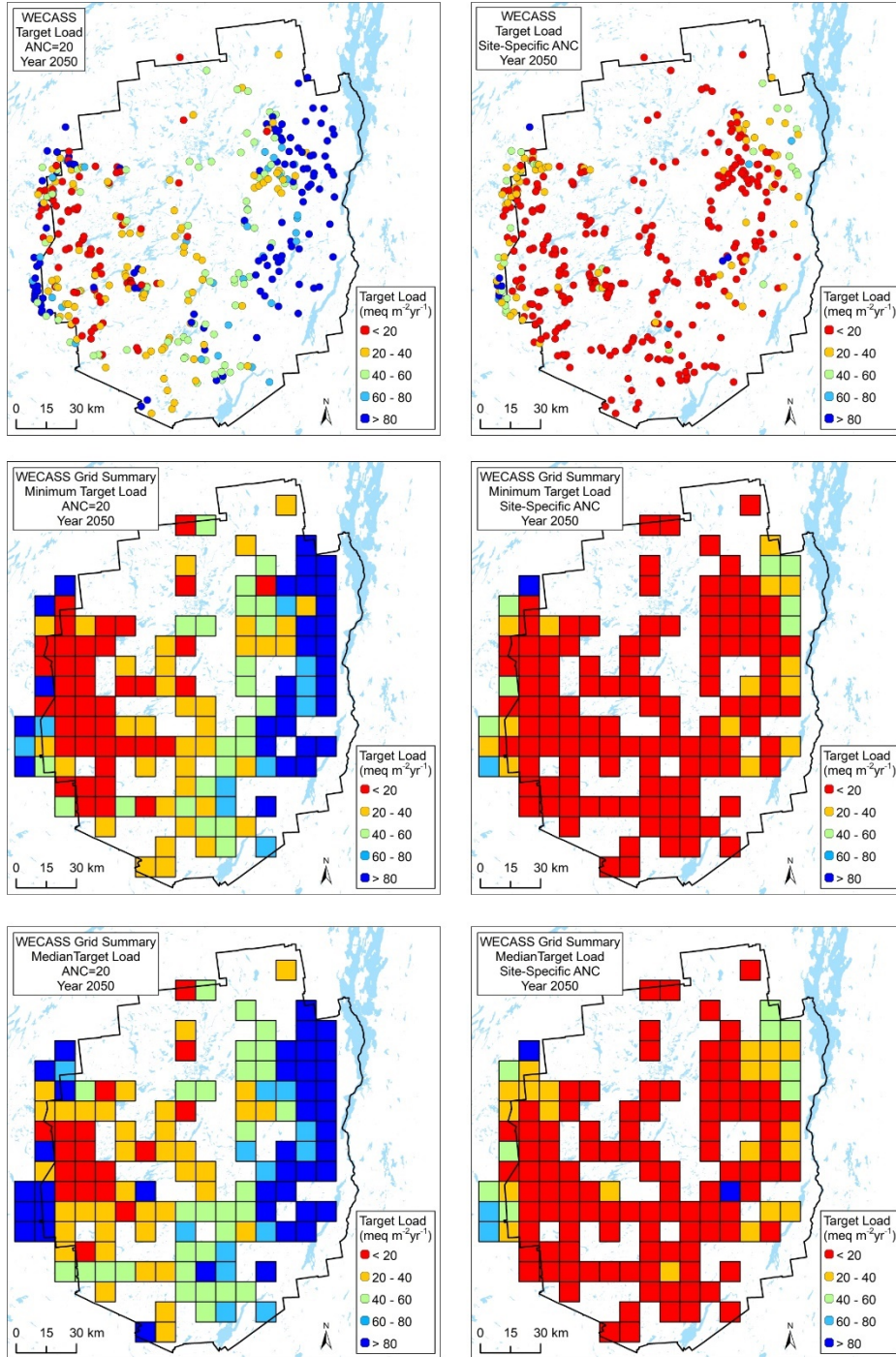


Figure 19. Spatial Representation of Predicted TL (Example 2)

Spatial representation of predicted TL for attaining ANC = 20 $\mu\text{eq L}^{-1}$ (left) and site-specific ANC (right) at WECASS sites by year 2150 (top panels); grid cell extrapolation of TL results (middle and bottom panels). The site-specific scenarios (right side of graphic) were based on achieving PnET-BGC estimates of preindustrial ANC minus 20 $\mu\text{eq L}^{-1}$.

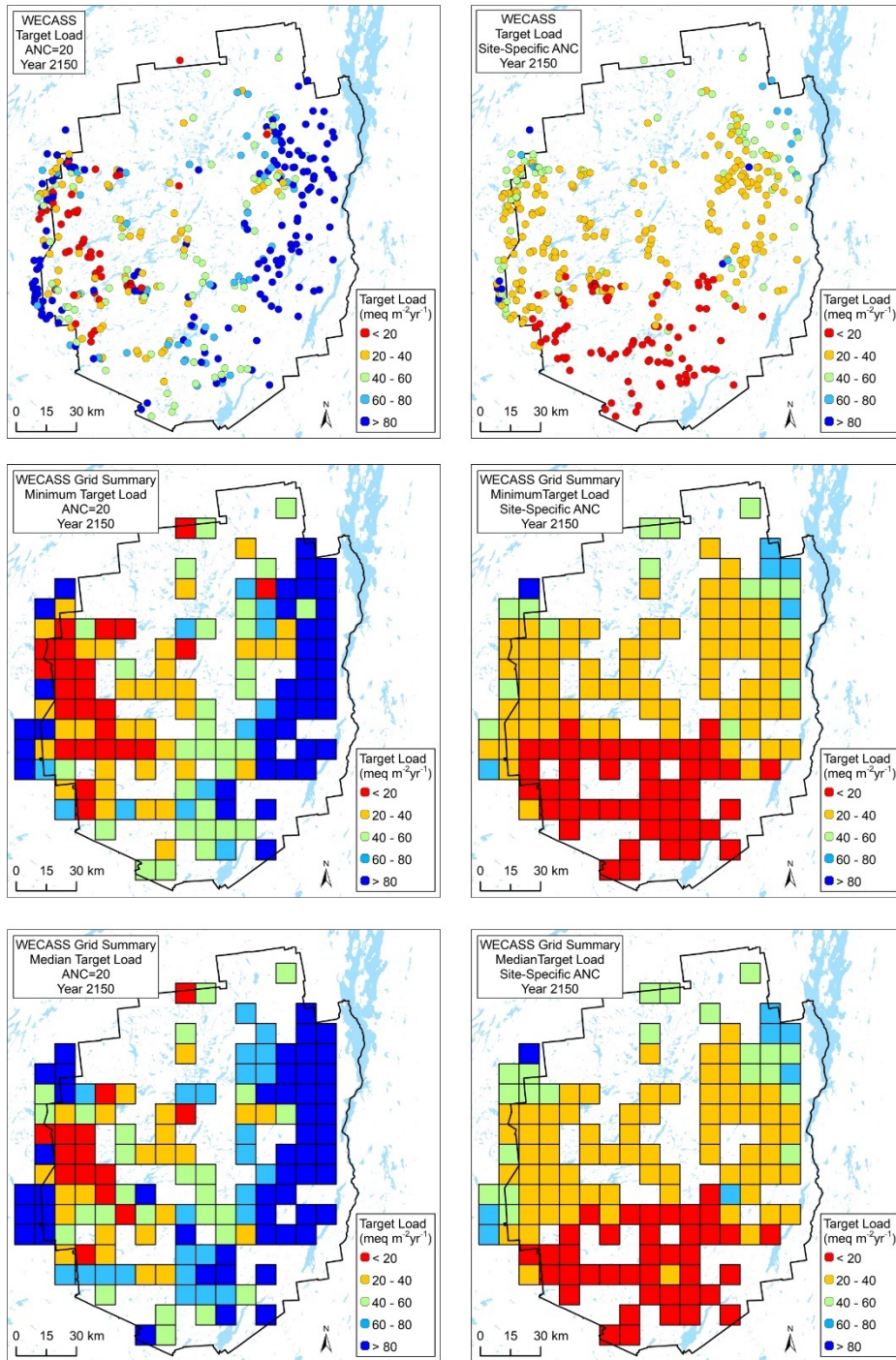


Figure 20. Spatial Representation of Exceedance of TL (Example 1)

Spatial representation of exceedance of TL for attaining ANC = 20 $\mu\text{eq L}^{-1}$ (left) and site-specific ANC (right) at WECASS sites by year 2050 (top panels); grid cell extrapolation of TL results (middle and bottom panels). The site-specific scenarios (right side of graphic) were based on achieving PnET-BGC estimates of preindustrial ANC minus 20 $\mu\text{eq L}^{-1}$.

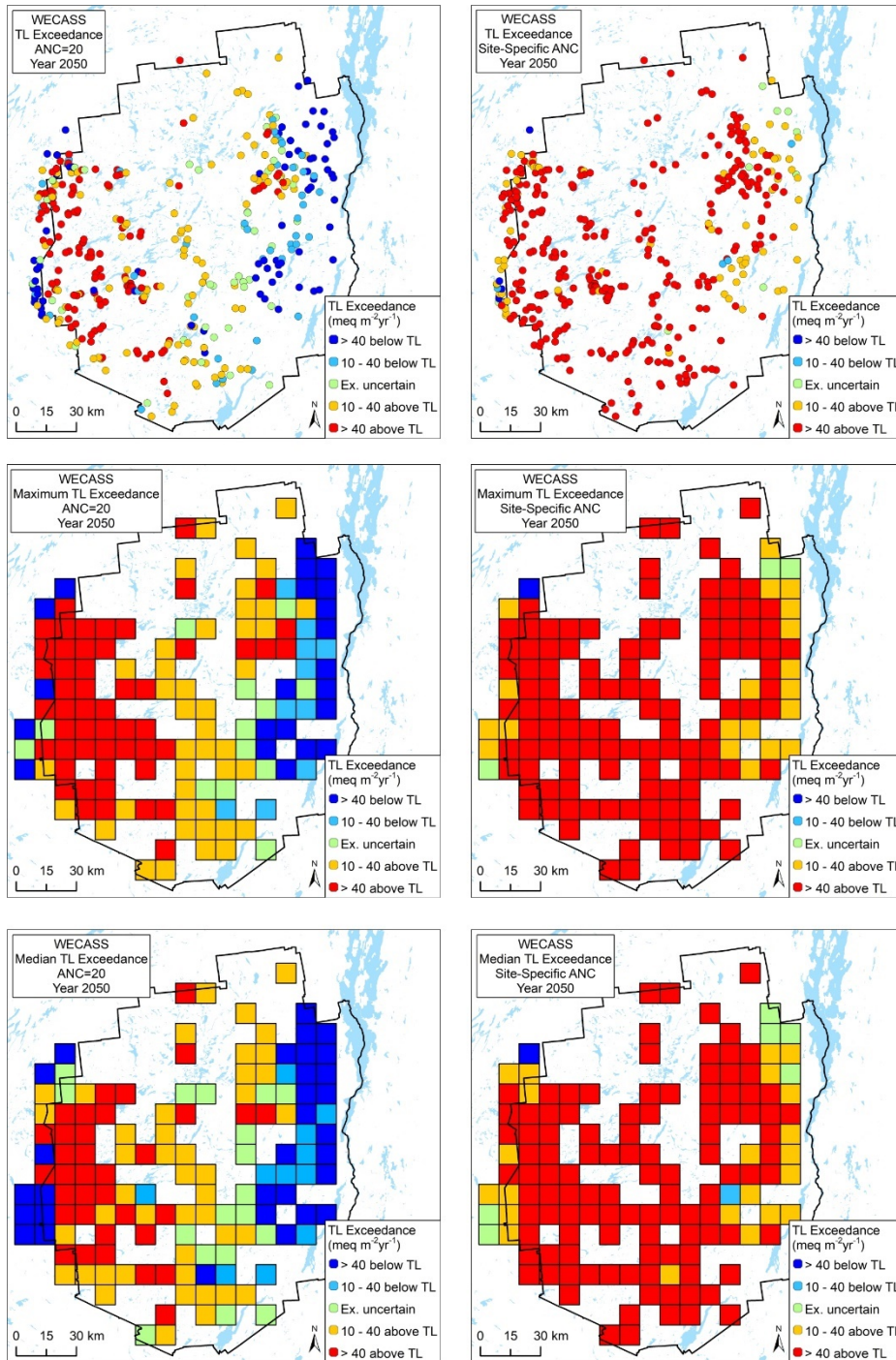
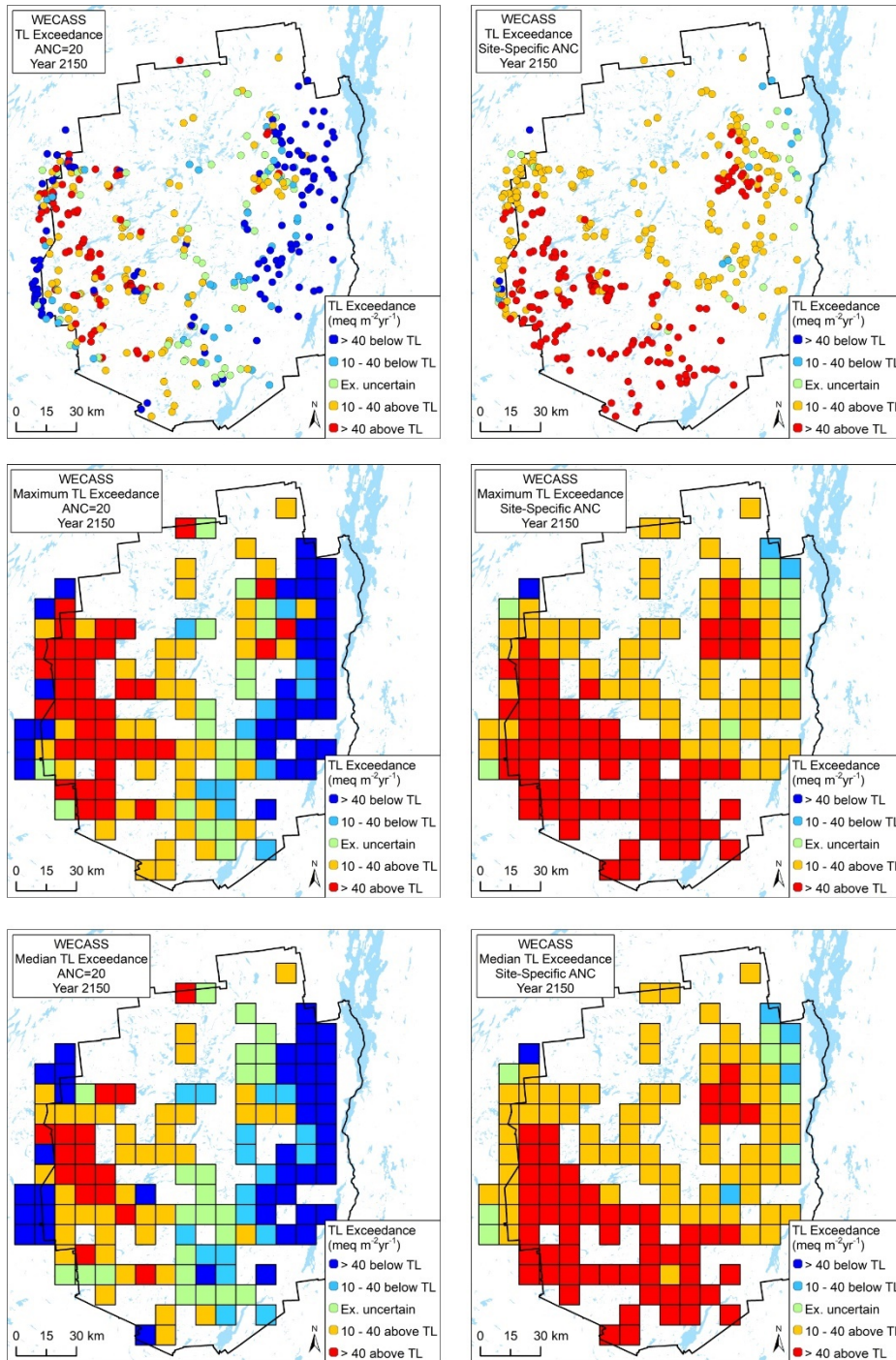


Figure 21. Spatial Representation of Exceedance of TL (Example 2)

Spatial representation of exceedance of TL for attaining ANC = 20 $\mu\text{eq L}^{-1}$ and site-specific ANC at WECASS sites by year 2150 (top panels); grid cell extrapolation of TL results (middle and bottom panels). The site-specific scenarios (right side of graphic) were based on achieving PnET-BGC estimates of preindustrial ANC minus 20 $\mu\text{eq L}^{-1}$.



4 Discussion

4.1 Stream Chemistry Simulations

Model simulations yielded projections of long-term changes in stream chemistry from the preindustrial period (1850) to the year 2200. Historical patterns in SO_4^{2-} coincided with increases in atmospheric S deposition at the start of the Industrial Revolution, followed by decreases in atmospheric deposition associated with controls on SO_2 emissions from the Clean Air Act and associated rules (Figure 7). Simulated stream SO_4^{2-} concentrations remained relatively high in 2015, several times higher than preindustrial values. The magnitude of the simulated stream SO_4^{2-} response to decreases in atmospheric S deposition also varied among study sites (Figure 7). This variability can be explained by differences among sites in characteristics including elevation, vegetation, soils, land cover, and model-calibrated soil SO_4^{2-} adsorption capacity.

Similarly, long-term increases in stream NO_3^- concentration are attributed to increases in NO_x emissions and atmospheric N deposition, perhaps coupled with decreases in forest demand for N with increasing stand age. The effects of disturbance associated with blow down events and salvage logging in the 1950s and 1960s in the Adirondack forest also contributed to historical increases in stream NO_3^- concentration. Consistent with the decreased NO_3^- deposition following implementation of the Clean Air Act and subsequent amendments and rules (e.g., the NO_x Budget Trading Program, Cross State Air Pollution Rule), a decreasing trend in stream NO_3^- concentration began around the year 2000. However, the mean value of stream NO_3^- for the 25 sites remained relatively high in 2015 ($33 \pm 17 \mu\text{mol L}^{-1}$) compared to preindustrial concentrations. The hindcast trends in stream NO_3^- were not only associated with decreases in atmospheric NO_x deposition, but also changes in meteorological conditions (most notably maximum monthly air temperature). Climatic drivers, including temperature and precipitation, are represented in the model and likely play a more important role in regulating monthly and yearly variation in stream NO_3^- concentrations than stream SO_4^{2-} concentrations because of strong N cycling through the forest vegetation and microbial processes which are influenced by meteorological conditions (McDonnell et al. 2018a). For example, increasing maximum monthly air temperature can result in loss of soil moisture due to increases in evapotranspiration, causing water stress and reduced tree growth. A decrease in tree N uptake can increase NO_3^- leaching to streams. The differences in stream NO_3^- response to historical changes in N deposition among study sites might also be attributed to inaccurate depiction of atmospheric N deposition to individual watersheds, watershed characteristics (particularly watershed retention of N), and the accuracy of the characterization of the land disturbance history of the watersheds.

In general, simulated stream SO_4^{2-} and NO_3^- concentrations were relatively low during the preindustrial period, whereas pH, ANC and soil % BS values were relatively high (Figure 7). Increasing acidic deposition increased stream SO_4^{2-} and NO_3^- concentrations, and coincided with decreases in ANC, pH, and soil % BS. Following peak atmospheric SO_4^{2-} and NO_3^- deposition and stream concentrations, simulated results showed slight increases in stream ANC, but no change in soil % BS out to the year 2200 under the future “business-as-usual” scenario. These results are consistent with previous modeling studies of historical acidification of surface water and soil in lake-watersheds of the Adirondack Park (Zhai et al. 2008, Wu and Driscoll 2009, Sullivan et al. 2011, Sullivan et al. 2012, Fakhraei et al. 2014, Zhou et al. 2015).

4.2 Target Loads

Target loads calculated in this analysis provide model estimates of the deposition loads of S and N required to return stream ANC to levels of $20 \mu\text{eq L}^{-1}$ (fixed ANC criteria) and to within $20 \mu\text{eq L}^{-1}$ of simulated preindustrial ANC (site specific ANC criteria). Model estimates suggest that most study streams had preindustrial ANC greater than $20 \mu\text{eq L}^{-1}$. The ANC and Al_i recoveries associated with decreases in acidic deposition would be expected to reduce or eliminate episodic excursions to potentially toxic levels of Al_i concentration (> 1.0 or $2.0 \mu\text{mol L}^{-1}$). Simulations of most sites showed that they were unable to recover to preindustrial ANC values by 2150 due to depletion of soil exchangeable base cations caused by historical acidic deposition (Table 14). In general, more substantial deposition reductions would be required in the future to achieve site-specific ANC recoveries (to within $20 \mu\text{eq L}^{-1}$ of preindustrial values) or to reach ANC benchmarks earlier, by the year 2050, for example, as compared with chemical recovery by 2150.

Table 14. Linear Regression Statistics for Predicting the TLs of Acidity in 2050 and 2150

Linear regression statistics for predicting the TLs of acidity in 2050 and 2150 as functions of mean observed stream ANC and fixed ANC criteria of ANC of 20 $\mu\text{eq L}^{-1}$ and site-specific ANC criteria preindustrial ANC minus 20 $\mu\text{eq L}^{-1}$ for years 2004 and 2005 for control of SO_4^{2-} , NO_3^- , and NH_4^+ deposition. Coefficients are significant at $P < 0.05$.

Target Year	ANC Criteria	Linear Regression Coefficients		
		Slope (m yr^{-1})	Intercept ($\text{meq m}^{-2} \text{ yr}^{-1}$)	R^2
2050	20 $\mu\text{eq L}^{-1}$	0.99	14.71	0.57
	Preindustrial ANC - 20 $\mu\text{eq L}^{-1}$	0.09	16.92	0.65
2150	20 $\mu\text{eq L}^{-1}$	1.11	25.59	0.66
	Preindustrial ANC - 20 $\mu\text{eq L}^{-1}$	0.05	31.17	0.52

Simulation results suggest that some of the damage to stream acid-base chemistry may be irreversible over multi-century time scales. Some streams had relatively low ANC prior to the advent of acidic deposition and modest depletion of soil available base cations may be difficult to recover in watersheds with low-weathering rates. Benchmarks based on model-simulated preindustrial ANC as criteria for recovery may be more appropriate than fixed ANC benchmarks as a basis for establishing recovery goals. However, in these forecast simulations, none of the 25 sites could achieve their preindustrial ANC by 2150 under even the most aggressive emissions reduction scenarios (100% reduction in SO_4^{2-} , NO_3^- , and NH_4^+ deposition). Due to this limitation in the maximum achievable chemical recovery, a simulated ANC to within 20 $\mu\text{eq L}^{-1}$ of a site's preindustrial value was used as the site-specific target in TL analyses at each site. Other TL and CL studies (cf., McDonnell et al. 2018b) have also concluded that the most acidified streams are unlikely to regain preindustrial ANC levels in response to reductions in acidic deposition.

The TLs to protect stream ANC were developed for the watersheds that were modeled to be recoverable with respect to the fixed (20 $\mu\text{eq L}^{-1}$) and site-specific ANC criteria (preindustrial ANC minus 20 $\mu\text{eq L}^{-1}$) under the SO_4^{2-} , NO_3^- , and NH_4^+ deposition reduction scenario for the years 2050 and 2150 (Table 10). Strong, positive correlations between measured stream ANC and the TLs at the individual modeled sites were observed (Figure 9). This pattern illustrates that streams with higher ANC tend to have higher TLs. These sites require less reduction in acidic deposition to achieve their ANC criterion values as compared with more acid-sensitive and affected streams. The linear regression models that estimated the TLs of acidity using measured stream ANC for the fixed and site-specific ANC criterion values for the years

2050 and 2150 are summarized in Table 14. For a given measured stream ANC, the TLs are higher for the year 2150 than for 2050, indicating that less reduction in acidic deposition is needed to achieve the same ANC target if a longer recovery period is considered. Generally, the empirical model fit for the fixed ANC target was stronger than the site-specific ANC target (Figure 9). This variability may be attributed to uncertainties in the simulation of preindustrial ANC, historical deposition and meteorological conditions, and estimation of watershed base cation weathering derived from the model calibration process.

4.3 Stream Discharge

An analysis of the effects of hydrologic variation on stream ANC in the Adirondack Park showed widespread sharp ANC decreases with increasing streamflow, a relationship that is well known based on many past investigations of sensitive surface waters (Eshleman et al. 1992, Wigington et al. 1996, Davies et al. 1999). This relationship is so well established that the term “episodic acidification” was introduced to describe this response (cf., Wigington et al. 1992). The current investigation confirmed that the decrease in ANC with increasing stream discharge becomes more pronounced as low-flow stream ANC increases, a relationship that is likely strongly driven by simple dilution, a largely natural phenomenon. This response is also likely affected by increases in NO_3^- and organic acids at high flow. The relationship of the magnitude of episodic acidification to the low-flow ANC is strong and robust at low-flow ANC values less than $90 \mu\text{eq L}^{-1}$ but shows greater scatter above this threshold. This pattern suggests that the relationship could be applied broadly in a regional assessment of episodic acidification of streams that were sampled only at low flow. This relationship highlights the reason for acidification concerns for streams with low-flow ANC values approaching $100 \mu\text{eq L}^{-1}$. Such streams may become sufficiently acidic for consecutive multi-day periods during spring snowmelt to cause deleterious effects on aquatic biota. Finally, this analysis of flow-related variation in stream ANC was applied to explore the implications for PnET-BGC model calibration and assessment. The high-flow stream samples were included in the averaged ANC values that were used in model calibration. There was further consideration of episodic acidification for only a small minority of the 25 modeled streams. Thus, the PnET-BGC model results are robust for evaluating episodic and moderately high-flow acidification at most of the streams modeled in this study.

4.4 Stream Biology

Contemporaneous data for stream chemistry and fisheries were analyzed and reported for 47 Adirondack streams to elucidate fish response functions applicable to streams of this region, and possibly elsewhere. Fisheries metrics included fish species richness (including presence/absence; equivalent to richness equal to 0 vs ≥ 1), total density, total biomass, and brook trout population density and biomass. The most effective richness metric explained one-third of the deviance in richness based on the concentration of Al_i . Fish were expected to occur in 86% of the streams that had baseflow Al_i less than $1.0 \mu\text{mol L}^{-1}$. The equation developed for Al_i concentration and the presence of more than 100 fish per 0.1 ha explained 36% of the deviance in observed probabilities. An estimated 98% of streams were expected to have at least 100 fish per 0.1 ha when Al_i was not detectable; nearly half (48%) of the streams would have at least 100 fish per 0.1 ha if Al_i was less than $1.0 \mu\text{mol L}^{-1}$. Equations for predicting community biomass based on stream ANC were somewhat better than equations based on Al_i concentrations. Nevertheless, fish biomass in at least one-third (36%) of the streams would be expected to have more than 1500 g per 0.1 ha if the Al_i concentrations were less than $1.0 \mu\text{mol L}^{-1}$. Similar relationships were developed for brook trout metrics. These analyses establish linkages between stream chemistry and fish responses to help place the modeled TL concentrations and stream-ANC predictions into an ecological (stream fishery) context.

The biological-response equations and functions are essentially empirical models which can be used to approximate the effects that deposition of N and S may have on metrics that indicate the health of fish communities and species' populations in headwater streams across the western Adirondack Park. All equations and functions can be used to predict the range in probabilities for observing biological (fish) indicators at certain levels for specific values of a chemical indicator (e.g., ANC, pH, and Al_i) in streams of the study area. The probabilities may also be interpreted as the proportion or percentage of study streams (with specific levels of a chemical indicator) that should exhibit various responses or levels of the fish indicator under summer 2014–2016 ANC, pH, and Al_i conditions. Probabilities for observing different levels of the same biological indicators under changing stream ANC, pH, and Al_i values (predicted to result from alternative target deposition loads of N and S) can be directly estimated using the equations or approximated using the curves. Accordingly, various ANC, pH, and Al_i thresholds for biological effects provide useful reference points to characterize current biological conditions and to evaluate anticipated changes if selected TLs of N and S are achieved in the study area.

The fish response functions and equations can be linked to acid-base chemistry data from individual streams or a group of streams and used as tools to characterize the condition of present-day fish assemblages and to approximate the preindustrial condition of fish assemblages, which can also help to identify attainable targets for biological recovery. The current summer chemistry and fish conditions are evident from the data used in the various response functions. For example, the present-day probability for observing at least one fish species would be 0.75 in a stream with summer ANC of 20 $\mu\text{eq L}^{-1}$ and about 75% of all streams with a summer ANC of 20 $\mu\text{eq L}^{-1}$ would be expected to have one or more fish species. Only 25% of such streams would have no resident fish (Figure 11A). In addition, the probability of at least 400 fish per 0.1 ha and at least 1500 g per 0.1 ha in any, and all streams with summer ANC of 20 $\mu\text{eq L}^{-1}$ is 0.13 and 0.23, respectively (Figures 11B, 11C). ANC hindcasts, based on stream chemistry observed at different discharge (Q) percentiles (Table 15) at each model site for year 1850, and forecasts for year 2050 and 2150, for the 25 modeled streams are summarized in Table 9.

The fish-response models, however, were derived using summer baseflow chemistry; thus, the acid-base chemistry would be considerably different from annual means and cannot be clearly related to the hindcast and forecast chemistry data to infer corresponding fish conditions under past or future deposition loading. Therefore, the hindcast estimates of mean annual ANC concentrations for 1850, estimates for 2015 (average of 61st flow percentile or Q_{61}), and predictions for year 2150 had to be adjusted to summer low-flow conditions to reflect comparable mean low-flow ANC conditions (the 27th flow percentile or Q_{27}) under which the summer 2014–2016 fish-surveys were completed (and water samples were collected). Estimates of ANC Q_{27} for each of the 25 PnET-BGC model sites were calculated using empirically ranked annual frequency distributions of daily flow data from one of four nearby USGS discharge-gauged sites (USGS station IDs 04253296, 01312000, 04256000, and 01343060), the linear relationship between the change in ANC and the change in discharge at the gauges, ANC data from samples collected on several dates at each on the 25 sites. A shift was applied to the ANC values associated with the discharge percentile on the original sample dates to that corresponding to the target Q_{27} as described for Appalachian streams in Lawrence et al. (2018b). The PnET-BGC model ANC Q_{27} estimates for each of the 25 streams in 1850, 2015, and 2150 (under seven N and S deposition loading scenarios and site-specific targets) are listed in Table 15. Estimates of ANC Q_{27} for the PnET-BGC model streams in 1850 averaged 191.0 $\mu\text{eq L}^{-1}$ with a median of 74.3 $\mu\text{eq L}^{-1}$. The probabilities for observing one or more species, >400 fish/0.1 ha, and >1500 g fish/0.1 ha in a representative stream (with the same median ANC Q_{27}) in 1850 would have been 0.84, 0.23, and 0.43, respectively (Figure 11).

Although these pre-industrial fish-community metrics, noted levels, and the proportion of streams expected to attain these levels might be good upper targets for biological recovery, they are twice as high as the 2015 median ANC Q_{27} for the 25 PnET-BGC model streams ($36.3 \mu\text{eq L}^{-1}$) and likely not feasible for many acidified streams in the region. Additionally, the probabilities for community richness, density, and biomass metrics that correspond to the 2015 median ANC Q_{27} are 0.78, 0.16, and 0.28, respectively. Although probability differences between 1850 and 2015 seem small; the probability for observing more than one fish species in a typical (summer median ANC of $36.3 \mu\text{eq L}^{-1}$) stream decreased by 7%, and the probabilities for observing moderate fish densities and biomass decreased by 30–35% over the 165-year period. Thus, the present-day probabilities (and percentages of streams) for most fish-community metrics remain substantially lower than historic values that were determined from hindcast ANC Q_{27} estimates and present-day (2014–2016) fish-response models.

Table 15. Calculated ANC Q₂₇ (µeq L⁻¹) in 1850, Estimated ANC Q₂₇ in 2015, and Predicted ANC Q₂₇ in 2150

The calculations were done under different N and S emission scenarios at the 25 PnET-BGC modeled streams.

Site	Calculated 1850 ANC Q ₂₇	Estimated 2015 ANC Q ₂₇	Predicted 2150 ANC Q ₂₇ (µeq L ⁻¹)							Site- specific ANC Q ₂₇
			Scenario 1: Business as usual (average of 2013-2015)	Scenario 2: Possible deposition future (Clean Power Plan)	Scenario 3: Additional deposition reduction 25%	Scenario 4: Additional deposition reduction 50%	Scenario 5: Additional deposition reduction 75%	Scenario 6: Additional deposition reduction 100%	Scenario 7: Increased deposition 15%	
North Buck	31.0	-33.9	-17.9	-17.5	-15.4	-12.9	-11.1	-8.5	-24.6	11.0
27026	25.7	-27.6	-21.9	-20.9	-20.1	-18.5	-16.4	-14.9	-32.3	5.7
35014	17.9	-26.2	-20.2	-19.5	-19.1	-18.5	-17.8	-17.2	-30.5	-2.1
T24	43.8	-7.7	10.4	11.4	13.3	16.2	19.1	22.0	8.7	23.8
WF	22.5	-7.1	0.7	1.3	2.5	4.1	5.5	7.2	-5.6	2.5
28011	43.6	-1.4	13.2	18.0	23.6	32.1	37.9	42.2	5.0	23.6
22019	41.2	1.4	6.7	11.6	12.7	15.0	18.9	21.3	-2.7	21.2
NW	49.2	4.2	17.8	20.9	26.1	30.1	37.6	45.1	9.8	29.2
12003	35.9	5.4	14.0	14.7	15.9	19.2	23.4	28.6	12.6	15.9
13008	59.3	24.9	32.0	34.4	37.1	40.2	43.2	46.3	29.7	39.3
South Buck	72.8	29.2	37.7	38.9	40.5	43.2	46.5	48.4	33.0	52.8
AMP	88.2	32.6	49.8	55.6	60.0	67.7	76.0	86.3	36.6	68.2
Buck Creek	72.9	36.3	44.7	46.8	50.4	55.6	58.9	66.1	42.0	52.9
28014	76.1	39.1	42.7	45.0	50.7	61.3	70.8	74.4	36.9	56.1
24002	74.3	39.8	45.3	47.5	51.5	55.5	59.4	63.4	44.3	54.3
Archer	163.6	125.5	134.7	135.7	136.9	139.6	142.0	144.3	120.2	143.6
N1	256.5	201.5	230.1	233.6	237.0	242.5	247.9	253.1	209.8	236.5
26008	276.1	225.1	238.3	246.0	248.4	255.7	263.2	271.7	227.8	256.1
30019	281.9	231.5	251.3	254.2	258.3	265.9	272.2	280.6	235.5	261.9
30009	311.4	270.4	284.3	285.5	289.3	295.2	301.0	307.0	266.3	291.4

Table 15 continued

Site	Predicted 2150 ANC Q ₂₇ (µeq L ⁻¹)									Site-specific ANC Q ₂₇
	Calculated 1850 ANC Q ₂₇	Estimated 2015 ANC Q ₂₇	Scenario 1: Business as usual (average of 2013-2015)	Scenario 2: Possible deposition future (Clean Power Plan)	Scenario 3: Additional deposition reduction 25%	Scenario 4: Additional deposition reduction 50%	Scenario 5: Additional deposition reduction 75%	Scenario 6: Additional deposition reduction 100%	Scenario 7: Increased deposition 15%	
28030	351.1	309.6	319.8	324.0	326.2	332.9	339.2	343.6	304.6	331.1
29012	410.1	345.9	361.3	363.0	367.1	373.4	379.6	385.9	348.0	390.1
27019	412.1	367.2	376.3	377.2	378.6	381.9	386.2	389.3	366.9	392.1
24001	554.0	438.6	534.0	535.0	537.3	540.7	546.1	550.7	527.3	534.0
S14	1004.1	848.7	908.4	909.7	912.1	917.9	922.4	926.8	898.1	984.1
mean	191.0	138.9	155.7	158.1	160.8	165.4	170.1	174.5	146.7	171.0
median	74.3	36.3	44.7	46.8	50.7	55.6	59.4	66.1	36.9	54.3

The response functions and equations (Baldigo et al. 2019b) can be used most effectively with the ANC projections from section 4.2 to predict how future fish assemblages at individual streams might change in response to various total loads of N and S, and/or to establish deposition loads that would be needed to meet some minimally acceptable biological targets (identified for protection or recovery) in the region. Two examples are used below to illustrate these applications. The first example uses the present-day (2015) median ANC Q_{27} from the 25 model streams ($36.3 \mu\text{eq L}^{-1}$) to describe total biomass probabilities and changes predicted to occur in probabilities in such a representative stream by 2150 if the ANC targets under scenario 6 were met. The probability for community biomass $>1500 \text{ g}/0.1 \text{ ha}$ under present-day ANC Q_{27} conditions is 0.28; which means a stream with a summer ANC of $36.3 \mu\text{eq L}^{-1}$ has a 0.28 probability of having more than 1500 g of fish/0.1 ha and that about 28% of streams with a summer ANC of $36.3 \mu\text{eq L}^{-1}$ should have $>1500 \text{ g fish}/0.1 \text{ ha}$. An individual stream such as the highly acidic stream North Buck, with a 2015 ANC Q_{27} of -33.9 currently has a 0.11 probability for $>1500 \text{ g fish}/0.1 \text{ ha}$. Decreasing deposition loads to the 1850 level (scenario 6) by year 2150 would increase ANC Q_{27} in the representative stream and in North Buck to 66.1 and $-8.5 \mu\text{eq L}^{-1}$, respectively, and consequently increase the probabilities for $>1500 \text{ g fish}/0.1 \text{ ha}$ to 0.39 and 0.16, respectively. Decreasing deposition loads to meet site-specific ANC Q_{27} targets by year 2150 would increase ANC Q_{27} in the representative stream and in North Buck to 54.3 and $11.0 \mu\text{eq L}^{-1}$, respectively, and increase the probabilities for $>1500 \text{ g fish}/0.1 \text{ ha}$ to 0.35 and 0.21, respectively. Although the probabilities for $>1500 \text{ g fish}/0.1 \text{ ha}$ would increase by 49% in the representative stream, and by 45% in North Buck under scenario 6, the probabilities for $>1500 \text{ g fish}/0.1 \text{ ha}$ would not change much in the representative stream but would increase by 91% at North Buck if the site-specific ANC targets were met by 2150. The 100% additional reduction in deposition loading (scenario 6) is likely not achievable and would affect ANC and fish assemblages in all streams alike, whereas, the site-specific targets are more conservative overall and generally benefit ANC levels and fish assemblages primarily in the most highly acidified streams.

Example 2 uses present-day (2015) and the 1850 ANC Q_{27} estimates for a representative (median ANC Q_{27}) stream and North Buck and the brook trout response equations to identify future ANC Q_{27} concentrations (and indirectly target deposition loads of N and S) that would be required to attain a theoretical brook trout recovery target. At present, the probability for low brook trout densities ($>100 \text{ trout}/0.1 \text{ ha}$) in a representative stream with an ANC Q_{27} of $36.3 \mu\text{eq L}^{-1}$ is 0.29 (Figure 13A), whereas the 1850 ANC Q_{27} data indicate a typical (median) stream would have an ANC Q_{27} of $74.3 \mu\text{eq L}^{-1}$ and the probability of $>100 \text{ trout}/0.1 \text{ ha}$ would equal 0.43. Although changes in deposition loads of N and S, and in acid-base chemistry in all study streams sufficient to reach pre-industrial ANC Q_{27} concentrations are unlikely, efforts to recover about half of the low-density

brook trout populations between 1850 and 2015 (i.e., increase the present-day probability of >100 trout/0.1 ha half way between 1850 (0.29) and 2015 (0.43) probabilities to 0.36) means that deposition loads of N and S would have to decrease enough so the ANC Q_{27} of individual streams (or the median from the group of 25 streams) increased by approximately $20 \mu\text{eq L}^{-1}$ (i.e., from $36.6 \mu\text{eq L}^{-1}$ to about $57 \mu\text{eq L}^{-1}$). This change is comparable to the $18 \mu\text{eq L}^{-1}$ increase in median ANC Q_{27} data (estimated for each of the 25 Adirondack streams with the PnET-BGC model) that would be necessary to meet site-specific ANC Q_{27} targets that are fixed at $20 \mu\text{eq L}^{-1}$ less than the 1850 ANC Q_{27} estimates.

The probabilities for achieving various benchmarks of fish response and the linear and nonlinear (absolute) relations may also be used to predict or extrapolate the future consequences of different S and N emission and deposition scenarios on fish assemblages in large groups of streams. For example, the logistic equations for describing the probabilities for various levels of brook trout population and community metrics (Figures 11–16), and equations listed in Baldigo et al. (2019b) were used to estimate the probabilities for all of the 25 model streams to have one or more fish species; total community density of at least 200 fish/0.1 ha; total community biomass of at least 1000 grams/0.1 ha; at least 100 brook trout/0.1 ha; and at least 500 grams of brook trout/0.1 ha under preindustrial (1850); ambient (2015); future 2150 scenarios 1, 2, 6, and 7; and the year 2150 site-specific TL ANC Q_{27} criterion (Figure 22). The individual probabilities for any given stream illustrate, not only the likelihood for observing the metric level expected in that stream under the various scenarios, but also the probability for the same condition to occur in other streams exhibiting the same summer (low-flow) ANC Q_{27} conditions. The various trajectories in Figure 22A show that the probability of one or more fish species is currently 0.64 in North Buck (2015), or another stream with the same ANC Q_{27} as North Buck, and this probability would increase to 0.74 if the site-specific TL ANC Q_{27} criterion for year 2150 was achieved. These values suggest that 64 out of every 100 streams with the same ANC Q_{27} should currently have one or more fish species, but the number of streams with 1 or more species would increase by 16% (to 74 out of 100 streams) in year 2150 if the site-specific TL ANC Q_{27} criterion was met. In addition, the linear and nonlinear relationships between summer ANC concentrations and estimates of fish community richness, total fish community density, total fish community biomass, density of brook trout, and biomass of brook trout (Figure 23) provide a basis for directly estimating these metrics for all 25 model streams under preindustrial (1850), ambient (2015), seven future 2150 scenarios, and the site-specific TL ANC criterion for year 2150 under summer baseflow ANC Q_{27} conditions.

The approximate number of modeled streams predicted to achieve two fish species, total community density of 200 fish/0.1 ha, total fish community biomass of 1000 grams/0.1 ha, 100 brook trout/0.1 ha, and 500 grams of brook trout/0.1 ha under preindustrial (1850), ambient (2015), seven future 2150 scenarios, and the site-specific TL ANC Q_{27} criterion for year 2150 are summarized in Figure 24 and described in section 4.6 below.

Figure 22. Estimated Probabilities for Each of the 25 Model Streams

Estimated probabilities for each of the 25 model streams to have (A) one or more fish species; (B) total fish community density of at least 200 fish/0.1 ha; (C) total fish community biomass of at least 1000 grams/0.1 ha; (D) at least 100 brook trout/0.1 ha; and (E) at least 500 grams of brook trout/0.1 ha under preindustrial (hindcast) (1850); ambient (2015); future 2150 scenarios 1, 2, 6, and 7; and the site-specific 2150 scenario at ANC Q₂₇ conditions.

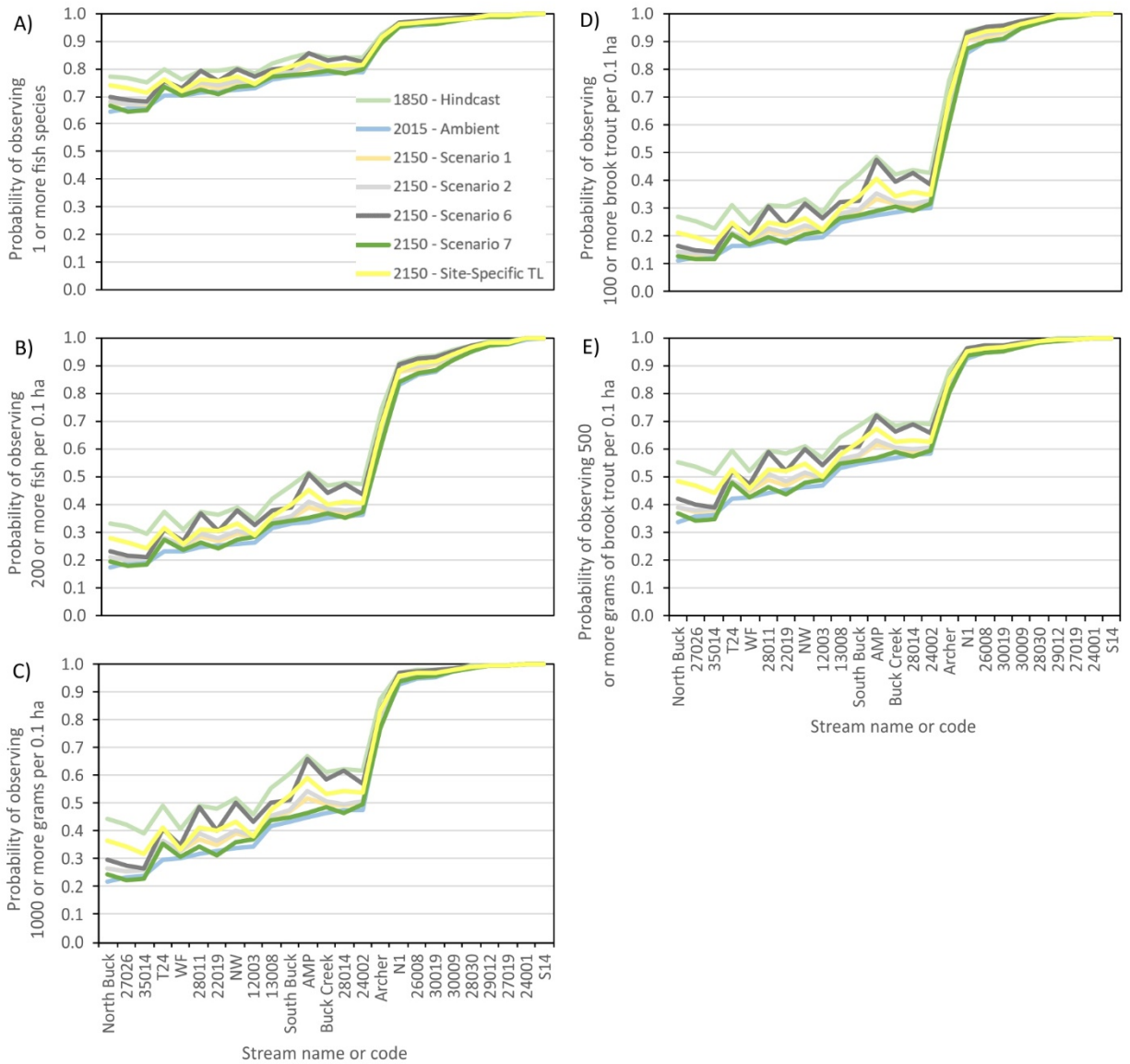


Figure 23. Linear and Nonlinear Relations between ANC Concentrations and Fish Communities/Brook Trout Population

Linear and nonlinear relations between ANC concentrations and (A) fish community richness, (B) fish community density, (C) fish community biomass, (D) density of brook trout populations, and (E) biomass of brook trout populations from 59 fish surveys in 47 streams in the western Adirondacks during summer 2014–2016 (from Baldigo et al. 2019a).

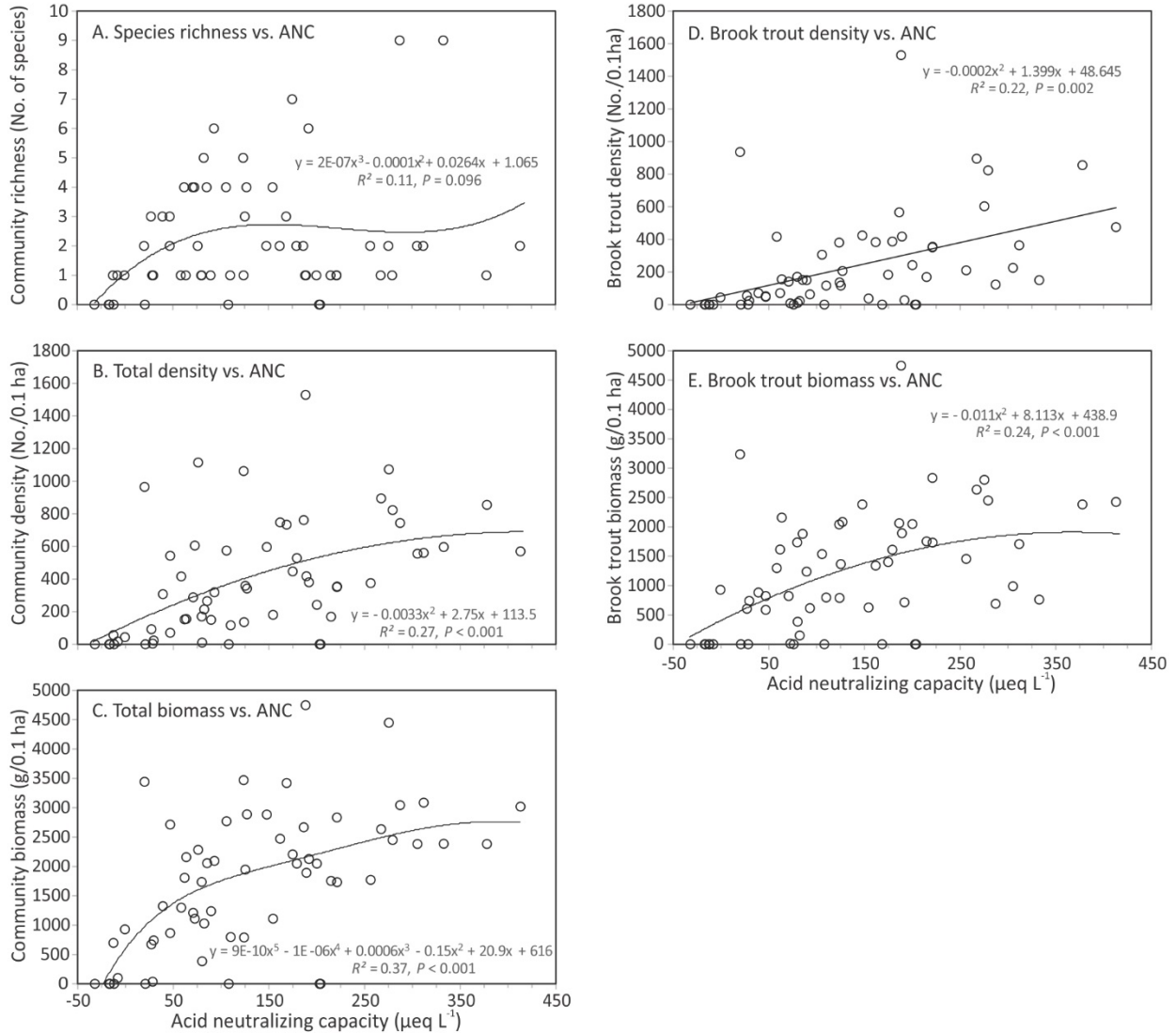
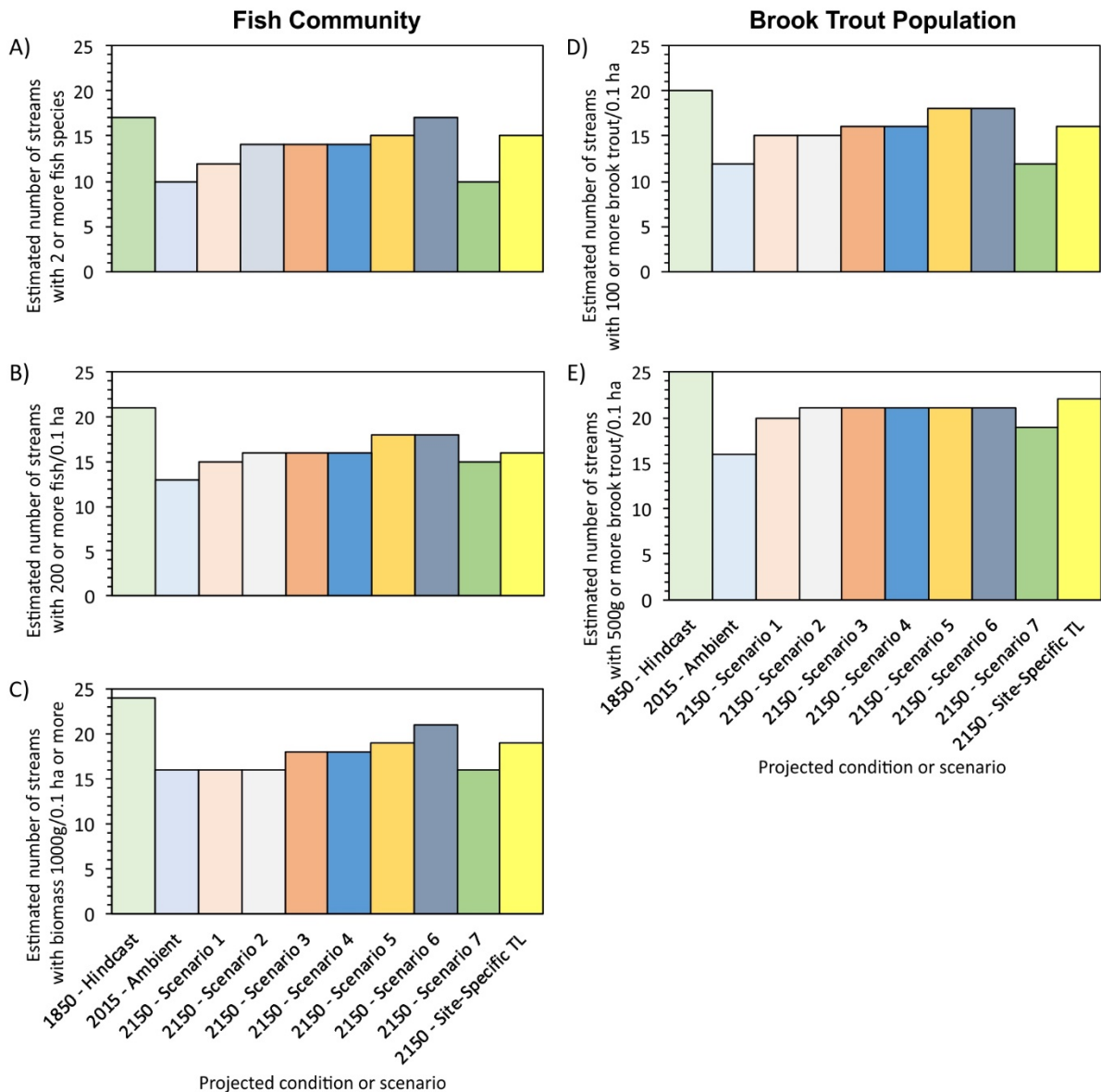


Figure 24. Projected Conditions or Scenarios for Fish Communities and Brook Trout Population

Number of the 25 model streams predicted to show the following: (A) two or more fish species, (B) total community density of ≥ 200 fish/0.1 ha, (C) total community biomass of ≥ 1000 grams/0.1 ha, (D) ≥ 100 brook trout/0.1 ha, and (E) ≥ 500 grams of brook trout/0.1 ha under pre-industrial (1850) versus the scenarios: 1850-Hindcast, ambient (2015), seven future 2150 scenarios and the site-specific 2150 scenario with ANC Q₂₇ conditions.



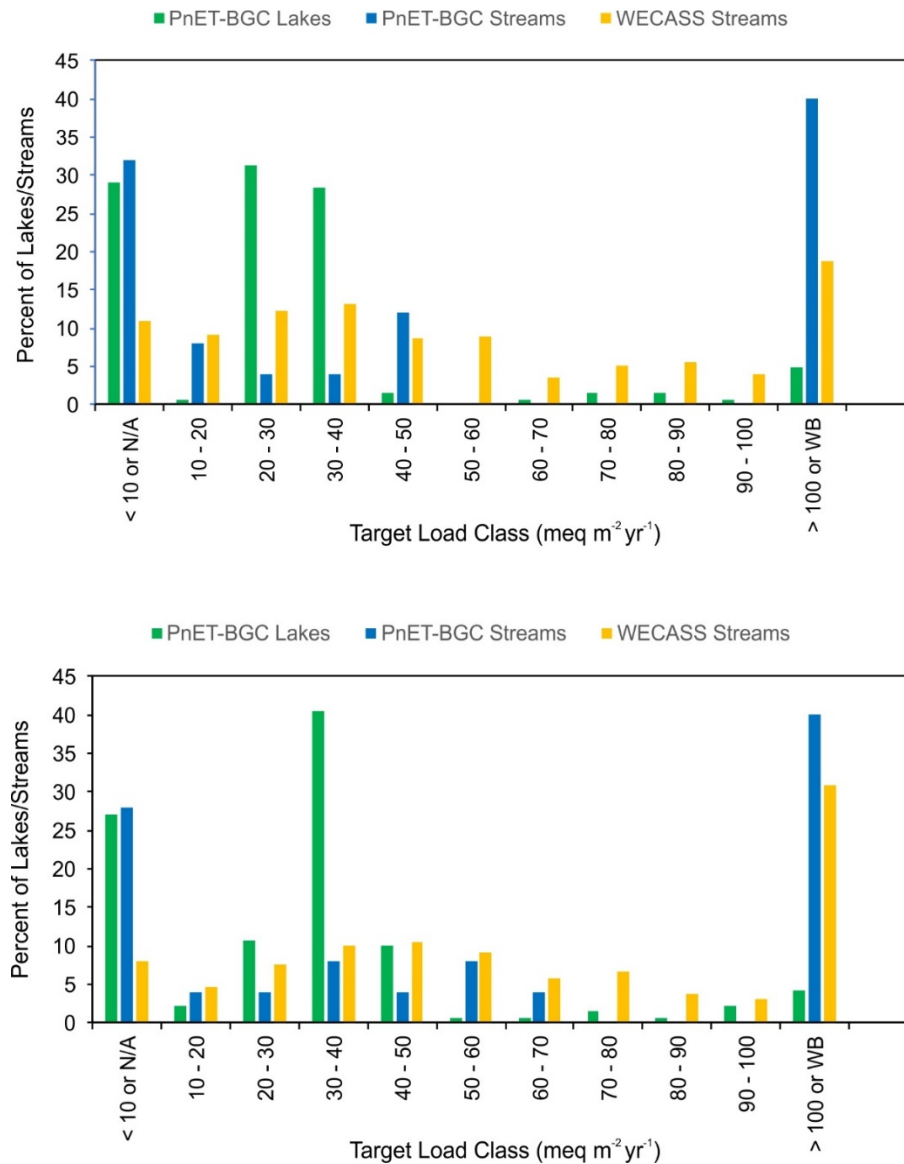
4.5 Comparison with Results for Adirondack Lakes

A direct comparison of the TL results for Adirondack streams versus lakes is of interest because Adirondack lakes have been well studied. Most of the previous work on TLs in this region has been conducted on Adirondack lakes. A rigorous comparison would require standardization of an endpoint year, sensitive criterion, choice of model, critical criterion level, and method of site selection. There is no database for Adirondack lakes that standardizes these items. The closest appropriate comparison with the stream modeling reported here is the Total Maximum Daily Load (TMDL) analysis of Fakhraei et al. (2014). In the TMDL study, 128 lakes were modeled that had been classified in 2010 by the State as “impaired” under Section 303(d) of the Clean Water Act due to high acidity. Approximately 97 of these lakes were determined to have ambient ANC $\leq 20 \mu\text{eq L}^{-1}$. Thus, these are among the most acid-sensitive lakes in the Adirondack Park.

About 30% of the lakes modeled by Fakhraei et al. (2014) were simulated by PnET-BGC to have TL less than $10 \text{ meq m}^{-2} \text{ yr}^{-1}$ (Figure 25). Almost the same percentage of streams modeled in this project had such very low TLs. Thus, the modeled stream (this study) and lake (TMDL study; Fakhraei et al. 2014) TLs are similar at the low end of the TL distribution. Modeled streams tended to more commonly have some high TL values ($> 100 \text{ meq m}^{-2} \text{ yr}^{-1}$), which reflects the selection of few relatively high ANC sites for modeling in the stream study reported here. The WECASS stream database showed more sites with low/moderate TL values ($20\text{--}40 \text{ meq m}^{-2} \text{ yr}^{-1}$) as compared with the modeled streams, suggesting that the regional population of WECASS streams is somewhat more acid-sensitive than the set of streams modeled here with PnET-BGC.

Figure 25. Comparison of Lake and Stream TLs to Protect Aquatic Biota against Low ANC

Comparison of lake and stream TLs to protect aquatic biota against ANC decreases to values below $20 \mu\text{eq L}^{-1}$ in the years 2050 (top) and 2150 (bottom). The lowest grouping ($<10 \text{ meq m}^{-2} \text{ yr}^{-1}$) includes “can’t get there from here” sites. The highest grouping ($>100 \text{ meq m}^{-2} \text{ yr}^{-1}$) includes sites classified as “well buffered (WB)”.



4.6 Integration of Biogeochemical, Hydrological, and Biological Models

This study was focused on developing a more complete understanding of historical, ambient, and expected future conditions of stream chemistry and biology for a diverse set of streams located throughout the Adirondack Mountain region. Among the primary components were the following:

1. A simulation of long-term temporal trends in water ANC derived from a dynamic biogeochemical model calibrated to stream and soil chemistry measured under moderately high to high-flow conditions that varied by site.
2. A linear regression model that could be used to adjust stream water ANC that was measured/modeled under a given flow condition (Q percentile) to the expected ANC under another flow condition.
3. A series of logistic regression models that estimate the probabilities for observing different levels of fish population and community metrics with regard to stream water ANC, Al_i , and pH measured during summer baseflow conditions at the time of fish surveys (i.e., the 27th percentile of the cumulative [annual] daily flows).
4. A series of linear and nonlinear regression equations that directly estimate the absolute (expected) fish population and community metrics with regard to stream water ANC, Al_i , and pH measured during summer baseflow conditions at the time of fish surveys (i.e., the 27th percentile of the cumulative [annual] daily flows).
5. An application of logistic and linear and nonlinear regression equations to predict either (a) the probabilities for observing different levels of fish population and community metrics or (b) the absolute fish metrics expected under historical, ambient, and future ANC levels at each of the 25 PnET-BGC model stream sites adjusted to the 27th percentile of cumulative (annual) daily flows.

In order to develop a concise description of the biological effects associated with historical, ambient, and potential future atmospheric N and S deposition; results from these components of the study were integrated to develop estimates of the expected number of species, density, and biomass in fish communities (Tables 16, 17, and 18) and the density and biomass of brook trout populations (Tables 19 and 20) under preindustrial (1850), ambient (2015), future (2150) scenario summer baseflow (Q_{27}) conditions, and a site-specific TL ANC Q_{27} criterion for year 2150 at each of the 25 PnET-BGC model stream sites.

About half of the study streams were projected to have lost one or more fish species since the preindustrial period. None of the future scenarios could fully recover the number of fish species expected to be present in all PnET-BGC modeled streams prior to year 1850. The different scenarios were associated with varying levels of recovery in total community density (Table 17), community biomass (Table 18), brook trout density (Table 19), and brook trout biomass (Table 20). A 100%

reduction in deposition beyond the U.S. Environmental Protection Agency Clean Power Plan (scenario 6) was the most effective modeled emissions scenario for biological recovery and would allow fish communities to more closely return to preindustrial conditions than with attainment of site-specific TLs, with the exception of brook trout biomass (Figure 22). Full biological recovery to preindustrial conditions would not be possible for some streams. The biological scenario results are dependent on the assumption that ANC is the only limiting factor for fish communities in these streams. Other aspects of stream impairment may affect the ability of these systems to fully recover from acidification impacts.

Table 16. Predicted Number of Fish Species for 24 Modeled Streams

The streams^a were modeled under preindustrial (1850), ambient (2015), and future (2150) scenario summer baseflow ANC Q₂₇ conditions.

Site	Preindustrial (1850)	Ambient (2015)	Future Scenario (2150)							Target Load	
			1	2	3	4	5	6	7	Site-Specific	
North Buck	2	0	1	1	1	1	1	1	1	0	1
35014	1	0	0	0	1	1	1	1	1	0	1
27026	2	0	0	0	0	1	1	1	1	0	1
T24	2	1	1	1	1	1	2	2	2	1	2
22019	2	1	1	1	1	1	2	2	2	1	2
12003	2	1	1	1	1	2	2	2	2	1	1
WF	2	1	1	1	1	1	1	1	1	1	1
South Buck	2	2	2	2	2	2	2	2	2	2	2
13008	2	2	2	2	2	2	2	2	2	2	2
24002	2	2	2	2	2	2	2	2	2	2	2
28011	2	1	1	1	2	2	2	2	2	1	2
28014	2	2	2	2	2	2	2	2	2	2	2
NW	2	1	1	2	2	2	2	2	2	1	2
Buck Creek	2	2	2	2	2	2	2	2	2	2	2
AMP	3	2	2	2	2	2	2	2	2	2	2
27019	3	3	3	3	3	3	3	3	3	3	3
Archer	3	3	3	3	3	3	3	3	3	3	3
30009	2	2	2	2	2	2	2	2	2	2	2

Table 16 continued

Site	Preindustrial (1850)	Ambient (2015)	Future Scenario (2150)							Target Load
			1	2	3	4	5	6	7	Site-Specific
26008	2	3	3	3	3	2	2	2	3	2
30019	2	3	3	3	2	2	2	2	3	2
29012	3	3	3	3	3	3	3	3	3	3
28030	3	2	2	3	3	3	3	3	2	3
N1	2	3	3	3	3	3	3	3	3	3
24001	9	4	8	8	8	8	9	9	7	8
Mean	3	3	3	3	3	3	3	3	3	3
Median	2	2	2	2	2	2	2	2	2	2

^a Stream S14 was not analyzed for predicting fish metrics because its ANC was very high, well beyond the level used to develop the fish metric equations. The acid-base chemistry of this lake would support relatively high richness over time, irrespective of acidic deposition.

Table 17. Predicted Fish Density (Number of Fish/0.1 ha) for 24 Modeled Streams

The streams^a were modeled under preindustrial (1850), ambient (2015), and future (2150) scenario summer baseflow ANC Q₂₇ conditions.

Site	Preindustrial (1850)	Ambient (2015)	Future Scenario (2150)							Target Load Site-Specific
			1	2	3	4	5	6	7	
North Buck	196	16	63	64	70	77	83	90	44	143
35014	162	39	57	59	60	62	64	65	27	108
27026	182	35	52	55	57	62	68	72	21	129
T24	228	92	142	145	150	157	165	173	137	177
22019	221	117	132	145	148	154	164	171	106	170
12003	208	128	151	153	157	165	176	190	148	157
WF	174	94	115	117	120	125	128	133	98	120
South Buck	296	191	213	216	220	226	234	239	201	250
13008	265	180	198	204	211	219	226	234	192	216
24002	300	218	231	237	246	256	265	275	229	253
28011	227	110	149	162	177	198	213	224	127	177
28014	304	216	225	231	244	270	292	300	210	257
NW	241	125	161	170	183	193	212	231	140	191
Buck Creek	297	209	230	235	244	256	264	281	223	250
AMP	330	200	242	256	267	285	303	326	210	286
27019	690	681	684	684	685	686	687	687	681	688
Archer	476	407	424	426	428	433	438	442	397	441
30009	652	617	630	631	635	640	644	649	613	636
26008	623	566	583	592	594	602	610	619	570	603
30019	628	574	598	601	605	613	619	627	579	609
29012	690	672	679	680	681	683	685	687	673	687
28030	675	651	658	660	662	666	669	671	647	665
N1	603	534	573	577	581	588	594	599	546	580
24001	631	689	647	646	645	642	638	634	652	647
Mean	519	432	462	466	471	479	486	494	446	488
Median	300	209	230	235	244	256	265	281	210	253

^a Stream S14 was not analyzed for predicting fish metrics because its ANC was very high, well beyond the level used to develop the fish metric equations. The acid-base chemistry of this lake would support relatively high richness over time, irrespective of acidic deposition.

Table 18. Predicted Fish Biomass (g/0.1 ha) for the 24 Modeled Streams

The streams^a were modeled under preindustrial (1850), ambient (2015), and future (2150) scenario summer baseflow ANC Q₂₇ conditions.

Site	Preindustrial (1850)	Ambient (2015)	Future Scenario (2150)							Target Load
			1	2	3	4	5	6	7	Site-Specific
North Buck	1140	-287	191	202	257	321	365	427	3	829
35014	946	-44	129	148	159	175	194	210	-177	572
27026	1066	-85	83	111	133	177	232	271	-233	731
T24	1297	447	819	836	870	919	966	1011	788	1038
22019	1268	646	750	840	860	899	963	1001	560	999
12003	1204	725	882	894	914	968	1032	1107	858	914
WF	1018	459	630	642	666	698	726	758	493	666
South Buck	1567	1115	1226	1240	1259	1291	1327	1347	1166	1392
13008	1454	1054	1153	1184	1218	1255	1290	1324	1122	1245
24002	1578	1251	1314	1338	1379	1419	1455	1490	1303	1407
28011	1295	586	867	948	1035	1154	1228	1279	717	1035
28014	1591	1242	1284	1310	1371	1471	1551	1579	1215	1424
NW	1356	701	945	994	1072	1128	1224	1312	807	1115
Buck Creek	1568	1209	1307	1330	1368	1420	1450	1513	1277	1393
AMP	1675	1161	1361	1419	1460	1526	1591	1663	1212	1530
27019	2810	2810	2816	2817	2818	2819	2820	2820	2810	2820
Archer	2060	1882	1927	1932	1937	1950	1961	1972	1856	1969
30009	2696	2544	2600	2605	2620	2641	2662	2682	2527	2627
26008	2568	2342	2403	2438	2449	2481	2514	2550	2355	2483
30019	2591	2372	2462	2475	2493	2525	2552	2586	2390	2508
29012	2812	2781	2804	2806	2810	2815	2818	2819	2785	2820
28030	2790	2690	2721	2733	2738	2755	2769	2777	2674	2751
N1	2485	2233	2365	2381	2397	2422	2446	2470	2272	2395
24001	3034	2782	2867	2873	2888	2913	2957	3000	2830	2867
Mean	2185	1947	2025	2035	2048	2069	2090	2110	1983	2094
Median	1578	1209	1307	1330	1371	1420	1455	1513	1215	1407

^a Stream S14 was not analyzed for predicting fish metrics because its ANC was very high, well beyond the level used to develop the fish metric equations. The acid-base chemistry of this lake would support relatively high richness over time, irrespective of acidic deposition.

Table 19. Predicted Brook Trout Density (Number of Brook Trout/0.1 ha) for the 24 Modeled Streams

The streams^a were modeled under preindustrial (1850), ambient (2015), and future (2150) scenario summer baseflow ANC Q₂₇ conditions.

Site	Preindustrial (1850)	Ambient (2015)	Future Scenario (2150)							Target Load Site-Specific
			1	2	3	4	5	6	7	
North Buck	92	1	24	24	27	31	33	37	14	64
35014	74	12	20	21	22	23	24	25	6	46
27026	85	10	18	19	20	23	26	28	3	57
T24	109	38	63	65	67	71	75	79	61	82
22019	106	51	58	65	66	70	75	78	45	78
12003	99	56	68	69	71	75	81	89	66	71
WF	80	39	50	50	52	54	56	59	41	52
South Buck	149	89	101	103	105	109	113	116	95	122
13008	131	83	93	96	100	104	109	113	90	103
24002	151	104	112	115	120	126	131	136	110	124
28011	109	47	67	74	82	93	101	107	56	82
28014	154	103	108	111	119	133	146	151	100	126
NW	117	55	73	78	85	91	101	111	62	89
Buck Creek	149	99	111	114	119	126	130	140	107	122
AMP	170	94	118	126	132	142	154	168	99	143
27019	584	529	540	542	543	547	552	556	529	560
Archer	271	220	233	234	236	239	242	245	213	244
30009	461	409	427	428	433	440	448	455	404	436
26008	416	351	368	378	381	390	400	411	355	391
30019	424	359	385	388	394	403	411	422	365	398
29012	581	503	522	524	529	537	544	552	506	557
28030	510	458	471	476	479	487	495	501	452	485
N1	391	321	358	362	366	373	380	387	331	366
24001	749	615	726	727	730	734	740	745	718	726
Mean	307	238	261	264	267	273	279	285	249	281
Median	151	99	111	114	119	126	131	140	100	124

^a Stream S14 was not analyzed for predicting fish metrics because its ANC was very high, well beyond the level used to develop the fish metric equations. The acid-base chemistry of this lake would support relatively high richness over time, irrespective of acidic deposition.

Table 20. Predicted Brook Trout Biomass (g/0.1 ha) for 24 Modeled Streams

The streams^a were modeled under preindustrial (1850), ambient (2015), and future (2150) scenario summer baseflow ANC Q₂₇ conditions.

Site	Preindustrial (1850)	Ambient (2015)	Future Scenario (2150)							Target Load Site-Specific
			1	2	3	4	5	6	7	
North Buck	680	151	290	293	311	332	347	369	233	527
35014	581	219	271	277	280	285	291	296	181	422
27026	640	207	256	265	272	285	303	316	166	485
T24	773	376	522	530	545	568	590	612	509	626
22019	755	451	493	532	541	558	589	607	417	606
12003	716	483	551	556	565	591	623	662	540	565
WF	615	380	444	449	459	472	483	496	393	459
South Buck	971	666	729	738	749	769	792	806	695	836
13008	881	634	687	705	724	747	769	791	670	740
24002	980	744	784	799	827	855	882	909	777	847
28011	771	427	544	581	624	688	730	761	479	624
28014	992	739	765	781	821	894	957	981	723	859
NW	811	473	580	604	643	673	728	782	517	666
Buck Creek	971	719	779	794	820	856	878	927	760	837
AMP	1068	691	815	855	885	937	991	1056	721	940
27019	1893	1918	1917	1916	1916	1915	1913	1911	1918	1910
Archer	1468	1282	1330	1335	1341	1354	1366	1378	1253	1374
30009	1886	1819	1846	1848	1855	1864	1873	1881	1810	1858
26008	1831	1701	1740	1761	1768	1786	1803	1822	1710	1787
30019	1842	1721	1775	1782	1792	1810	1823	1839	1733	1801
29012	1895	1914	1918	1918	1918	1917	1916	1913	1915	1911
28030	1916	1884	1896	1900	1902	1907	1911	1913	1878	1906
N1	1788	1622	1717	1727	1737	1752	1766	1780	1651	1735
24001	1519	1857	1599	1595	1586	1573	1551	1533	1623	1599
S14*	NA	NA	NA	NA	NA	NA	NA	NA	NA	NA
Mean	1583	1351	1433	1443	1456	1477	1497	1516	1390	1501
Median	980	719	779	794	821	856	882	927	723	847

^a Stream S14 was not analyzed for predicting fish metrics because its ANC was very high, well beyond the level used to develop the fish metric equations. The acid-base chemistry of this lake would support relatively high richness over time, irrespective of acidic deposition.

Stream ANC values were combined with estimates of flow percentiles based on about 300 streams sampled during synoptic surveys across the Adirondack Park to evaluate site-specific and regional episodic acidification patterns. Results indicate a relationship between low-flow stream ANC and the rate at which ANC declines as stream discharge increases, which is consistent across the region. Declines in ANC with increasing discharge are larger as low-flow ANC increases, a relation that has been described in previous studies of episodic acidification in Adirondack streams, but never quantified as in this study. This relation is likely driven by dilution of base cation concentrations during high-intensity rain events and rapid snowmelt, especially in streams with ANC higher than $200 \mu\text{eq L}^{-1}$. However, a role for increases in NO_3^- and organic acids is also likely but would have to be evaluated through detailed analysis that is beyond the scope of the current investigation.

The minimum ANC values reached during high flow in these Adirondack streams was evaluated by exploring the 85th percentile discharge values, which is exceeded at a given point on about 55 days during an average year. Regional mean relations developed for these streams indicate that a stream with a low-flow ANC (15th percentile) of $50 \mu\text{eq L}^{-1}$ would decline to a high-flow value of about $5 \mu\text{eq L}^{-1}$. Similarly, a stream with low-flow ANC of $100 \mu\text{eq L}^{-1}$ would decline to about $23 \mu\text{eq L}^{-1}$ at high flow. Such values may be of concern because of a likely association with high concentrations of Al_i .

4.7 Management Implications

Results of this research suggest, and in many cases confirm, that many low-order Adirondack streams have low TLs to achieve fixed or site-specific benchmarks for ANC and Al_i recovery. Many streams, especially in the southwestern portion of the Adirondack Park, are currently in exceedance of these TLs. This finding applies to the 25 streams modeled using PnET-BGC in this study and to the broader group of streams found throughout the region to which the modeled site results were extrapolated. Many other streams, especially some of those located in the eastern portion of the Adirondack region, have relatively high TLs and are relatively insensitive to acidic deposition.

The strongest predictor of fisheries response to changes in acidic deposition is the concentration of Al_i , with clear benchmarks near 1.0 and $2.0 \mu\text{mol L}^{-1}$. These TLs and exceedances are sensitive to flow conditions at the time of sample collection. Stream chemistry data used to support this modeling study were largely based on sampling during moderate to moderately high flows, which reflected conditions when concentrations of Al_i were more likely to be elevated above toxicity thresholds in acid-sensitive

watersheds. These findings are therefore generally applicable to periods when toxic conditions for brook trout and other fish species can occur. However, because stream water sampling occurred during moderate to moderately high flows, which occur commonly throughout the year, the modeling was based on a realistic representation of the chemical conditions to which fish were exposed.

Modeling results indicate that many Adirondack streams currently exceed their TLs needed to support healthy fisheries. This information will help inform the management of natural resources and to determine whether and to what extent further emissions reductions or other restoration options might be helpful. The finding that some streams may not be able to regain their preindustrial water chemistry in response to further reductions in the emissions and deposition of S and N, and in some cases may be unable to regain values within $20 \mu\text{eq L}^{-1}$ of preindustrial ANC, suggests that a management strategy such as watershed liming might be considered an option to accelerate recovery (Lawrence et al., 2016).

Under current conditions, the addition of calcium carbonate in the form of pulverized limestone (lime) or other bases would promote further recovery, rather than prevent additional harm. Addition of lime directly to lakes or streams can have some short-term benefits to specific ecosystem components but may not be appropriate for advancing long-term ecosystem recovery (Lawrence et al. 2016). Addition of lime to a watershed could provide acid buffering to reduce or eliminate mobilization of Al_i and improve the availability of base cation nutrients for utilization by both terrestrial and aquatic plants and animals in the short term (Lawrence et al. 2016). However, the extent and duration of potential benefits of watershed liming to accelerate recovery from acidic deposition remains uncertain.

Placing the results of this study in the context of ecosystem services can also be helpful in developing management strategies that promote recovery because environmental degradation caused by acidic deposition may affect a wide variety of ecosystem services that are important to human beneficiaries, such as anglers, bird watchers, artists, tourists, and many others (O'Dea et al. 2017). Target loads provide estimates of the pollution levels at which ecosystem services become compromised and an ecosystem transitions from a sustaining to non-sustaining condition (Sullivan 2012, Sullivan 2015). However, environmental policies based on the protection or restoration of ecosystem services may conflict with public opinions about governmental intervention, economic growth, and the cost of energy, which can be resolved during the development of appropriate public policies (Burns and Sullivan 2015).

5 References

- Aber, J.D. and C.A. Federer. 1992. A generalized, lumped-parameter model of photosynthesis, evapotranspiration and net primary production in temperate and boreal forest ecosystems. *Oecologia* 92:463-474.
- Aber, J.D. and R. Freuder. 2000. Variation among solar radiation data sets for the Eastern US and its effects on predictions of forest production and water yield. *Clim. Res.* 15:33-43.
- Aber, J.D., S.V. Ollinger, and C.T. Driscoll. 1997. Modeling nitrogen saturation in forest ecosystems in response to land use and atmospheric deposition. *Ecol. Model.* 101:61-78.
- April, R., R. Newton, and L. Truettner Coles. 1986. Chemical weathering in two Adirondack watersheds: Past and present-day rates. *GSA Bulletin* 97(10):1232-1238. 10.1130/0016-7606(1986)97<1232:CWITAW>2.0.CO;2.
- Arseneau, K.M.A., C.T. Driscoll, C.M. Cummings, G. Pope, and B.F. Cumming. 2016. Adirondack (NY, USA) reference lakes show a pronounced shift in chrysophyte species composition since ca. 1900. *J. Paleolimnol.* 56(4):349-364. 10.1007/s10933-016-9922-2.
- Baker, J.P., J. Van Sickle, C.J. Gagen, D.R. DeWalle, W.E. Sharpe, R.F. Carline, B.P. Baldigo, P.S. Murdoch, D.W. Bath, W.A. Kretser, H.A. Simonin, and P.J. Wigington, Jr. 1996. Episodic acidification of small streams in the northeastern United States: effects on fish populations. *Ecol. Appl.* 6(2):423-437.
- Baldigo, B.P., G.B. Lawrence, and H.A. Simonin. 2007. Persistent mortality of brook trout in episodically acidified streams of the southwestern Adirondack Mountains, New York. *Trans. Am. Fish. Soc.* 136:121-134.
- Baldigo, B.P., S.D. George, G.B. Lawrence, and E.A. Paul. 2019a. Acidification impacts and goals for gauging recovery of brook trout populations and fish communities in streams of the western Adirondack Mountains, New York, USA. *Trans. Am. Fish. Soc.* 148:373-392. doi:10.1002/tafs.10137.
- Baldigo, B.P., G.B. Lawrence, R.W. Bode, H.A. Simonin, K.M. Roy, and A.J. Smith. 2009. Impacts of acidification on macroinvertebrate communities in streams of the western Adirondack Mountains, New York, USA. *Ecol. Indicat.* 9:226-239.
- Baldigo, B.P., S.D. George, C.T. Driscoll, S. Shao, T.J. Sullivan, D.A. Burns, and G.B. Lawrence. 2019b. Probabilistic relationships between indicators of acid-base chemistry and fish assemblages in streams of the western Adirondack Mountains, New York, USA. *Canadian Journal of Fisheries and Aquatic Sciences.* 10.1139/cjfas-2018-0260.
- Baldigo, B.P., P.S. Murdoch, and D.A. Burns. 2005. Stream acidification and mortality of brook trout (*Salvelinus fontinalis*) in response to timber harvest in Catskill Mountain watersheds, New York, USA. *Can. J. Fish. Aquat. Sci.* 42(5):1168-1183.

- Bates, R.A. 1999. Response of basic cations in soil water to experimental addition of N and S compounds to forest soils in the Adirondack region of New York. Master's Thesis, Syracuse University, Syracuse, NY.
- Beier, C.M., J. Caputo, G.B. Lawrence, and T.J. Sullivan. 2017. Loss of ecosystem services due to chronic pollution of forests and surface waters in the Adirondack region (USA). *J. Environ. Manage.* 191:19-27. DOI: 10.1016/j.jenvman.2016.12.069.
- Blume, L.J., P.W.S. B. A. Schumacher, K.A. Cappel, M. L. Papp, R.D.V. Remortel, D.S. Coffey, M.G. Johnson, and D.J. Chaloud. 1990. Handbook of methods for acid deposition studies: Laboratory analyses for soil chemistry. EPA/600/4-90/023. U.S. Environmental Protection Agency, Washington, DC.
- Bobbink, R., K. Hicks, J. Galloway, T. Spranger, R. Alkemade, M. Ashmore, M. Bustamante, S. Cinderby, E. Davidson, F. Dentener, B. Emmett, J.-W. Erisman, M. Fenn, F.S. Gilliam, A. Nordin, L. Pardo, and W. DeVries. 2010. Global assessment of nitrogen deposition effects on terrestrial plant diversity: a synthesis. *Ecol. Appl.* 20:30-59.
- Brown, T.L. and N.A. Connelly. 1986. Tourism and employment in the Adirondack Park. *Annals of Tourism Research* 13(3):481-489.
- Bulger, A.J., B.J. Cosby, C.A. Dolloff, K.N. Eshleman, J.R. Webb, and J.N. Galloway. 1999. SNP:FISH, Shenandoah National Park: Fish in Sensitive Habitats. Project Final Report to National Park Service. University of Virginia, Charlottesville, VA.
- Burns, D.A. and T.J. Sullivan. 2015. Critical loads of Atmospheric Deposition to Adirondack Lake Watersheds: A Guide for Policymakers. New York State Energy Research and Development Authority, Albany, NY. 14 pp.
- Burns, D.A., J. Lynch, B.J. Cosby, M. Fenn, and J.S. Baron 2011. National Acid Precipitation Assessment Program Report to Congress 2011: An integrated assessment, National Science and Technology Council, Washington, D.C., 114 p.
- Burns, D.A., M.R. McHale, C.T. Driscoll, and K.M. Roy. 2006. Response of surface water chemistry to reduced levels of acid precipitation: comparison of trends in two regions of New York. *Hydrol. Process.* 20:1611-1627.
- Chen, L. and C.T. Driscoll. 2004. An evaluation of processes regulating spatial and temporal patterns in Lake Sulfate. *Glob. Biogeochem. Cycles* 18(3). DOI 10.1029/2003GB002169.
- Chen, L. and C.T. Driscoll. 2005a. Regional assessment of the response of acid-base status of lake-watersheds in the Adirondack region of New York to changes in atmospheric deposition using PnET-BGC. *Environ. Sci. Technol.* 39:787-794.
- Chen, L. and C.T. Driscoll. 2005b. Regional application of an integrated biogeochemical model to northern New England and Maine. *Ecol. Appl.* 15(3):1783-1797.

- Christopher, S.F., M.J. Mitchell, M.R. McHale, E.W. Boyer, D.A. Burns, and C. Kendall. 2008. Factors controlling nitrogen release from two forested catchments with contrasting hydrochemical responses. *Hydrol. Process.* 22(1):46-62. doi:10.1002/hyp.6632.
- Cronan, C.S., W.A. Reiners, R.C.J. Reynolds, and G.E. Lang. 1978. Forest floor leaching: contributions from mineral, organic, and carbonic acids in New Hampshire subalpine forests. *Science* 200(4339):309-311.
- Davies, T.D., M. Tranter, P.J. Wigington, K.N. Eshleman, N.E. Peters, J. Van Sickle, D.R. DeWalle, and P.S. Murdoch. 1999. Prediction of episodic acidification in North-eastern USA: an empirical/mechanistic approach. *Hydrol. Process.* 13(8):1181-1195. 10.1002/(SICI)1099-1085(19990615)13:8<1181::AID-HYP767>3.0.CO;2-9.
- Driscoll, C.T. 1985. Aluminum in acidic surface waters: chemistry, transport, and effects. *Environ. Health Perspect.* 63:93-104. 10.2307/3430034.
- Driscoll, C.T., M.D. Lehtinen, and T.J. Sullivan. 1994. Modeling the acid-base chemistry of organic solutes in Adirondack, New York, lakes. *Water Resour. Res.* 30:297-306.
- Driscoll, C.T., J.P. Baker, J.J. Bisogni, and C.L. Schofield. 1980. Effect of aluminum speciation on fish in dilute acidified waters. *Nature* 284:161-164.
- Driscoll, C.T., K.M. Driscoll, M.J. Mitchell, and D.J. Raynal. 2003. Effects of acidic deposition on forest and aquatic ecosystems in New York State. *Environ. Pollut.* 123:327-336.
- Driscoll, C.T., K.M. Driscoll, K.M. Roy, and J. Dukett. 2007. Changes in the chemistry of lakes in the Adirondack region of New York following declines in acidic deposition. *Water Air Soil Pollut.* 22(6):1181-1188.
- Driscoll, C.T., K.M. Driscoll, H. Fakhraei, and K. Civerolo. 2016. Long-term temporal trends and spatial patterns in the acid-base chemistry of lakes in the Adirondack region of New York in response to decreases in acidic deposition. *Atmos. Environ.* 146:5-14. <https://doi.org/10.1016/j.atmosenv.2016.08.034>.
- Driscoll, C.T., R.M. Newton, C.P. Gubala, J.P. Baker, and S.W. Christensen. 1991. Adirondack Mountains. *In*: Charles, D.F. (Ed.) *Acidic Deposition and Aquatic Ecosystems: Regional Case Studies*. Springer-Verlag, New York, NY. pp. 133-202.
- Driscoll, C.T., J.J. Buonocore, J.I. Levy, K.F. Lambert, D. Burtraw, S.B. Reid, H. Fakhraei, and J. Schwartz. 2015. US power plant carbon standards and clean air and health co-benefits. *Nature Climate Change* 5:535. 10.1038/nclimate2598.
- Driscoll, C.T., G.B. Lawrence, A.J. Bulger, T.J. Butler, C.S. Cronan, C. Eagar, K.F. Lambert, G.E. Likens, J.L. Stoddard, and K.C. Weathers. 2001. Acidic deposition in the northeastern United States: sources and inputs, ecosystem effects, and management strategies. *BioScience* 51(3):180-198.

- Eshleman, K.N., P.J. Wigington, Jr., T.D. Davies, and M. Tranter. 1992. Modelling episodic acidification of surface waters: the state of science. *Environmental pollution (Barking, Essex : 1987)* 77(2-3):287-295.
- Fakhraei, H. and C.T. Driscoll. 2015. Proton and Aluminum Binding Properties of Organic Acids in Surface Waters of the Northeastern U.S. *Environ. Sci. Technol.* 49(5):2939-2947. 10.1021/es504024u.
- Fakhraei, H., C.T. Driscoll, P. Selvendiran, J.V. DePinto, J. Bloomfield, S. Quinn, and H.C. Rowell. 2014. Development of a total maximum daily load (TMDL) for acid-impaired lakes in the Adirondack region of New York. *Atmos. Environ.* 95:277-287. 10.1016/j.atmosenv.2014.06.039.
- Fakhraei, H., C.T. Driscoll, J.R. Renfro, M.A. Kulp, T.F. Blett, P.F. Brewer, and J.S. Schwartz. 2016. Critical loads and exceedances for nitrogen and sulfur atmospheric deposition in Great Smoky Mountains National Park, United States. *Ecosphere* 7(10):1-28. 10.1002/ecs2.1466.
- Fitzpatrick, F.A., I.R. Waite, J. D'Arconte, M.R. Meador, M.A. Maupin, and M.E. Gurtz. 1998. Revised methods for characterizing stream habitat in the National Water-Quality Assessment Program. *Water Resources Investigations Report 98-4052*. U.S. Geological Survey.
- Galloway, J.N. and E.B. Cowling. 2002. Reactive nitrogen and the world: 200 years of change. *Ambio* 31:64-71.
- Gbondo-Tugbawa, S.S. and C.T. Driscoll. 2003. Factors controlling long-term changes in soil pools of exchangeable basic cations and stream acid neutralizing capacity in a northern hardwood forest ecosystem. *Biogeochemistry* 63:161– 185.
- Gbondo-Tugbawa, S.S., C.T. Driscoll, J.D. Aber, and G.E. Likens. 2001. Evaluation of an integrated biogeochemical model (PnET-BGC) at a northern hardwood forest ecosystem. *Water Resour. Res.* 37(4):1057-1070.
- Gensemer, R.W. and R.C. Playle. 1999. The bioavailability and toxicity of aluminum in aquatic environments. *Crit. Rev. Environ. Sci. Tech.* 29(4):315-450.
- George, S.D. and B.P. Baldigo. 2018. Adirondack and Catskill Stream-Fish Survey Dataset. U.S. Geological Survey, Troy, NY. doi: 10.5066/F70C4V25.
- Gilliam, F.S., D.A. Burns, C.T. Driscoll, S.D. Frey, G.M. Lovett, and S.A. Watmough. 2018. Decreased atmospheric nitrogen deposition in eastern North America: Predicted responses of forest ecosystems. *Environ. Pollut.* <https://doi.org/10.1016/j.envpol.2018.09.135>.
- Gran, G. 1952. Determination of the equivalence point in potentiometric titrations. *Int. Congr. Anal. Chem.* 77:661-671.
- Greaver, T.L., T.J. Sullivan, J.D. Herrick, M.C. Barber, J.S. Baron, B.J. Cosby, M. Deerhake, R. Dennis, J.J.D. Dubois, C. Goodale, A.T. Herlihy, G.B. Lawrence, L. Liu, J. Lynch, and K. Novak. 2012. Ecological effects of nitrogen and sulfur air pollution in the US: what do we know? *Frontiers in Ecology and the Environment*. doi:10.1890/110049 10(7):365-372.

- Gubala, C.P., C.T. Driscoll, R.M. Newton, and C.F. Schofield. 1991. The chemistry of a near-shore lake region during spring snowmelt. *Environ. Sci. Technol.* 25(12):2024-2030.
- Hemond, H.F. 1994. Role of organic acids in acidification of fresh waters. *In*: Steinberg, C.E.W. and R.F. Wright (Eds.). *Acidification of Freshwater Ecosystems: Implications for the Future*. John Wiley & Sons Ltd., Chichester. pp. 103-116.
- Husar, R.B., T.J. Sullivan, and D.F. Charles. 1991. Historical trends in atmospheric sulfur deposition and methods for assessing long-term trends in surface water chemistry. *In*: Charles, D.F. (Ed.) *Acidic Deposition and Aquatic Ecosystems: Regional Case Studies*. Springer-Verlag, New York. pp. 65-82.
- Ito, M., M.J. Mitchell, and C.T. Driscoll. 2002. Spatial patterns of precipitation quantity and chemistry and air temperature in the Adirondack region of New York. *Atmos. Environ.* 36:1051-1062.
- Janssen, P.H.M. and P.S.C. Heuberger. 1995. Calibration of process-oriented models. *Ecol. Model.* 83(1):55-66. [https://doi.org/10.1016/0304-3800\(95\)00084-9](https://doi.org/10.1016/0304-3800(95)00084-9).
- Jenkins, M.A., S. Jose, and P.S. White. 2007. Impacts of an exotic disease and vegetation change on foliar calcium cycling in Appalachian Forests. *Ecol. Appl.* 17(3):869-881.
- Johnson, A.H., A.J. Moyer, J.E. Bedison, S.L. Richter, and S.A. Willig. 2008. Seven decades of calcium depletion in organic horizons of Adirondack forest soils. *Soil Sci. Soc. Am. J.* 72:1824-1830. doi:10.2136/sssaj2006.0407.
- Johnson, D.W. and S.E. Lindberg. 1992. *Atmospheric Deposition and Forest Nutrient Cycling: A Synthesis of the Integrated Forest Ecological Series*. Springer, New York. 707 pp.
- Jørgensen, S.E. and G. Bendricchio (Eds.). 2001. *Fundamentals of Ecological Modelling* (3rd ed.), Amsterdam; New York.
- Josephson, D.C., J.M. Robinson, J. Chiotti, K.J. Jirka, and C.E. Kraft. 2014. Chemical and biological recovery from acid deposition within the Honnedaga Lake watershed, New York, USA. *Environ. Monitor. Assess.* 186(7):4391-4409. 10.1007/s10661-014-3706-9.
- Kang, P.-G. and M.J. Mitchell. 2013. Bioavailability and size-fraction of dissolved organic carbon, nitrogen, and sulfur at the Arbutus Lake watershed, Adirondack Mountains, NY. *Biogeochemistry* 115(1):213-234. 10.1007/s10533-013-9829-1.
- Lawrence, G.B., B. Momen, and K.M. Roy. 2004. Use of stream chemistry for monitoring acidic deposition effects in the Adirondack Region of New York. *J. Environ. Qual.* 33:1002-1009.
- Lawrence, G.B., D.A. Burns, and K. Riva-Murray. 2016. A new look at liming as an approach to accelerate recovery from acidic deposition effects. *Sci. Total Environ.* 562:35-46. <https://doi.org/10.1016/j.scitotenv.2016.03.176>.
- Lawrence, G.B., H.A. Simonin, B.P. Baldigo, K.M. Roy, and S.B. Capone. 2011. Changes in the chemistry of acidified Adirondack streams from the early 1980s to 2008. *Environ. Pollut.* 159:2750-2758.

- Lawrence, G.B., J.E. Dukett, N. Houck, P. Snyder, and S. Capone. 2013. Increases in dissolved organic carbon accelerate loss of toxic Al in Adirondack lakes recovering from acidification. *Environ. Sci. Technol.* 47(13):7095-7100. 10.1021/es4004763.
- Lawrence, G.B., Antidormi, M.R., McDonnell, T.C., Sullivan, T.J., and Bailey, S.W., 2020, Adirondack New York soil chemistry data, 1992-2017: U.S. Geological Survey data release, <https://doi.org/10.5066/P9YAWR0N>
- Lawrence, G.B., W.C. Shortle, M.B. David, K.T. Smith, R.A.F. Warby, and A.G. Lapenis. 2012. Early indications of soil recovery from acidic deposition in U.S. red spruce forests. *Soil Sci. Soc. Am. J.* 76:1407-1417. 10.2136/sssaj2011.0415.
- Lawrence, G.B., S.I. Passy, K.L. Pound, S.D. George, D.A. Burns, and B.P. Baldigo. 2018a. Results of the 2010-2011 East-Central Adirondack Stream Survey (ECASS). 18-26. New York State Energy Research and Technology Authority, Albany, NY.
- Lawrence, G.B., J.W. Sutherland, C.W. Boylen, S.A. Nierzwicki-Bauer, B. Momen, B.P. Baldigo, and H.A. Simonin. 2007. Acid rain effects on aluminum mobilization clarified by inclusion of strong organic acids. *Environ. Sci. Technol.* 41(1):93-98.
- Lawrence, G.B., B.P. Baldigo, K.M. Roy, H.A. Simonin, R.W. Bode, S.I. Passy, and S.B. Capone. 2008a. Results from the 2003-2005 Western Adirondack Stream Survey. Final Report 08-22. New York State Energy Research and Development Authority (NYSERDA).
- Lawrence, G.B., T.C. McDonnell, T.J. Sullivan, M. Dovciak, S.W. Bailey, M.R. Antidormi, and M.R. Zarfos. 2018b. Soil base saturation combines with beech bark disease to influence composition and structure of sugar maple-beech forests in an acid rain-impacted region. *Ecosystems* 21(4):795-810. 10.1007/s10021-017-0186-0.
- Lawrence, G.B., K.M. Roy, B.P. Baldigo, H.A. Simonin, S.B. Capone, J.W. Sutherland, S.A. Nierzwicki-Bauer, and C.W. Boylen. 2008b. Chronic and episodic acidification of Adirondack streams from acid rain in 2003-2005. *J. Environ. Qual.* 37:2264-2274.
- Lawrence, G.B., P.W. Hazlett, I.J. Fernandez, R. Ouimet, S.W. Bailey, W.C. Shortle, K.T. Smith, and M.R. Antidormi. 2015a. Declining acidic deposition begins reversal of forest-soil acidification in the northeastern U.S. and eastern Canada. *Environ. Sci. Technol.* 49:13103-13111.
- Lawrence, G.B., T.J. Sullivan, D.A. Burns, S.A. Bailey, B.J. Cosby, M. Dovciak, H.A. Ewing, T.C. McDonnell, R. Minocha, J. Quant, K.C. Rice, J. Siemion, and K. Weathers. 2015b. Acidic Deposition along the Appalachian Trail Corridor and its Effects on Acid-Sensitive Terrestrial and Aquatic Resources. Results of the Appalachian Trail MEGA-Transect Atmospheric Deposition Effects Study. Natural Resource Report NPS/NRSS/ARD/NRR—2015/996. National Park Service, Fort Collins, CO.
- Lawrence, G.B., T.C. McDonnell, and T.J. Sullivan. 2017. Adirondack New York vegetation data 2000-2015, 2000-2015: U.S. Geological Survey data release. <https://doi.org/10.5066/F70000B3>.

- McDonnell, T.C., T.J. Sullivan, and C.M. Beier. 2018a. Influence of climate on long-term recovery of Adirondack Mountain lakewater chemistry from atmospheric deposition of sulfur and nitrogen. *Adir. J. Environ. Stud.* 22:20-45.
- McDonnell, T.C., W.A. Jackson, B.J. Cosby, and T.J. Sullivan. 2018b. Atmospheric Deposition Effects Modeling for Resource Management on Southern Appalachian National Forests. Report prepared for USDA Forest Service, Asheville, NC. E&S Environmental Chemistry, Inc., Corvallis, OR.
- McNab, W.H. and P.E. Avers. 1994. Ecological subregions of the United States: section descriptions. U.S. Department of Agriculture, Forest Service, Washington, D.C. 267 pp.
- McNeil, B.E., R.E. Martell, and J.M. Read. 2006. GIS and biogeochemical models for examining the legacy of forest disturbance in the Adirondack Park, NY, USA. *Ecol. Model.* 195(3):281-295. <https://doi.org/10.1016/j.ecolmodel.2005.11.028>.
- Meador, M.R., J.P. McIntyre, and K.H. Pollock. 2003. Assessing the efficacy of single-pass backpack electrofishing to characterize fish community structure. *Trans. Am. Fish. Soc.* 132(1):39-46. [10.1577/1548-8659\(2003\)132<0039:ATEOSP>2.0.CO;2](https://doi.org/10.1577/1548-8659(2003)132<0039:ATEOSP>2.0.CO;2).
- Mitchell, M.J., G. Lovett, S. Bailey, D. Burns, D. Buso, T.A. Clair, F. Courchesne, L. Duchesne, C. Eimers, I. Fernandez, D. Houle, D.S. Jeffries, G.E. Likens, M.D. Moran, C. Rogers, D. Schwede, J. Shanley, K.C. Weathers, and R. Vet. 2011. Comparisons of watershed sulfur budgets in southeast Canada and northeast US: new approaches and implications. *Biogeochemistry* 103:181-207. DOI [10.1007/s10533-010-9455-0](https://doi.org/10.1007/s10533-010-9455-0).
- Neff, J.C., A.R. Townsend, G. Gleixner, S.J. Lehman, J. Turnbull, and W.D. Bowman. 2002. Variable effects of nitrogen additions on the stability and turnover of soil carbon. *Nature* 419(6910):915-917. http://www.nature.com/nature/journal/v419/n6910/supinfo/nature01136_S1.html.
- Nilsson, J. and P. Grennfelt. 1988. Critical Loads for Sulphur and Nitrogen. *Miljorapport 1988:15*. Nordic Council of Ministers, Copenhagen.
- O'Dea, C., S. Anderson, T. Sullivan, D. Landers, and F. Casey. 2017. Impacts to ecosystem services from aquatic acidification: using FECS-CS to understand the impacts of air pollution. *Ecosphere* 8(5):e01807. [10.1002/ecs2.1807](https://doi.org/10.1002/ecs2.1807).
- Ollinger, S.V., R.G. Lathrop, J.M. Ellis, J.D. Aber, G.M. Lovett, and S.E. Millham. 1993. A spatial model of atmospheric deposition for the northeastern US. *Ecol. Appl.* 3(3):459-472.
- Page, B.D. and M.J. Mitchell. 2008. Influences of a calcium gradient on soil inorganic nitrogen in the Adirondack Mountains, New York. *Ecol. Appl.* 18:1604-1614.
- Pourmokhtarian, A., C.T. Driscoll, J.L. Campbell, and K. Hayhoe. 2012. Modeling potential hydrochemical responses to climate change and increasing CO₂ at the Hubbard Brook Experimental Forest using a dynamic biogeochemical model (PnET-BGC). *Water Resour. Res.* 48(7):W07514. [10.1029/2011WR011228](https://doi.org/10.1029/2011WR011228).

- Pourmokhtarian, A., C.T. Driscoll, J.L. Campbell, K. Hayhoe, A.M.K. Stoner, M.B. Adams, D. Burns, I. Fernandez, M.J. Mitchell, and J.B. Shanley. 2017. Modeled ecohydrological responses to climate change at seven small watersheds in the northeastern United States. *Glob. Change Biol.* 23(2):840-856. doi:10.1111/gcb.13444.
- R Core Team. 2013. R: A Language and Environment for Statistical Computing. R Foundation for Statistical Computing, Vienna, Austria.
- Schaberg, P.G., D.H. DeHayes, G.J. Hawley, G.R. Strimbeck, J.R. Cumming, P.F. Murakami, and C.H. Borer. 2000. Acid mist, soil Ca and Al alter the mineral nutrition and physiology of red spruce. *Tree Physiol.* 20:73-85.
- Schwede, D.B. and G.G. Lear. 2014. A novel hybrid approach for estimating total deposition in the United States. *Atmos. Environ.* 92:207-220. <http://dx.doi.org/10.1016/j.atmosenv.2014.04.008>.
- Shepard, J.P., M.J. Mitchell, T.J. Scott, Y.M. Zhang, and D.J. Raynal. 1989. Measurements of wet and dry deposition in a northern hardwood forest. *Water Air Soil Pollut.* 48:225-238.
- Simonin, H.A., W.A. Kretser, D.W. Bath, M. Olson, and J. Gallagher. 1993. *In situ* bioassays of brook trout (*Salvelinus fontinalis*) and blacknose dace (*Rhinichthys atratulus*) in Adirondack streams affected by episodic acidification. *Can. J. For. Res.* 50:902-912.
- Simonson, T.D., J. Lyons, and P.D. Kanehl. 1994. Quantifying Fish Habitat in Streams: Transect Spacing, Sample Size, and a Proposed Framework. *N. Am. J. Fish. Manage.* 14(3):607-615. 10.1577/1548-8675(1994)014<0607:QFHIST>2.3.CO;2.
- Stager, J.C., S. McNulty, C. Beier, and J. Chiarenzelli. 2009. Historical Patterns and Effects of Changes In Adirondack Climates Since the Early 20th Century. *Adir. J. Environ. Stud.* 15(2):Article 5.
- StatPoint. 2010. STATGRAPHICS® Centurion XVI User Manual. StatPoint Technologies, Inc., Warrenton, VA. 305 pp.
- Strayer, D.L. 2010. Alien species in fresh waters: ecological effects, interactions with other stressors, and prospects for the future. *Freshw. Biol.* 55(s1):152-174. doi:10.1111/j.1365-2427.2009.02380.x.
- Sullivan, T.J. 2012. Combining ecosystem service and critical load concepts for resource management and public policy. *Water* 4:905-913. doi:10.3390/w4040905.
- Sullivan, T.J. 2015. Air Pollutant Deposition and Its Effects on Natural Resources in New York State. Cornell University Press, Ithaca, NY. 307 pp.
- Sullivan, T.J., B.J. Cosby, C.T. Driscoll, T.C. McDonnell, and A.T. Herlihy. 2011. Target loads of atmospheric sulfur deposition to protect terrestrial resources in the Adirondack Mountains, New York against biological impacts caused by soil acidification. *J. Environ. Stud. Sci.* 1(4):301-314.
- Sullivan, T.J., B.J. Cosby, C.T. Driscoll, T.C. McDonnell, A.T. Herlihy, and D.A. Burns. 2012. Target loads of atmospheric sulfur and nitrogen deposition for protection of acid sensitive aquatic resources in the Adirondack Mountains, New York. *Water Resour. Res.* 48:doi:10.1029/2011WR011171.

- Sullivan, T.J., B.J. Cosby, C.T. Driscoll, T.C. McDonnell, A.T. Herlihy, and D.A. Burns. 2014. Critical Loads of Sulfur and Nitrogen for Protection of Acid Sensitive Aquatic and Terrestrial Resources in the Adirondack Mountains. Summary Report. Report No. 14-11. New York State Energy Research and Development Authority (NYSERDA), Albany, NY.
- Sullivan, T.J., I.J. Fernandez, A.T. Herlihy, C.T. Driscoll, T.C. McDonnell, N.A. Nowicki, K.U. Snyder, and J.W. Sutherland. 2006a. Acid-base characteristics of soils in the Adirondack Mountains, New York. *Soil Sci. Soc. Am. J.* 70:141-152.
- Sullivan, T.J., G.B. Lawrence, S.W. Bailey, T.C. McDonnell, C.M. Beier, K.C. Weathers, G.T. McPherson, and D.A. Bishop. 2013. Effects of acidic deposition and soil acidification on sugar maple in the Adirondack Mountains, New York. *Environ. Sci. Technol.* 47:12687-12694. 10.1021/es401864w.
- Sullivan, T.J., C.T. Driscoll, C.M. Beier, D. Burtraw, I.J. Fernandez, J.N. Galloway, D.A. Gay, C.L. Goodale, G.E. Likens, G.M. Lovett, and S.A. Watmough. 2018. Air pollution success stories in the United States: The value of long-term observations. *Environ. Sci. Policy* 84:69-73. <https://doi.org/10.1016/j.envsci.2018.02.016>.
- Sullivan, T.J., C.T. Driscoll, B.J. Cosby, I.J. Fernandez, A.T. Herlihy, J. Zhai, R. Stemberger, K.U. Snyder, J.W. Sutherland, S.A. Nierzwicki-Bauer, C.W. Boylen, T.C. McDonnell, and N.A. Nowicki. 2006b. Assessment of the Extent to Which Intensively-Studied Lakes Are Representative of the Adirondack Mountain Region. Final Report 06-17. New York State Energy Research and Development Authority, Albany, NY.
- Sullivan, T.J., D.F. Charles, J.A. Bernert, B. McMartin, K.B. Vaché, and J. Zehr. 1999. Relationship between landscape characteristics, history, and lakewater acidification in the Adirondack Mountains, New York. *Water Air Soil Pollut.* 112:407-427.
- Sutherland, J.W., F.W. Acker, J.A. Bloomfield, C.W. Boylen, D.F. Charles, R.A. Daniels, L.W. Eichler, J.L. Farrell, R.S. Feranec, M.P. Hare, S.L. Kanfoush, R.J. Preall, S.O. Quinn, H.C. Rowell, W.F. Schoch, W.H. Shaw, C.A. Siegfried, T.J. Sullivan, D.A. Winkler, and S.A. Nierzwicki-Bauer. 2015. Brooktrout Lake case study: Biotic recovery from acid deposition 20 years after the 1990 Clean Air Act Amendments. *Environ. Sci. Technol.* 49(5):2665-2674. 10.1021/es5036865.
- Thomas, G.W. 1982. Exchangeable cations. *In*: Page, A.L. (Ed.) *Methods of Soil Analysis. Part 2. Chemical and Microbiological Properties.* American Society of Agronomy, Soil Science Society of America, Madison, WI. pp. 159-165.
- Thorndike, E. 1999. New York's Adirondack Park: Where U.S. wilderness preservation began. *International Journal of Wilderness* 5(1):9-14.
- U.S. Environmental Protection Agency. 2008. Integrated Science Assessment for Oxides of Nitrogen and Sulfur -- Ecological Criteria. EPA/600/R-08/082F. National Center for Environmental Assessment, Office of Research and Development, Research Triangle Park, NC.

- U.S. Environmental Protection Agency. 2009. Risk and Exposure Assessment for Review of the Secondary National Ambient Air Quality Standards for Oxides of Nitrogen and Oxides of Sulfur: Final. EPA-452/R-09-008a. Office of Air Quality Planning and Standards, Health and Environmental Impacts Division, Research Triangle Park, NC.
- U.S. Environmental Protection Agency. 2017. Integrated Science Assessment (ISA) for Oxides of Nitrogen, Oxides of Sulfur and Particulate Matter - Ecological Criteria (First External Review Draft). EPA/600/R-16/372. U.S. Environmental Protection Agency, Washington, DC.
- U.S. Geological Survey, 2018, USGS water data for the Nation: U.S. Geological Survey National Water Information System, accessed January 15, 2018, at <https://doi.org/10.5066/F7P55KJN>
- van Breemen, N., J. Mulder, and C.T. Driscoll. 1983. Acidification and alkalization of soils. *Plant Soil* 75:283-308.
- Van Deventer, J.S. and W.S. Platts. 1985. A computer software system for entering, managing, and analyzing fish capture data from streams. U.S. Forest Service Research Note INT-352.
- van Sickle, J., J.P. Baker, H.A. Simonin, B.P. Baldigo, W.A. Kretser, and W.E. Sharpe. 1996. Episodic acidification of small streams in the northeastern United States: fish mortality in field bioassays. *Ecol. Appl.* 6(2):408-421.
- Wigington, P.J., Jr., T.D. Davies, M. Tranter, and K.N. Eshleman. 1992. Comparison of episodic acidification in Canada, Europe and the United States. *Environ. Pollut.* 78(1-3):29-35.
- Wigington, P.J., Jr., D.R. DeWalle, P.S. Murdoch, W.A. Kretser, H.A. Simonin, J. Van Sickle, and J.P. Baker. 1996. Episodic acidification of small streams in the northeastern United States: ionic controls of episodes. *Ecol. Appl.* 6(2):389-407.
- Wu, W. and C.T. Driscoll. 2009. Application of the PnET-BGC – An integrated biogeochemical model – To assess the surface water ANC recovery in the Adirondack region of New York under three multi-pollutant proposals. *J. Hydrol.* 378(3):299-312. <https://doi.org/10.1016/j.jhydrol.2009.09.035>.
- Zhai, J., C.T. Driscoll, T.J. Sullivan, and B.J. Cosby. 2008. Regional application of the PnET-BGC model to assess historical acidification of Adirondack Lakes. *Water Resour. Res.* 44:W01421, doi:01410.01029/02006WR005532.
- Zhou, Q., C.T. Driscoll, and T.J. Sullivan. 2015. Responses of 20 lake-watersheds in the Adirondack region of New York to historical and potential future acidic deposition. *Sci. Total Environ.* 511:186-194. <http://dx.doi.org/10.1016/j.scitotenv.2014.12.044>.
- Zippin, C. 1958. The removal method of population estimation. *The Journal of Wildlife Management* 22(1):82-90. 10.2307/3797301.

Appendix A. Regression Models Used to Reconstruct the Historical Wet Deposition at Huntington Wildlife Forest between 1900 and 1978

The regression models were developed using annual national emissions (Tg yr^{-1}) and concentration in precipitation (mg L^{-1}) measured at an NADP site in the Adirondacks (NY20) during the period 1979-2015.

Concentration in Precipitation	=	Intercept	+	Slope	x	National Emission	R ²	P-Value
Ca ²⁺		1.701		0.681		PM ₁₀	0.63	<0.001
Mg ²⁺		-0.151		0.358		PM ₁₀	0.59	<0.001
K ⁺		0.126		0.047		PM ₁₀	0.34	<0.001
Na ⁺		-0.321		0.598		PM ₁₀	0.49	<0.001
NH ₄ ⁺		6.07		0.201		NO _x	0.09	0.065
NO ₃ ⁻		-6.603		1.202		NO _x	0.75	<0.001
Cl ⁻		0.986		0.388		PM ₁₀	0.43	<0.001
SO ₄ ²⁻		-3.012		1.893		SO ₂	0.70	<0.001

Appendix B. Model Calibration Input Data

This appendix summarizes the soil chemistry, watershed characteristics, land disturbance, and stream chemistry data used in model calibrations developed in this study.

B.1 Soil Chemistry

All soil samples that provided model calibration data for this study were sieved (2 mm) before analysis and were passed through an additional 1 mm sieve before pH, and carbon (C) and N analysis. All soil samples from the Buck watersheds, the WASS, the ASMP surveys and a single watershed within the drainage of Honnedaga Lake were analyzed in the USGS New York Water Science Center Laboratory for moisture content (oven dried at 65 °C and 105 °C for organic and mineral samples, respectively); exchangeable Ca, Mg, Na, and K (unbuffered 1 M NH₄Cl vacuum extraction); loss on ignition; and pH (0.01 M CaCl₂ slurry) following USEPA standard methods for acidic forest soils (Blume et al. 1990). Concentrations of C and N were determined by a thermo combustion elemental analyzer using the methods of the instrument manufacturer. Exchangeable Al was determined by 1 M KCl batch extraction and measurement by an inductively coupled plasma optical spectrometer (ICP). Exchangeable acidity was determined by 1 M KCl batch extraction and measurement by titration (Thomas 1982). Exchangeable H⁺ was calculated by subtracting exchangeable Al from exchangeable acidity. Effective cation exchange capacity was calculated as the sum of exchangeable acidity and exchangeable base cations (Ca, Mg, K, and Na). All data from these chemical analyses are available in Lawrence et al. (2017). Base saturation was calculated as the sum of exchangeable base cations divided by the effective cation exchange capacity.

B.2 Watershed Characteristics and Land Disturbance

Vegetation was classified by type for model application: northern hardwood, spruce-fir, red maple and red oak mixture, and red pine (Aber et al. 1997). The set of vegetation parameters was determined for each watershed based on a land cover geographic information system (GIS) data layer for the Adirondack region. The expected element content in vegetation was derived from measurements at the HWF (Johnson and Lindberg 1992).

Land disturbance history was incorporated into model simulations, although the Adirondack region has generally experienced limited human disturbance. The land disturbance information was obtained through Adirondack Park Agency GIS data layers, including a 1916 land cover map, information on major blow down events, and historical records of disturbance (McNeil et al. 2006). Most land disturbance in the

study watersheds from logging and associated fire occurred prior to 1916; however, major forest blow down events occurred in 1950 and 1995 (Sullivan et al. 1999). To account for the substantial disturbance that occurred from logging and fire around 1916, 80% removal of biomass at that time was assumed. Forest blow down and storms in 1950 and 1995 were accounted for in the simulations by assuming 50% and 40% biomass removal, respectively.

Weathering rate inputs for the PnET-BGC model simulations were obtained through model calibration (Table B-1.), using the observed stream water solute concentrations and soil chemistry. Weathering rates and other soil parameters (i.e., water holding capacity, soil mass, cation exchange coefficients, soil SO_4^{2-} adsorption capacity) were held constant over the simulation period. The model-calibrated base cation weathering rates among the 25 model sites were roughly in the same range as estimates of long-term weathering rates at Adirondack watersheds made by April et al. (1986): $0.62 \pm 0.21 \text{ keq ha}^{-1} \text{ year}^{-1}$ for Woods Lake and $0.50 \pm 0.25 \text{ keq ha}^{-1} \text{ year}^{-1}$ for Panther Lake. Soil cation exchange of Ca^{2+} , Mg^{2+} , Na^+ , H^+ , Al^{3+} , K^+ and NH_4^+ are depicted in PnET-BGC using Gaines-Thomas coefficients derived from soil solution concentrations and exchangeable base cation pools measured at Adirondack sites (Bates 1999). The adsorption of SO_4^{2-} , was modeled using a pH-dependent isotherm (Gbondon-Tugbawa et al. 2001).

Table B-1. Calibrated Model Parameters for 25 Simulated Streams

No.	Sites	Weathering Rate (g/m ² /month)					CEC (eq kg ⁻¹)	SO ₄ ²⁻ Adsorption (mol kg ⁻¹)	DOC Partitionin g	Site Density ^a
		Ca ²⁺	Mg ²⁺	Na ⁺	K ⁺	Cl ⁻				
3	North Buck	0.068	0.012	0.036	0.012	0.012	0.089	0.016	0.850	0.024
24	35014	0.055	0.010	0.032	0.013	0.009	0.085	0.021	0.582	0.021
20	27026	0.055	0.008	0.030	0.011	0.009	0.088	0.015	0.526	0.021
6	T24	0.034	0.004	0.030	0.008	0.009	0.080	0.011	0.485	0.018
23	22019	0.058	0.012	0.036	0.015	0.008	0.085	0.015	0.624	0.021
11	12003	0.062	0.012	0.045	0.012	0.009	0.082	0.016	0.835	0.019
10	WF	0.080	0.012	0.027	0.010	0.006	0.086	0.008	0.388	0.014
4	South Buck	0.072	0.012	0.042	0.012	0.010	0.092	0.012	0.485	0.016
22	13008	0.078	0.013	0.042	0.014	0.009	0.088	0.009	0.640	0.021
19	24002	0.096	0.016	0.040	0.013	0.010	0.093	0.015	0.568	0.021
21	28011	0.072	0.012	0.030	0.010	0.009	0.090	0.016	0.485	0.017
14	28014	0.082	0.018	0.045	0.010	0.009	0.086	0.008	0.385	0.015
9	NW	0.080	0.015	0.032	0.010	0.070	0.092	0.016	0.360	0.014
2	Buck Creek	0.122	0.016	0.036	0.012	0.010	0.090	0.014	0.582	0.021
7	AMP	0.194	0.021	0.048	0.013	0.010	0.097	0.016	0.505	0.020
13	27019	0.195	0.018	0.041	0.013	0.009	0.101	0.009	0.520	0.020
1	Archer	0.194	0.021	0.045	0.010	0.010	0.101	0.016	0.588	0.021
17	30009	0.203	0.023	0.055	0.013	0.009	0.100	0.014	0.530	0.020
12	26008	0.145	0.023	0.050	0.015	0.008	0.095	0.012	0.485	0.018
18	30019	0.208	0.026	0.052	0.013	0.022	0.103	0.014	0.676	0.023
16	29012	0.205	0.024	0.048	0.013	0.018	0.107	0.016	0.445	0.018
15	28030	0.210	0.027	0.034	0.012	0.009	0.100	0.013	0.625	0.022
8	N1	0.240	0.021	0.035	0.011	0.006	0.103	0.015	0.450	0.018
25	24001	0.245	0.025	0.029	0.015	0.010	0.104	0.009	0.582	0.021
5	S14	0.320	0.029	0.043	0.010	0.010	0.108	0.016	0.320	0.015

^a mol of organic anions per mol of organic C of each site

B.3 Stream Sampling Design and Methods

The WASS involved sampling of streams within the drainages of the Black and Oswegatchie River basins during August base flow in 2003 and 2004, spring snowmelt in 2004 and 2005, and late October high flow in 2003. The base flow sampling in 2003 presented in Lawrence et al. (2008) was not included in this analysis because it was conducted during extreme low-flow conditions when approximately one-quarter of the streams were dry. Samples were collected from approximately 195 WASS streams during each survey. To select streams within the study region for inclusion in WASS sampling, all streams that fit the following criteria were identified: (1) appeared on a USGS 1:24,000-scale quadrangle map, (2) accessible by hiking to and from the sampling location within approximately 1 hour, and (3) watershed did not contain upstream lakes or ponds that drained more than 25% of the total drainage area defined by the sampling point. From the 565 WASS streams that fit these criteria, 200 streams (total drainage area = 284 km²) were randomly selected for sampling. Stream order of the sampled streams ranged from 1 to 3, but most were first order. To reduce variability related to changing flow conditions at the time of sampling, the samples for each survey were collected on three consecutive days, with a few exceptions that were collected on the fourth consecutive day. Results of the WASS surveys were provided by Lawrence et al. (2011). Some WASS streams were sampled at the same locations on additional dates for comparison with historical data.

In the ECASS, stream samples were collected throughout the remainder of the Adirondack Ecological Region (McNab and Avers 1994) that were not within the Black and Oswegatchie River basins. The same criteria and randomized stream selection used in the WASS was also used in the ECASS. Approximately 200 streams were sampled in surveys conducted once during August base flows in 2010, once during spring snowmelt in 2011 and once during autumn after leaf drop in 2011.

Resampling of WASS streams was done in 2014–2015 to evaluate the response of the streams to the decreasing trend in wet atmospheric deposition of SO₄²⁻ that occurred in the region between the two sampling periods (2002–2005 and 2014–2015). Of the original 200 WASS sites, 64 were resampled once during snowmelt in 2014 and 2015, and once in the summer and fall of 2014. Stream selection for resampling was based on a random design stratified by four ranges of base-cation surplus (BCS), an acidification index that includes effects of strongly acidic acids (Lawrence et al. 2007). The BCS is similar to ANC but relates more directly to Al_i. The ranges in BCS (expressed in µeq L⁻¹) were defined

to represent streams that were severely acidic ($BCS < -30$), acidic ($-30 < BCS < 25$), weakly buffered ($25 < BCS < 75$), and moderately buffered ($75 < BCS < 250$) during spring snowmelt. These BCS ranges correspond approximately to the following ANC ranges: severely acidic ($ANC < 0.0$), acidic ($0.0 < ANC < 40$), weakly buffered ($40 < ANC < 80$), and moderately buffered ($80 < ANC < 250$).

Continuous records of stream chemistry were also available for use in this project from the three long-term monitoring watersheds associated with Buck Creek. Continuous measurements (weekly or biweekly) of ANC, and pH were collected by the USGS at the sampling site located on the main stem of Buck Creek (referred to as Main Buck) for the period 1991 through 2015. Stage-activated auto samples were also collected from March 2001 through 2015. Additional ANC and pH data from Main Buck were available intermittently from 1982 through 1985. The full suite of chemical measurements needed for monitoring and assessment of stream acid-base chemistry was also available for the streams in the North and South Buck Creek tributary watersheds from 1999 through 2015. Stage-activated auto samples were collected through the full record, and manually collected samples were taken at the tributary sites biweekly from May 2000 through 2015. Further information on Buck Creek stream chemistry can be found in Lawrence et al. (2011).

The WECASS stream samples were analyzed in the laboratory of the Adirondack Lakes Survey Corporation (ALSC) for concentrations of constituents needed to calculate the BCS (Ca^{2+} , Mg^{2+} , Na^+ , K^+ , SO_4^{2-} , NO_3^- , Cl^- and dissolved organic carbon [DOC]), as well as total monomeric Al (Al_m), organic monomeric Al (Al_o), Si, NH_4^+ , ANC, and pH following USEPA approved methods described elsewhere (Burns et al. 2006). Inorganic monomeric Al (Al_i) was calculated as the difference between Al_m and Al_o . Buck Creek stream samples were chemically analyzed for Ca^{2+} , Mg^{2+} , Na^+ , K^+ , SO_4^{2-} , NO_3^- , Cl^- , DOC, Si, NH_4^+ , ANC, and pH, at the Rensselaer Polytechnic Institute Keck Laboratory from January 1999 through May 1999. Buck Creek stream samples were analyzed for Al_m and Al_o at the USGS laboratory in Troy, NY, from January 1999 through September 2008 and for Ca^{2+} , Mg^{2+} , Na^+ , K^+ , SO_4^{2-} , NO_3^- , Cl^- , DOC, Si, NH_4^+ , ANC, and pH from June 1999 through September 2008. Samples from a stream in the Honnedaga Lake drainage were also collected approximately monthly and during high-flow events from 2011 to 2016 and analyzed in the USGS laboratory in Troy, NY, for the constituents listed above, following the same analysis methods. Buck Creek stream samples were analyzed at the ALSC laboratory from October 2008 through December 2015 for all analytes previously measured at the USGS Troy laboratory. In each lab,

the same USEPA methods were used (<https://nepis.epa.gov/Exe/ZyPDF.cgi?Dockey=30000TA0.PDF>; accessed January 15, 2018). Analysis of 99 samples at both the Keck and USGS Troy laboratories indicated an average difference between laboratories of less than 5 $\mu\text{mol L}^{-1}$, for all analyses except DOC (33 $\mu\text{mol C L}^{-1}$) and Si (6.4 $\mu\text{mol L}^{-1}$). Analysis of 155 stream samples collected from three sites in 2006 to 2008 and analyzed in the ALSC and USGS Troy laboratories showed a mean difference of 0.7 $\mu\text{mol L}^{-1}$. Stream chemistry data are available through the U.S. Geological Survey, National Water Information System—Web interface (U.S. Geological Survey, 2018).

Appendix C. The Role of Hydrologic Variation in WECASS stream Chemistry: ANC – Q Relations and Duration of Episodic Acidification

The relation between ANC_{max} and $\Delta ANC/\Delta Q$ based on the median measured ANC values at 309 of the WECASS streams that were part of this analysis is shown in Figure C-1. As ANC_{max} increases, $\Delta ANC/\Delta Q$ decreases. This pattern indicates that the magnitude of the decrease in ANC is reduced under increasing discharge as the low-flow ANC value decreases. This finding is consistent with past investigations of episodic acidification (Eshleman et al. 1992, Wigington et al. 1996, Davies et al. 1999). These data indicate that there is a robust regional episodic acidification relation across streams of the Adirondacks. This relation shows little scatter among these streams at ANC values less than about $90 \mu eq L^{-1}$, and greater scatter at higher ANC values (Figure C-1). The reasons for this greater scatter among the higher ANC streams are unclear, but these streams are relatively unimportant because they have ANC values well above biologically relevant thresholds. A preliminary exploration of landscape factors that may explain deviation from the regional relation for the higher ANC streams showed significant correlations between the magnitude of the residuals and some soil texture and depth metrics as well as soil pH (results not shown). This preliminary analysis suggests that soil permeability and pH may influence the magnitude of episodic acidification among these Adirondack streams, but further analysis would be needed to confirm this initial result.

The largest driver of the relation shown in Figure C-1 is likely to be simple dilution of base cation concentrations during hydrological episodes by rapid runoff derived from shallow flow paths, an increasingly important component of streamflow as discharge increases (Wigington et al. 1996). Dilution is a natural phenomenon and would occur even in the absence of acidic deposition. The rapid runoff entering the stream at high flow may have originated from dilute but non-acidic (no or low sulfuric or nitric acid) rainfall or snowmelt. However, at least part of the runoff that influences stream ANC under high flow reflects the influence of rapid biogeochemical processes in the soil such as cation exchange. Soil base cation pools that have been depleted by acidic deposition are likely less able to counter base cation dilution under current conditions, as compared with the period prior to the advent of acidic deposition. Dilution is likely to become an increasingly dominant driver of episodic acidification as low-flow ANC increases, which explains in part the inverse relation shown in Figure C-1 and Table C-1. However, other processes are likely to contribute to episodic acidification as well, including increases in

nitric and organic acids (Wigington et al. 1996). Sulfate typically dilutes under high flow in surface waters of the Adirondacks, indicating that sulfuric acid is not a likely contributor to episodic acidification in these waters, but rather has the opposite effect of minimizing ANC declines at high flow (Wigington et al. 1996). Further analysis of the drivers of episodic acidification in these streams could be performed through exploration of the charge balance ANC, but such an analysis is beyond the scope of this investigation.

Figure C-1. Relation between ANC_{max} and $\Delta ANC/\Delta Q$ at 309 Streams Sampled as Part of the WASS and ECASS Studies in the Adirondack Mountains

Each point represents the median value for a stream site. The solid line represents the best fit least squares linear regression through the data points, with the y-intercept, slope, and r^2 values shown. The dashed lines represent the 95% prediction intervals of the regression relation.

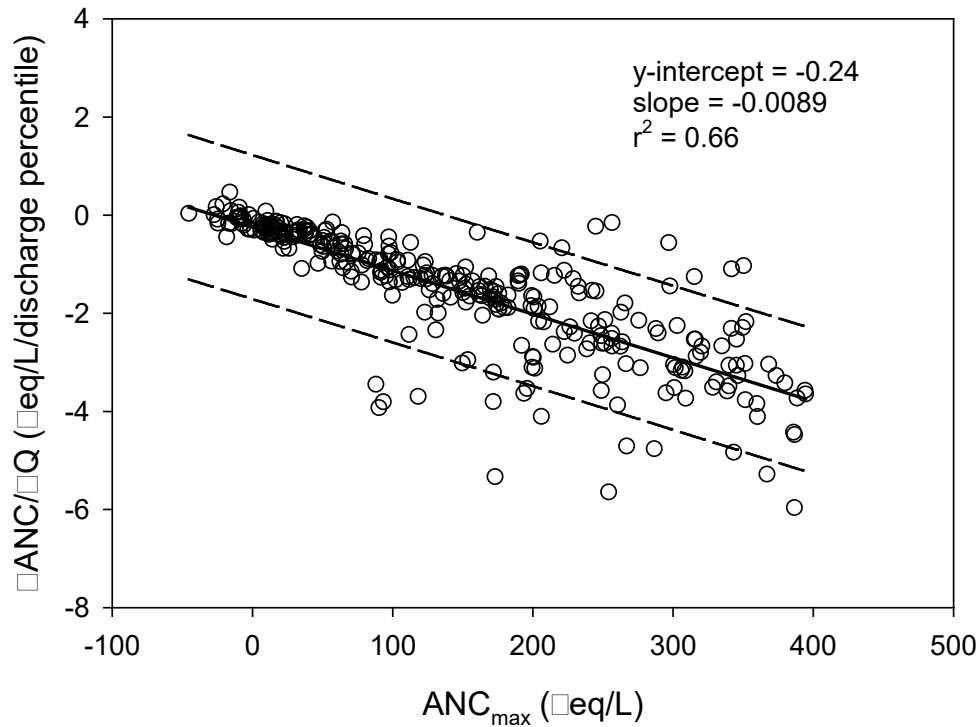


Table C-1. ANC at Low Flow (Q₁₅), Median Flow (Q₅₀), High Flow (Q₈₅), and the Low Flow

The high-flow ANC difference is based on the regression relations described in the caption of Figure 20.

Low Flow ANC at Q ₁₅ ($\mu\text{eq L}^{-1}$)	Median Flow ANC at Q ₅₀ ($\mu\text{eq L}^{-1}$)	High Flow ANC at Q ₈₅ ($\mu\text{eq L}^{-1}$)	Low Flow–High Flow ANC Difference ($\mu\text{eq L}^{-1}$)
-25	-24	-23	2
0	-7	-14	14
50	27	5	45
100	62	23	77
150	96	41	109
200	130	60	140
300	198	97	203
400	267	133	267

At low-flow ANC in the range of -25 to 0 $\mu\text{eq L}^{-1}$, little episodic acidification is predicted as discharge increases from low flow (Q₁₅) to high flow (Q₈₅). However, such streams are considered chronically acidic and not likely to support a healthy, diverse aquatic biological community even in the absence of pronounced episodic acidification. A hypothetical acid-sensitive Adirondack stream is estimated to decrease from low-flow ANC of 50 $\mu\text{eq L}^{-1}$ to high-flow ANC of 5 $\mu\text{eq L}^{-1}$, a value that would likely be accompanied by elevated and toxic Al_i concentrations. Even a stream with low-flow ANC of 100 $\mu\text{eq L}^{-1}$ is expected to decline to ANC of 23 $\mu\text{eq L}^{-1}$ at high flow, a value of potential concern depending on the persistence of that low ANC condition. At a higher low-flow ANC of 200 $\mu\text{eq L}^{-1}$ and above, the episodic decreases in ANC from low flow are large, but ANC values are expected to remain above those of concern with respect to the health of aquatic biota (Figure C-2).

Episodic acidification of streams is associated with mortality of caged brook trout held in streams of the Adirondacks and nearby regions (Baldigo et al. 2005, 2007). Concentrations of Al_i typically explain the most variation in fish mortality patterns among the related chemical constituents, and Al_i is generally viewed as the primary cause of fish mortality. An Al_i concentration of 2 $\mu\text{mol L}^{-1}$ appears to be an important threshold above which mortality increases sharply with exposures of as little as 2–4 days duration (Baldigo et al. 2007). This Al_i concentration threshold typically occurs when ANC values are about 0 to 20 $\mu\text{eq L}^{-1}$ in Adirondack streams, with some variation driven largely by DOC concentrations (Lawrence et al. 2007).

Because of the important role of duration of exposure to toxic conditions as well as intensity in promulgating deleterious effects on aquatic biota, we evaluated consecutive days of high flow at Buck Creek for the water year 2003 through 2015 study period. The results shown in Table C-2 indicate that flows of Q_{85} or greater lasting for two days and three to five days were common in Buck Creek during 2003–2015. Furthermore, continuous periods of six days or more of high flow were observed in every year during 2003–2015. In fact, 10 of 13 years had high-flow periods of 10 or more consecutive days, with some years exceeding 20 consecutive days. These high-flow periods that lasted 10 days or more all occurred during the spring snowmelt season of March to April. These results indicate that lengthy periods of high flow and episodic acidification occurred during every study year in Buck Creek and presumably most or all Adirondack streams—and that these periods of high flow are especially prolonged during spring snowmelt.

Figure C-2. Estimated ANC at Low Flow (Q_{15}), Median Flow (Q_{50}), and High Flow (Q_{85})

The data is based on the median $\Delta\text{ANC}/\Delta Q$ value at 309 Adirondack streams as a function of the ANC_{max} value as defined in the text. Best fit least squares linear regression relations are shown for each flow condition. These regression equations are as follows: $Q_{15} = 5.11 + (0.98 * \text{ANC}_{\text{max}})$, $r^2 = 0.92$, $p < 0.001$, $Q_{50} = -3.36 + (0.67 * \text{ANC}_{\text{max}})$, $r^2 = 0.90$, $p < 0.001$, $Q_{85} = -11.82 + (0.36 * \text{ANC}_{\text{max}})$, $r^2 = 0.53$, $p < 0.001$.

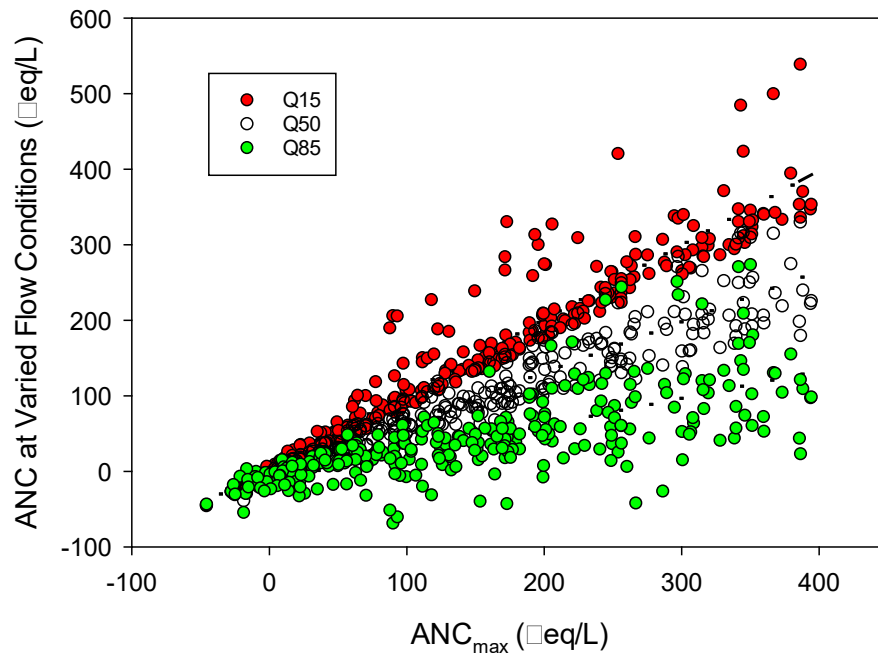


Table C-2. Consecutive Days that Stream Discharge Remained at Values of Q_{85} or Greater for Water Years 2003–2015 at Buck Creek near Inlet, NY

Water Year	1 day	2 days	3-5 days	6-10 days	11+ days	Maximum days
2003	5	4	2	-	2	15
2004	4	7	8	1	-	10
2005	2	5	5	1	1	12
2006	2	5	8	5	2	12
2007	5	1	6	4	-	9
2008	8	5	4	-	1	20
2009	6	4	8	1	1	12
2010	3	8	3	-	1	11
2011	2	5	6	1	1	22
2012	5	3	5	1	-	9
2013	6	7	5	1	-	6
2014	3	12	4	2	-	10
2015	2	6	3	-	1	14

Appendix D. Watershed Characteristics Used as Candidate Predictor Variables for Target Load Extrapolation

Variable ID	Description	Units	Source
CurrentANC	Measured stream water acid neutralizing capacity from WECASS	$\mu\text{eq L}^{-1}$	Cf., Lawrence et al. (2018)
CurrentBCS	Measured stream water base cation surplus from WECASS	$\mu\text{eq L}^{-1}$	Cf., Lawrence et al. (2018)
CurrentDep	Average (2014-2015) Total N+S deposition	$\text{meq m}^{-2} \text{yr}^{-1}$	Schwede and Lear (2014)
TotalDep60	Average (1955-2015) Total N+S deposition	$\text{meq m}^{-2} \text{yr}^{-1}$	Ito et al. (2002), Schwede and Lear (2014)
lat	Average latitude	degrees	N/A
lon	Average longitude	degrees	N/A
elev	Average elevation	m	https://nationalmap.gov/elevation.html
slope	Average slope	degrees	Derived from elevation
con42	Percent coniferous forest from NLCD 2011	%	https://www.mrlc.gov/
conmix	Percent coniferous + 50% mixed forest from NLCD 2011	%	https://www.mrlc.gov/
decid41	Percent deciduous forest from NLCD 2011	%	https://www.mrlc.gov/
decmix	Percent deciduous + 50% mixed forest from NLCD 2011	%	https://www.mrlc.gov/
mixed43	Percent mixed forest	%	https://www.mrlc.gov/
sand	Average percent sand	%	https://www.nrcs.usda.gov/wps/portal/nrcs/detail/soils/survey/?cid=nrcs142p2_053627 ; https://www.nrcs.usda.gov/wps/portal/nrcs/detail/soils/survey/geo/?cid=nrcs142p2_053629
silt	Average percent silt	%	https://www.nrcs.usda.gov/wps/portal/nrcs/detail/soils/survey/?cid=nrcs142p2_053627 ; https://www.nrcs.usda.gov/wps/portal/nrcs/detail/soils/survey/geo/?cid=nrcs142p2_053629
clay	Average percent clay	%	https://www.nrcs.usda.gov/wps/portal/nrcs/detail/soils/survey/?cid=nrcs142p2_053627 ; https://www.nrcs.usda.gov/wps/portal/nrcs/detail/soils/survey/geo/?cid=nrcs142p2_053629
soilph1to1	Average soil pH (1:1 slurry)	%	https://www.nrcs.usda.gov/wps/portal/nrcs/detail/soils/survey/?cid=nrcs142p2_053627 ; https://www.nrcs.usda.gov/wps/portal/nrcs/detail/soils/survey/geo/?cid=nrcs142p2_053629

depth_rz	Average depth to root zone	%	https://www.nrcs.usda.gov/wps/portal/nrcs/detail/soils/survey/?cid=nrcs142p2_053627; https://www.nrcs.usda.gov/wps/portal/nrcs/detail/soils/survey/geo/?cid=nrcs142p2_053629
soc	Average soil organic carbon	%	https://www.nrcs.usda.gov/wps/portal/nrcs/detail/soils/survey/?cid=nrcs142p2_053627; https://www.nrcs.usda.gov/wps/portal/nrcs/detail/soils/survey/geo/?cid=nrcs142p2_053629

Appendix E. Ambient Stream Chemistry from WECASS

In this appendix, WECASS stream chemistry results used as the basis for regionalizing modeling results are summarized. Mean pH varied from 5.63 to 6.11 among the four WASS surveys shown in Table E-1, but the 5th and 95th percentiles varied from 4.55 to 7.47 among the 195 streams sampled in just one (August 2004) stream survey (Table E-1.) Although mean pH values exhibited clear seasonal variation, the range in pH values among the individual streams was similar in each of the surveys, particularly for the most acidic streams. The WASS included streams that were chronically acidic.

Values of mean BCS in the WASS varied by $124 \mu\text{eq L}^{-1}$ among surveys but varied by $677 \mu\text{eq L}^{-1}$ between the 5th and 95th percentile among streams in the August 2004 survey (Table E-1). ANC exhibited similar, although somewhat smaller variation (mean generally near $70 \mu\text{eq L}^{-1}$) in comparison to BCS, and summer base flow values averaged across all streams were approximately $100 \mu\text{eq L}^{-1}$ higher than mean values for either spring snowmelt survey (Table E-1). In each of the surveys, the mean concentration of Al_i equaled or exceeded $2 \mu\text{mol L}^{-1}$, which has been shown previously to cause mortality in young-of-the-year brook trout. Concentrations of nontoxic Al_o were somewhat higher than those of Al_i in each of the surveys, except those conducted during spring snowmelt (March 2004 and 2005). Concentrations of Al_i at the 95th percentile were 13 and $12 \mu\text{mol L}^{-1}$ in the March 2004 and March 2005 surveys, respectively, far in excess of concentrations that can be tolerated by fish (Baldigo et al. 2007).

Table E-1. Results of the Western Adirondack Stream Surveys (WASS)

The table shows the number of streams sampled, mean flow (L s^{-1}) during the survey, and the mean and range (5th percentile and 95th percentile) of chemical measurements made in each of the four sampling surveys. The base cation surplus (BCS) and acid-neutralizing capacity by Gran titration (ANC_G) are expressed as $\mu\text{eq L}^{-1}$. The remaining measurements are expressed as $\mu\text{mol L}^{-1}$.

WASS				
Survey Date	Oct. 27-30 2003	Aug. 16-18 2004	Mar. 29-31 2004	Mar. 29-Apr. 1 2005
No. of streams	196	195	188	190
Mean flow	446	30.2	255	182
pH	5.58	6.11	5.63	5.85
	4.45 to 7.01	4.55 to 7.47	4.43 to 7.16	4.58 to 7.21

Table E-1 continued

WASS				
Survey Date	Survey Date	Survey Date	Survey Date	Survey Date
BCS	58	153	29	51
	-72 to 241	-73 to 604	-97 to 224	-87 to 284
ANC _G	78	168	62	74
	-32 to 251	-19 to 578	-27 to 246	-18 to 311
Inorganic Al	3	2	3	3
	0 to 9	0 to 6	0 to 13	0 to 12
Organic Al	5	4	3	3
	1 to 9	1 to 9	1 to 6	1 to 6
DOC	792	712	412	417
	312 to 1350	142 to 1986	147 to 693	163 to 704
SO ₄ ²⁻	53	38	46	45
	40 to 71	14 to 58	37 to 61	35 to 57
NO ₃ ⁻	6	6	36	31
	0 to 16	1 to 16	5 to 77	6 to 72
Cl ⁻	26	14	34	21
	9 to 77	4 to 50	5 to 49	7 to 56
Ca ²⁺	71	93	62	65
	19 to 141	19 to 269	20 to 134	22 to 149
Mg ²⁺	23	31	19	22
	7 to 61	6 to 99	7 to 48	8 to 55
Na ⁺	41	44	46	38
	18 to 89	16 to 83	18 to 63	21 to 65
K ⁺	11	6	9	10
	4 to 19	1 to 14	5 to 13	5 to 15
Si	117	158	105	120
	77 to 185	81 to 247	75 to 178	81 to 181
NH ₄ ⁺	0	1	1	1
	0 to 1	0 to 2	0 to 2	0 to 4

The mean concentration of DOC in the October 2003 survey was $792 \mu\text{mol L}^{-1}$, the highest of the four surveys, although the value for the August 2004 survey approached this level (Table E-1). Mean concentrations of SO_4^{2-} showed limited seasonal variation and only ranged from 38 to $53 \mu\text{mol L}^{-1}$ among the four WASS surveys (Table E-1). In contrast, NO_3^- concentrations showed distinct seasonal variation, with high concentrations during the March 2004 and March 2005 surveys and low concentrations during the August 2004 survey and the October 2003 survey. Mean concentrations of Cl^- were lowest in the August 2004 survey and highest in the March 2004 survey, but the concentration range was greatest in the October 2003 survey.

Some seasonality was observed in Ca^{2+} and Mg^{2+} concentrations, with highest concentrations during the August 2004 survey, and lowest concentrations during the March surveys (Table E-1). This pattern was likely indicative of deeper subsurface flow paths in summer base flow than during the high-flow periods of spring snowmelt. Little or no seasonality was apparent in the mean concentrations of Na^+ and K^+ (Table E-1). Mean concentrations of NH_4^+ were near the analytical reporting limit in each of the surveys, and few streams had concentrations that exceeded $2 \mu\text{mol L}^{-1}$. Effects of season and flow on stream chemistry were reflected in variations in the mean concentrations of sampling periods in the WASS and ECASS (Table E-1, Table E-2). These data indicated that the most acidic conditions occurred during snowmelt and the least acidic conditions occurred during August samplings in both surveys. Mean pH in the WASS ranged from 5.58 in the 2004 snowmelt sampling period to 6.11 in the August 2004 sampling (Table E-1), and in the ECASS from 6.63 in the 2011 snowmelt sampling to 6.88 in the August 2010 sampling (Table E-2). Similarly, mean values of ANC were lower during snowmelt than August by approximately $100 \mu\text{eq L}^{-1}$ in the WASS and more than $200 \mu\text{eq L}^{-1}$ in the ECASS.

Table E-2. Results of the East-Central Adirondack Stream Surveys (ECASS)

The table shows the number of streams sampled, mean flow ($L s^{-1}$) during the survey, and the mean and range (5th percentile and 95 percentile) of chemical measurements made in each of the four sampling surveys. The base cation surplus (BCS) and acid-neutralizing capacity by Gran titration (ANC_G) are expressed as $\mu eq L^{-1}$. The remaining measurements are expressed as $\mu mol L^{-1}$.

ECASS			
Survey Date	Aug. 9-11 2010	Apr. 18-20 2011	Oct. 31-Nov 2 2011
No. of streams	178	195	203
Mean flow	21	352	40
pH	6.88	6.33	6.67
	5.42 to 7.79	4.87 to 7.33	4.99 to 7.53
BCS	307	83	169
	-6.5 to 985	-46 to 277	-31 to 565
ANCG	316	89	181
	9.7 to 1025	-5 to 295	-1.6 to 560
Inorganic Al	0.3	0.8	0.3
	0 to 0.7	0 to 3.4	0 to 1.3
Organic Al	1.8	2.3	2.1
	1.3 to 2.7	1.2 to 4.1	1.1 to 4.1
DOC	273	277	253
	102 to 661	124 to 493	107 to 483
SO42-	43	34	39
	23 to 60	24 to 47	25 to 51
NO3-	9.2	17	9.6
	0.6 to 23.9	0.1 to 52	0 to 29
Cl-	9.2	7.9	9.4
	5.3 to 16	4.5 to 13	5.7 to 16
Ca2+	133	61	87
	26 to 383	21 to 135	23 to 219
Mg2+	50	21	32
	10 to 139	6.4 to 48	7.5 to 87
Na+	58	28	40
	29 to 96	18 to 43	21 to 69
K+	4.8	3.3	3.8
	0.7 to 10	0.7 to 7.1	1.0 to 8.5
Si	203	103	151
	108 to 297	63 to 157	82 to 232
NH4+	0.6	0.6	0.3
	0 to 1.2	0 to 1.1	0 to 0.8

Average values of BCS for all WASS and ECASS sampling periods were above zero, with the lowest mean value being $29 \mu\text{eq L}^{-1}$ during the WASS 2004 snowmelt sampling. Because a BCS value of $0 \mu\text{eq L}^{-1}$ represents the threshold for mobilization of Al_i (Lawrence et al. 2007), positive mean values for all sampling periods were reflected by low mean concentrations of Al_i .

Mean concentrations of DOC in WASS streams were considerably higher during the August and October samplings than during the snowmelt samplings (Table E-1), but mean concentrations in the ECASS streams were highly similar during each of the sampling periods (Table E-2). The mean concentrations of Al_o fit these same patterns in the WASS and ECASS surveys, which was consistent with the strong control DOC typically exerts over Al_o concentrations. Mean concentrations of SO_4^{2-} showed limited variation among sampling periods of both the WASS and ECASS. In contrast, NO_3^- concentrations showed distinct differences among sampling periods, with high concentrations during the snowmelt sampling periods and low concentrations during the August 2004 and October sampling periods in both the WASS and ECASS. In the WASS, mean concentrations of Cl^- were lowest in the August 2004 sampling whereas in the ECASS, concentrations for each of the sampling periods were similarly low.

Mean concentrations of Ca^{2+} and Mg^{2+} in the WASS and ECASS were highest during the August samplings and lowest during the snowmelt samplings, but Na^+ and K^+ , which often behave similarly to Ca^{2+} and Mg^{2+} , did not show large differences among the sampling periods in either survey (Table E-1, Table E-2). Mean concentrations of Si were highest during the August sampling and similar during the snowmelt and October samplings in the WASS, and also highest in the August ECASS sampling, although the mean for the October ECASS sampling was considerably higher than for the August sampling. Mean concentrations of NH_4^+ were extremely low during all sampling periods of both surveys.

Spatial variations of chemistry among individual streams varied widely within both the WASS and ECASS regions. For example, pH values ranged from 4.55 to 7.47, and ANC varied from -19 to $578 \mu\text{eq L}^{-1}$, between the 5th and 95th percentiles in WASS streams during the August sampling (Table E-1). Concentrations of Al_i for these percentiles in WASS streams sampled in the 2004 snowmelt ranged from zero to a highly toxic level of $13 \mu\text{mol L}^{-1}$ (Table E-2). Ranges were also large for measures of acidification in the ECASS, but these ranges reflected less acidification than those seen in the WASS. For example, pH in the August ECASS sampling ranged from 5.42 to 7.79, and ANC ranged from 9.7 to $1025 \mu\text{eq L}^{-1}$ for the 5th and 95th percentiles. The generally lower level of

acidification in the ECASS than the WASS was also reflected in the snowmelt Al_i range of 0 to $3.4 \mu\text{mol L}^{-1}$ for those percentiles in the ECASS region. Nevertheless, the range in pH for 5th and 95th percentiles of the 2005 WASS snowmelt sampling was 4.58 to 7.21, which was similar to the ECASS snowmelt range of 4.87 to 7.33. Overall, these data exhibited a wide range in acidity levels from severely acidic to circumneutral within both study regions.

The greatest range in DOC concentrations in both the WASS (Table E-1) and ECASS (Table E-2) occurred in August samplings, and the minimum concentrations were similar in the two surveys. However, highest DOC concentrations in WASS streams during August and October were much greater by a factor of two or more than those measured in the ECASS, whereas the snowmelt ranges in the two surveys were similar. Ranges of SO_4^{2-} were relatively high in the WASS August sampling, ranging from 14 to $58 \mu\text{mol L}^{-1}$ from the 5th to the 95th percentile, but otherwise similar between WASS and ECASS samplings. Concentrations of NO_3^- for these percentiles ranged from less than 10 to over $70 \mu\text{mol L}^{-1}$ in the WASS snowmelt samplings, but from only 0 to $16 \mu\text{mol L}^{-1}$ in the WASS August sampling. Similarly, NO_3^- concentrations for these percentiles ranged from 0.1 to $52 \mu\text{mol L}^{-1}$ in the ECASS snowmelt sampling and only 0.6 to $24 \mu\text{mol L}^{-1}$ in the ECASS August sampling. The low end of the ranges for Cl^- were similar between WASS and ECASS samplings, but the highest concentrations of WASS streams were considerably higher than those of ECASS streams.

Concentrations of Ca^{2+} and Mg^{2+} exhibited the lowest ranges in the snowmelt samplings of both surveys, largely because concentrations were reduced under elevated flows (Table E-1, Table E-2). However, ranges tended to be greater for the ECASS samplings than the WASS samplings because of the difference in the highest concentration values. For example, the Ca^{2+} concentrations for 5th and 95th percentiles of the August WASS sampling ranged from 19 to $269 \mu\text{mol L}^{-1}$, whereas the concentrations for these percentiles of the August ECASS ranged from 26 to $383 \mu\text{mol L}^{-1}$. Concentration ranges for Na^+ and K^+ were smaller than those observed for Ca^{2+} and Mg^{2+} and were similar between WASS and ECASS samplings. Concentration ranges for Si exhibited the same relationships among samplings and between surveys as Ca^{2+} and Mg^{2+} . Like the mean concentrations for WASS and ECASS samplings, the concentration ranges for NH_4^+ were small because little NH_4^+ was measured in any of the streams.

APPENDIX F. USGS Identification Numbers Needed for Data Retrieval from the National Water Information System (NWIS) Database

NWIS ID	Descriptive Text	Latitude	Longitude
04253294	South Tributary Buck Creek, BB07	43.741597	-74.710970
04253295	North Tributary Buck Creek, AB07	43.743562	-74.712254
04253296	Main Buck Creek, BC01	43.743947	-74.722194
434531074473001	AEAP, EW01	43.758611	-74.791667
434801074505701	AEAP, EW03	43.800278	-74.849167
434903074525401	AEAP, EW06	43.817500	-74.881667
434353074530001	AEAP, EW08	43.731389	-74.883333
434252074540201	AEAP, EW09	43.714444	-74.900556
434417074445501	AEAP, EW11	43.738056	-74.748611
434948074515801	AEAP, EW13	43.830000	-74.866111
434458074481701	AEAP, EW16	43.749444	-74.804722
434836074030201	ASM, NW	43.810000	-74.050778
441424074155501	ASM, AMP	44.240250	-74.265361
440034074184801	ASM, N1	44.009611	-74.313500
434816074494201	ASM, WF	43.804667	-74.828361
434054074421001	Benedict Creek, Benedict Brook	43.681722	-74.702972
441549075114301	WECASS 1001, Former_WASS	44.263831	-75.195383
432652074243301	WECASS 1003, Former_ECASS	43.447992	-74.409178
432455074331601	WECASS 1004, Former_ECASS	43.415297	-74.554675
441750075121501	WECASS 1005, Former_WASS	44.297306	-75.204269
432407074343701	WECASS 1005s, Former_ECASS	43.402167	-74.577000
441512075092701	WECASS 1006, Former_WASS	44.253353	-75.157519
441556075110701	WECASS 1007, Former_WASS	44.265556	-75.185489
432806074304801	WECASS 1007s, Former_ECASS	43.468417	-74.513556
431631074402401	WECASS 1008a, Former_ECASS	43.275278	-74.673444
431625074401001	WECASS 1008b, Former_ECASS	43.273833	-74.669667
441731075125901	WECASS 1009, Former_WASS	44.291972	-75.216408
432157074255501	WECASS 1010, Former_ECASS	43.366078	-74.432200
432626074315201	WECASS 1011, Former_ECASS	43.440756	-74.531242
432522074523301	WECASS 1012, Former_ECASS	43.422911	-74.875989
432416074340801	WECASS 1013, Former_ECASS	43.404519	-74.568894
432245074591901	WECASS 1014, Former_ECASS	43.379192	-74.988681
441615075083301	WECASS 1016, Former_WASS	44.270839	-75.142653
441741075083101	WECASS 1017, Former_WASS	44.294789	-75.142086
441503075085501	WECASS 1019, Former_WASS	44.250844	-75.148619

Table F continued

NWIS ID	Descriptive Text	Latitude	Longitude
441520075084301	WECASS 1020, Former_WASS	44.255800	-75.145375
441008074233401	WECASS 126	44.168889	-74.392778
440750074262301	WECASS 144	44.130667	-74.439722
442845074264601	WECASS 179	44.479417	-74.446333
441140073505301	WECASS 2007a, Slide_Brook	44.194608	-73.848064
441130073504301	WECASS 2007b, Brothers_Trail	44.191794	-73.845464
440900073555301	WECASS 2011, Former_ECASS	44.150056	-73.931472
435651073495601	WECASS 223	43.947500	-73.832306
442833074274101	WECASS 235	44.475917	-74.461472
440730074292201	WECASS 241	44.125167	-74.489583
444319073493501	WECASS 26	44.721972	-73.826444
441345073525501	WECASS 2E, Former_ECASS	44.229272	-73.882056
441749075163901	WECASS 2W, Former_WASS	44.296969	-75.277600
435917073432801	WECASS 44	43.988278	-73.724667
440908073444901	WECASS 73	44.152222	-73.747139
440900074305901	WECASS 92	44.150111	-74.516611
442931074233001	WECASS 94	44.492194	-74.391694
441953073590801	WECASS 0	44.331639	-73.985561
440759073442801	WECASS 10	44.133181	-73.741208
441905075043301	WECASS 1017B, Orebed Creek	44.318250	-75.075983
432417074470401	WECASS 102	43.404814	-74.784533
434024073374201	WECASS 103	43.673594	-73.628503
432217074252801	WECASS 104	43.371600	-74.424619
441820073485301	WECASS 105	44.305750	-73.814861
441031073370601	WECASS 107	44.175403	-73.618506
441140073301401	WECASS 108	44.194689	-73.504069
441258073314701	WECASS 109	44.216358	-73.529919
442518073394401	WECASS 11	44.421897	-73.662481
442758073531101	WECASS 110	44.466378	-73.886436
440016075193501	WECASS 11001	44.004506	-75.326628
440250075171901	WECASS 11008	44.047372	-75.288664
440239075165601	WECASS 11010	44.044328	-75.282408
440320075184201	WECASS 11011	44.055775	-75.311803
440351075175501	WECASS 11012, Unnamed	44.064272	-75.298736
440530075163801	WECASS 11014	44.091789	-75.277264
440711075171501	WECASS 11019	44.119942	-75.287767
440710075173501	WECASS 11020	44.119569	-75.293139
440701075192101	WECASS 11022	44.117147	-75.322747
440657075191301	WECASS 11023	44.115983	-75.320492
440606075200201	WECASS 11025	44.101719	-75.333908

Table F Continued

NWIS ID	Descriptive Text	Latitude	Longitude
440154075184701	WECASS 11027	44.031914	-75.313175
443535073421401	WECASS 112	44.593069	-73.703986
440007073431901	WECASS 113	44.002086	-73.722033
441957073314601	WECASS 114	44.332678	-73.529664
442156073504901	WECASS 115	44.365678	-73.847058
433914074241401	WECASS 116	43.653906	-74.404092
434850073560401	WECASS 117	43.814022	-73.934539
441452074232501	WECASS 119	44.247892	-74.390544
433005074183801	WECASS 120	43.501447	-74.310594
440151075084801	WECASS 12003	44.030897	-75.146819
440125075084201	WECASS 12008	44.023786	-75.145056
440654075073001	WECASS 12012	44.115014	-75.125158
440720075060001	WECASS 12012A, Mud Creek	44.122494	-75.100150
440705075141901	WECASS 12017	44.118075	-75.238642
440729075143701	WECASS 12019	44.124908	-75.243669
440430075142201	WECASS 12020	44.075128	-75.239719
440603075143001	WECASS 12022	44.100961	-75.241822
440610075143701	WECASS 12023	44.102939	-75.243831
440613075144301	WECASS 12024	44.103836	-75.245458
440303075131601	WECASS 12027	44.050856	-75.221144
441712074041001	WECASS 123	44.286700	-74.069472
432452074432101	WECASS 124	43.414447	-74.722775
441654073394201	WECASS 125	44.281742	-73.661894
431942074023401	WECASS 127	43.328561	-74.042900
440742073391001	WECASS 128	44.128356	-73.652889
431517074211201	WECASS 129	43.254925	-74.353489
441702073411801	WECASS 130	44.283992	-73.688378
440201075053401	WECASS 13008	44.033656	-75.092789
440213075062701	WECASS 13009	44.036972	-75.107519
440239075051001	WECASS 13012	44.044194	-75.086314
440647075041601	WECASS 13019	44.113261	-75.071169
434211074150201	WECASS 131	43.703181	-74.250808
435327074245401	WECASS 132	43.890944	-74.415028
434343074013501	WECASS 134	43.728764	-74.026492
430823074303201	WECASS 138	43.139769	-74.509031
435740074240801	WECASS 139	43.961272	-74.402339
441812073424301	WECASS 14	44.303358	-73.712008
435441074242501	WECASS 140	43.911467	-74.407125
442059073491001	WECASS 142	44.349889	-73.819697
440141074015301	WECASS 143	44.028253	-74.031456

Table F continued

NWIS ID	Descriptive Text	Latitude	Longitude
434211074065801	WECASS 145	43.703233	-74.116308
435024074255001	WECASS 147	43.840117	-74.430697
434848073512801	WECASS 148	43.813356	-73.857831
435626074265101	WECASS 15	43.940711	-74.447661
434233074160501	WECASS 150	43.709178	-74.268211
440019074505101	WECASS 15001	44.005500	-74.847756
440005074491401	WECASS 15002	44.001408	-74.820700
440821073381401	WECASS 151	44.139267	-73.637222
431943074051001	WECASS 153	43.328650	-74.086275
431731074023501	WECASS 153B, Glasshouse Creek	43.292011	-74.043136
440841073475901	WECASS 154	44.144828	-73.799761
435806074030401	WECASS 156	43.968428	-74.051339
440005074463501	WECASS 15650	44.001556	-74.776444
440003074464601	WECASS 15651	44.001083	-74.779639
440008074465301	WECASS 15652	44.002472	-74.781611
440005074470201	WECASS 15653	44.001444	-74.783917
440004074471601	WECASS 15654	44.001125	-74.787833
440001074472301	WECASS 15655	44.000417	-74.789806
440000074473801	WECASS 15656	44.000000	-74.793917
435951074475001	WECASS 15657	43.997722	-74.797389
440126074502101	WECASS 15670	44.023917	-74.839389
440128074500701	WECASS 15671	44.024556	-74.835472
440134074495301	WECASS 15672	44.026306	-74.831528
440141074494301	WECASS 15673	44.028306	-74.828778
440149074493201	WECASS 15674	44.030361	-74.825694
440148074491801	WECASS 15675	44.030028	-74.821833
440149074490301	WECASS 15676	44.030278	-74.817750
440152074485001	WECASS 15677	44.031139	-74.813917
435201074254001	WECASS 157	43.866956	-74.427978
434304074070901	WECASS 159	43.717839	-74.119197
432413074181801	WECASS 16	43.403728	-74.305164
441214073571301	WECASS 162	44.204036	-73.953844
434916073492501	WECASS 163	43.821167	-73.823764
434733073504201	WECASS 164	43.792528	-73.845008
434308074034901	WECASS 165	43.719114	-74.063664
434147074033101	WECASS 166	43.696575	-74.058786
433942074223901	WECASS 167	43.661714	-74.377725
433049074093101	WECASS 168, Unnamed	43.513750	-74.158631
440703073345901	WECASS 17	44.117733	-73.583089
435705075165501	WECASS 17002	43.951592	-75.281969

Table F continued

NWIS ID	Descriptive Text	Latitude	Longitude
435610075184901	WECASS 17007	43.936294	-75.313669
435630075184701	WECASS 17008	43.941789	-75.313075
435431075180201	WECASS 17009	43.908686	-75.300822
435308075171401	WECASS 17016	43.885764	-75.287261
435405075153301	WECASS 17018, Unnamed	43.901586	-75.259206
441051073494401	WECASS 171	44.181078	-73.828894
432141074222001	WECASS 172	43.361611	-74.372228
435650073592601	WECASS 175	43.947319	-73.990739
431818074121301	WECASS 176	43.305000	-74.203700
435851074030701	WECASS 177, Unnamed	43.981050	-74.052131
435145073454301	WECASS 180	43.862525	-73.762181
435352075032701	WECASS 18001	43.897814	-75.057589
435403075031401	WECASS 18002	43.900878	-75.053981
435450075025601	WECASS 18003	43.913936	-75.049011
435233075044401	WECASS 18004	43.876103	-75.078975
435529075122601	WECASS 18007, Unnamed	43.924944	-75.207250
435852075112301	WECASS 18010	43.981225	-75.189839
441344073444201	WECASS 183	44.229069	-73.745083
442440073484001	WECASS 184	44.411247	-73.811139
435943075114201	WECASS 18500, W.Br. Oswegatchie River	43.995278	-75.195000
431557074140901	WECASS 188	43.266042	-74.235844
442600074253001	WECASS 189	44.433347	-74.425122
435540074454401	WECASS 19002	43.927925	-74.762492
435531074484701	WECASS 19003	43.925317	-74.813328
435755074483401	WECASS 19006	43.965286	-74.809464
435830074473601	WECASS 19010	43.975072	-74.793350
435905074465901	WECASS 19011	43.984958	-74.783089
442101073512801	WECASS 192	44.350450	-73.857839
440144074291301	WECASS 194	44.028956	-74.487058
432234074132601	WECASS 197	43.376319	-74.224122
433105074175801	WECASS 199	43.518256	-74.299658
442018073484101	WECASS 200	44.338533	-73.811489
441042073435701	WECASS 2000	44.178392	-73.732522
435540074420101	WECASS 20001	43.927869	-74.700328
435600074411501	WECASS 20002	43.933597	-74.687717
435651074414101	WECASS 20003	43.947572	-74.694747
440714073502701	WECASS 2001	44.120819	-73.841067
440609073491401	WECASS 2002	44.102536	-73.820603
441214073500601	WECASS 2003	44.204033	-73.835208
442322073535101	WECASS 2004	44.389589	-73.897578

Table F continued

NWIS ID	Descriptive Text	Latitude	Longitude
442506073520001	WECASS 2005	44.418381	-73.866889
442243073542001	WECASS 2006	44.378683	-73.905822
440945073483301	WECASS 2008	44.162633	-73.809400
440738073591201	WECASS 2009	44.127264	-73.986858
431934074545101	WECASS 201	43.326239	-74.914350
440813073573301	WECASS 2010	44.137039	-73.959369
440956073540901	WECASS 2012	44.165758	-73.902622
433348074221201	WECASS 204	43.563394	-74.370211
440949073470101	WECASS 206	44.163878	-73.783692
432139074193601	WECASS 209	43.360928	-74.326942
434444074052901	WECASS 21	43.745572	-74.091658
434644075202101	WECASS 21003	43.779106	-75.339192
434739075191601	WECASS 21005	43.794375	-75.321131
434908075212501	WECASS 21009	43.818939	-75.357075
434915075190901	WECASS 21013	43.820942	-75.319406
435054075153501	WECASS 21016	43.848372	-75.259958
433123074233301	WECASS 211	43.523211	-74.392756
434916074210101	WECASS 212, Unnamed	43.821114	-74.350392
443437074032801	WECASS 213	44.577078	-74.057794
444252074264401	WECASS 214	44.714703	-74.445789
435714074020701	WECASS 215	43.953969	-74.035350
432532074183401	WECASS 216	43.425811	-74.309567
443920074164401	WECASS 217	44.655794	-74.278892
443924074165001	WECASS 217A, Crandall Brook	44.656889	-74.280597
434503073503001	WECASS 218	43.751028	-73.841919
441324074200401	WECASS 22	44.223344	-74.334661
432820074145201	WECASS 220	43.472350	-74.247969
434754075002501	WECASS 22001	43.798336	-75.007147
434723075005401	WECASS 22002	43.789964	-75.015103
435004075012401	WECASS 22003	43.834619	-75.023569
435032075000901	WECASS 22004	43.842275	-75.002550
435001075001701	WECASS 22005	43.833722	-75.004914
435128075002301	WECASS 22007	43.858033	-75.006533
435106075044101	WECASS 22011, Sunday Creek	43.851933	-75.078314
435139075082201	WECASS 22017, Unnamed	43.860919	-75.139558
435115075093901	WECASS 22019	43.854408	-75.161067
434628075122101	WECASS 22024	43.774472	-75.206083
435129075140301	WECASS 22032	43.858333	-75.234244
432253073463901	WECASS 221	43.381483	-73.777756
440955074305001	WECASS 222	44.165453	-74.513914

Table F continued

NWIS ID	Descriptive Text	Latitude	Longitude
431000074294001	WECASS 224	43.166922	-74.494692
442058073453501	WECASS 225	44.349692	-73.759772
435524073440001	WECASS 226	43.923422	-73.733461
435539073441601	WECASS 226A, Unnamed	43.927686	-73.737803
434043073354101	WECASS 227	43.678867	-73.594811
433632073533001	WECASS 228	43.609128	-73.891842
441600073381201	WECASS 229	44.266667	-73.636922
432720073590701	WECASS 230	43.455681	-73.985494
434637074464701	WECASS 23001	43.777147	-74.779989
434547074582101	WECASS 23003	43.763128	-74.972606
434539074583801	WECASS 23004	43.760969	-74.977328
435056074570101	WECASS 23012	43.848928	-74.950422
434652074565401	WECASS 23014	43.781128	-74.948489
443706073384301	WECASS 231	44.618558	-73.645411
434300073530301	WECASS 232	43.716728	-73.884397
432303074560401	WECASS 233	43.384275	-74.934672
434805073494101	WECASS 234	43.801617	-73.828147
434623074491001	WECASS 23501, Eagle Creek	43.773222	-74.819444
435733073312201	WECASS 236	43.959439	-73.522789
434551074473501	WECASS 23640, Black Bear Mtn Bk	43.764167	-74.793056
434557074471701	WECASS 23641, Black Bear Mtn Bk	43.765833	-74.788056
434603074470301	WECASS 23642, Black Bear Mtn Bk	43.767500	-74.784167
434605074464701	WECASS 23643, Black Bear Mtn Bk	43.768056	-74.779722
434609074463101	WECASS 23644, Black Bear Mtn Bk	43.769167	-74.775278
434613074461601	WECASS 23645, Black Bear Mtn Bk	43.770278	-74.771111
434617074455901	WECASS 23646, Black Bear Mtn Bk	43.771389	-74.766389
434620074454501	WECASS 23647, Black Bear Mtn Bk	43.772222	-74.762500
434621074453401	WECASS 23648, Black Bear Mtn Bk	43.772500	-74.759444
441120073552501	WECASS 237	44.188994	-73.923878
441058073591701	WECASS 238	44.182814	-73.988267
432302074572801	WECASS 239, Unnamed	43.384072	-74.957936
432741074260501	WECASS 24	43.461639	-74.434764
440451073293001	WECASS 240	44.080853	-73.491772
434606074424901	WECASS 24001	43.768447	-74.713675
434544074411101	WECASS 24002	43.762253	-74.686622
434547074420701	WECASS 24002A, Seventh Lake Inlet	43.763261	-74.702181
441551073324101	WECASS 242	44.264353	-73.544850
441540073515201	WECASS 243	44.261331	-73.864689
435459073391001	WECASS 244	43.916594	-73.652894
434643073545001	WECASS 245	43.778686	-73.914094

Table F continued

NWIS ID	Descriptive Text	Latitude	Longitude
434547074421001	WECASS 24500, Seventh Lake Inlet	43.763111	-74.703028
431805074090401	WECASS 246	43.301594	-74.151356
433948073573401	WECASS 248	43.663611	-73.959594
441044073294101	WECASS 249	44.179008	-73.494917
435103073425801	WECASS 250	43.851094	-73.716203
434005075160601	WECASS 25002	43.668275	-75.268608
433811075180601	WECASS 25003	43.636589	-75.301817
433753075211101	WECASS 25006	43.631400	-75.353111
433851075210501	WECASS 25007	43.647522	-75.351469
433922075210201	WECASS 25009	43.656167	-75.350650
434008075205301	WECASS 25011	43.669142	-75.348122
434006075200101	WECASS 25013	43.668375	-75.333728
434127075200801	WECASS 25015	43.691058	-75.335592
434139075213801	WECASS 25018	43.694314	-75.360800
434242075215601	WECASS 25021	43.711675	-75.365622
434249075215601	WECASS 25022	43.713747	-75.365633
434336075205601	WECASS 25023	43.726853	-75.348953
442716073505501	WECASS 251	44.454533	-73.848611
441446074151301	WECASS 252, Unnamed	44.246350	-74.253781
442414075095001	WECASS 253	44.404033	-75.163953
433830073555601	WECASS 254	43.641942	-73.932406
434450075200101	WECASS 25500, Independence River	43.747333	-75.333611
434308075152201	WECASS 25501, Otter Creek	43.719111	-75.256361
441121073365701	WECASS 256	44.189172	-73.616042
442445073542301	WECASS 257	44.412700	-73.906614
440340073411001	WECASS 258	44.061264	-73.686189
443337074011601	WECASS 259	44.560336	-74.021306
442223074015001	WECASS 260	44.373289	-74.030803
434012075040501	WECASS 26006	43.670100	-75.068286
434001075045401	WECASS 26008	43.667211	-75.081928
433940075053201	WECASS 26009	43.661169	-75.092336
433949075063801	WECASS 26011	43.663764	-75.110572
433822075143901	WECASS 26021	43.639517	-75.244303
434116075135701	WECASS 26028	43.687892	-75.232711
434118075133101	WECASS 26030	43.688358	-75.225517
434116075125501	WECASS 26031	43.687861	-75.215222
434106075123101	WECASS 26032	43.685239	-75.208756
434317075125401	WECASS 26044	43.721603	-75.215214
434254075144401	WECASS 26046	43.715058	-75.245603
441715073551001	WECASS 261	44.287506	-73.919706

Table F continued

NWIS ID	Descriptive Text	Latitude	Longitude
432623074280401	WECASS 262	43.439817	-74.467944
442724074215601	WECASS 264	44.456917	-74.365781
442638073520601	WECASS 265	44.444136	-73.868411
434438074431901	WECASS 270	43.743947	-74.722194
434025074585901	WECASS 27002	43.673811	-74.983317
434029074590401	WECASS 27002A, Unnamed	43.674750	-74.984444
434107074591301	WECASS 27003, Unnamed	43.685336	-74.987158
433849074575101	WECASS 27005	43.647067	-74.964350
433837074571401	WECASS 27006	43.643731	-74.954061
433800074550101	WECASS 27010	43.633536	-74.917128
434142074533201	WECASS 27014	43.695103	-74.892347
434442074473801	WECASS 27015	43.745028	-74.793894
434359074471801	WECASS 27016	43.733314	-74.788347
434301074453701	WECASS 27018	43.717050	-74.760347
434256074453801	WECASS 27019	43.715700	-74.760600
434217074465001	WECASS 27020	43.704756	-74.780628
434211074462301	WECASS 27021	43.703122	-74.773064
434207074453801	WECASS 27022	43.702194	-74.760781
434204074452401	WECASS 27023	43.701378	-74.756811
434211074452401	WECASS 27024	43.703089	-74.756928
434208074450901	WECASS 27025	43.702269	-74.752711
434154074445701	WECASS 27026	43.698481	-74.749378
434049074462001	WECASS 27027	43.680339	-74.772281
434100074462601	WECASS 27027A, Unnamed	43.683500	-74.773917
434421074584901	WECASS 27036	43.739269	-74.980442
434427074584401	WECASS 27037	43.741069	-74.978950
434446074562301	WECASS 27039	43.746369	-74.939950
443409074051501	WECASS 271	44.569361	-74.087750
441232073405301	WECASS 272	44.208931	-73.681511
434410073591101	WECASS 273	43.736281	-73.986531
433605074065001	WECASS 274	43.601578	-74.114061
440615073413201	WECASS 275	44.104169	-73.692358
442328073513201	WECASS 276	44.391361	-73.859114
434414074445701	WECASS 27680, Wheeler Creek	43.737333	-74.749306
434416074445601	WECASS 27681, Wheeler Creek	43.737944	-74.749056
434450074452901	WECASS 27682, Wheeler Creek	43.747333	-74.758167
434350074452901	WECASS 27683, Wheeler Creek	43.730667	-74.758167
434339074451401	WECASS 27684, Wheeler Creek	43.727544	-74.753917
434338074450101	WECASS 27685, Wheeler Creek	43.727250	-74.750528
434340074444201	WECASS 27686, Wheeler Creek	43.727833	-74.745250

Table F continued

NWIS ID	Descriptive Text	Latitude	Longitude
434342074442901	WECASS 27687, Wheeler Creek	43.728500	-74.741389
434324074571301	WECASS 27690, Beaver Brook	43.723528	-74.953722
434329074570601	WECASS 27691, Beaver Brook near Old Forge NY	43.724806	-74.951833
434331074565601	WECASS 27692, Beaver Brook	43.725528	-74.948917
434335074564501	WECASS 27693, Beaver Brook	43.726556	-74.946083
434341074563401	WECASS 27694, Beaver Brook	43.728222	-74.942833
434344074562701	WECASS 27695, Beaver Brook	43.729139	-74.941000
434348074561701	WECASS 27696, Beaver Brook	43.730167	-74.938250
434351074560901	WECASS 27697, Beaver Brook	43.731056	-74.935944
434845073302501	WECASS 277	43.812603	-73.507017
433540073505701	WECASS 278	43.594469	-73.849386
432248074400001	WECASS 279	43.380242	-74.666669
431606074120201	WECASS 28	43.268611	-74.200561
431733074144101	WECASS 280	43.292661	-74.244733
434056074440401	WECASS 28004	43.682419	-74.734556
434101074420301	WECASS 28006	43.683867	-74.700925
434051074415901	WECASS 28007, Pine Grove Creek	43.680892	-74.699947
433953074400801	WECASS 28010	43.664869	-74.669144
433918074403501	WECASS 28011	43.655078	-74.676514
433854074411501	WECASS 28013	43.648444	-74.687708
433909074403201	WECASS 28013B, Otter Brook	43.652500	-74.675556
433820074410001	WECASS 28014	43.639069	-74.683419
434124074393301	WECASS 28017	43.690053	-74.659328
434105074393501	WECASS 28018	43.684742	-74.659978
434208074354501	WECASS 28022	43.702361	-74.596086
434208074343001	WECASS 28024, Silver Run	43.702286	-74.575236
434500074441601	WECASS 28030	43.750047	-74.737983
433920074403401	WECASS 28037	43.655708	-74.676386
434057074425001	WECASS 28039	43.682731	-74.713958
434145074413201	WECASS 28041	43.696000	-74.692303
431555074214301	WECASS 281	43.265283	-74.362019
433342073434001	WECASS 282	43.561811	-73.727889
434216074343401	WECASS 28501, Cellar Brook	43.704611	-74.576361
434136074360701	WECASS 28503, Silver Run downstream	43.693361	-74.602000
434211074340001	WECASS 28602, Silver Run	43.703250	-74.566667
434210074334001	WECASS 28603, Silver Run	43.702944	-74.561306
434210074332201	WECASS 28604, Silver Run	43.703000	-74.556361
434212074330501	WECASS 28605, Silver Run	43.703389	-74.551528
434213074324401	WECASS 28606, Silver Run	43.703833	-74.545778

Table F continued

NWIS ID	Descriptive Text	Latitude	Longitude
434211074333001	WECASS 28607, Silver Run	43.703306	-74.558389
434213074321301	WECASS 28608, Silver Run	43.703722	-74.537139
434211074315801	WECASS 28609, Silver Run	43.703250	-74.532972
434213074340801	WECASS 28610, Silver Run Trib	43.703778	-74.569056
434218074335701	WECASS 28611, Silver Run Trib	43.705028	-74.565972
434221074334301	WECASS 28612, Silver Run Trib	43.705944	-74.562194
434228074333301	WECASS 28613, Silver Run Trib	43.707917	-74.559417
434233074333001	WECASS 28614, Silver Run Trib	43.709278	-74.558333
434236074332601	WECASS 28615, Silver Run Trib	43.710139	-74.557222
434240074332201	WECASS 28616, Silver Run Trib	43.711306	-74.556139
434004074401701	WECASS 28620, S. Br. Moose River Trib	43.667944	-74.671611
434000074401301	WECASS 28621, S. Br. Moose River Trib	43.666806	-74.670500
433955074401101	WECASS 28622, S. Br. Moose River Trib	43.665389	-74.669861
433958074395001	WECASS 28624, S. Br. Moose River Trib	43.666361	-74.664111
434003074393801	WECASS 28625, S. Br. Moose River Trib	43.667583	-74.660583
434008074392501	WECASS 28626, S. Br. Moose River Trib	43.668944	-74.656972
434013074391001	WECASS 28627, S. Br. Moose River Trib	43.670278	-74.652944
434438074430701	WECASS 28631, Buck Creek	43.744083	-74.718778
434436074425401	WECASS 28632, Buck Creek	43.743528	-74.715222
434433074424201	WECASS 28633, Buck Creek	43.742722	-74.711667
434431074422901	WECASS 28634, Buck Creek	43.741944	-74.708222
434422074422201	WECASS 28635, Buck Creek	43.739472	-74.706306
434412074422101	WECASS 28636, Buck Creek	43.736889	-74.705833
434411074420801	WECASS 28637, Buck Creek	43.736444	-74.702389
433423075183301	WECASS 29002	43.573089	-75.309300
433422075153301	WECASS 29003	43.572853	-75.259392
433453075182501	WECASS 29005	43.581650	-75.306992
433613075184301	WECASS 29008	43.603875	-75.312183
433702075200701	WECASS 29009	43.617317	-75.335553
433324075165001	WECASS 29012	43.556864	-75.280742
433021075113001	WECASS 30001	43.505906	-75.191808
433102075073801	WECASS 30002	43.517250	-75.127381
433117075073501	WECASS 30003	43.521664	-75.126400
433206075055601	WECASS 30004	43.535197	-75.098953
433553075062101	WECASS 30009	43.598219	-75.105869
433325075083601	WECASS 30012, Unnamed	43.557119	-75.143436
433313075114301	WECASS 30013	43.553800	-75.195550
433243075124601	WECASS 30013A, Cropsey Creek	43.545444	-75.212917
433223075122001	WECASS 30016	43.539828	-75.205653
433208075122301	WECASS 30016A, Cummings Creek	43.535806	-75.206500

Table F continued

NWIS ID	Descriptive Text	Latitude	Longitude
433548075110101	WECASS 30019	43.596681	-75.183794
433639075093101	WECASS 30023	43.610944	-75.158681
433636075084101	WECASS 30026, Unnamed	43.610061	-75.144800
433130074555201	WECASS 31007	43.525133	-74.931383
433014074585101	WECASS 31009, Otter Brook	43.503903	-74.980889
433010074585901	WECASS 31010	43.502914	-74.983114
433011074590001	WECASS 31010A, Unnamed	43.503222	-74.983472
433044074565301	WECASS 31011, Unnamed	43.512267	-74.948222
433706074564501	WECASS 31015, Unnamed	43.618425	-74.945903
442300073495101	WECASS 32, Unnamed	44.383539	-73.831019
433730074435701	WECASS 32001	43.625058	-74.732700
434916073562801	WECASS 34	43.821144	-73.941156
432622075075801	WECASS 34006	43.439447	-75.133025
432720075091001	WECASS 34500, Little Woodhall Creek	43.455556	-75.152778
435132073534001	WECASS 35	43.859083	-73.894603
432602075060201	WECASS 35004	43.434167	-75.100639
432708075053101	WECASS 35005	43.452453	-75.092142
432806075033501	WECASS 35008	43.468411	-75.059775
432718075001801	WECASS 35012	43.455100	-75.005006
432910075001001	WECASS 35014	43.486256	-75.002906
434307074185401	WECASS 36	43.718650	-74.315033
435306073455901	WECASS 39	43.885031	-73.766514
441353073474701	WECASS 4	44.231442	-73.796611
435813073491301	WECASS 40	43.970508	-73.820472
431320074321001	WECASS 41	43.222492	-74.536125
440403074021901	WECASS 42	44.067614	-74.038814
440151074015501	WECASS 45	44.031033	-74.032117
434758073580401	WECASS 46	43.799456	-73.968003
431632074332401	WECASS 49	43.275692	-74.556819
442851073365401	WECASS 5	44.480939	-73.615194
432730074312101	WECASS 500	43.458611	-74.522572
440752075152001	WECASS 5001	44.131364	-75.255822
440946075182701	WECASS 5002	44.162928	-75.307614
441323075182701	WECASS 5005	44.223247	-75.307678
432654074313101	WECASS 501	43.448353	-74.525358
433136074231001	WECASS 502	43.526772	-74.386150
431048074393401	WECASS 503	43.180056	-74.659711
430712074380501	WECASS 504	43.120178	-74.634967
430905074414901	WECASS 505	43.151614	-74.697217
433113074221401	WECASS 51	43.520542	-74.370647

Table F continued

NWIS ID	Descriptive Text	Latitude	Longitude
432407074425401	WECASS 52	43.401953	-74.715142
442307073294101	WECASS 53	44.385344	-73.494800
441248073540501	WECASS 56	44.213575	-73.901508
441432073504301	WECASS 57	44.242339	-73.845519
434131073430801	WECASS 59	43.692139	-73.718939
432355074380801	WECASS 60	43.398686	-74.635636
440933075105901	WECASS 6004	44.159322	-75.183156
440934075111301	WECASS 6004A, Unnamed	44.159603	-75.187017
440932075133301	WECASS 6007	44.159156	-75.226053
441034075143101	WECASS 6009	44.176228	-75.242131
441041075144001	WECASS 6010	44.178114	-75.244514
441218075131001	WECASS 6012	44.205175	-75.219594
441240075125301	WECASS 6013	44.211125	-75.214986
441255075143901	WECASS 6014	44.215389	-75.244419
441352075131401	WECASS 6015	44.231372	-75.220569
441418075081501	WECASS 6019	44.238436	-75.137567
441242075073401	WECASS 6020, Yellow Creek	44.211708	-75.126239
432122074175901	WECASS 62	43.356267	-74.299742
434820074190201	WECASS 63	43.805825	-74.317369
432002074105701	WECASS 64	43.333928	-74.182711
435446074285901	WECASS 65	43.912778	-74.483158
441021073573601	WECASS 67	44.172594	-73.960275
435704074263401	WECASS 68	43.951383	-74.442997
434305074185601	WECASS 70	43.718206	-74.315633
440754075064901	WECASS 7001	44.131864	-75.113692
440859075065901	WECASS 7003, Unnamed	44.149778	-75.116478
440912075061901	WECASS 7003B, Unnamed	44.153344	-75.105392
441053075044101	WECASS 7005	44.181411	-75.078131
441415075070901	WECASS 7017	44.237556	-75.119281
441408075063501	WECASS 7018	44.235583	-75.109761
441408075062001	WECASS 7019	44.235767	-75.105628
441252075052101	WECASS 7024	44.214533	-75.089317
441329075033701	WECASS 7027	44.224906	-75.060536
441332075024401	WECASS 7028	44.225814	-75.045636
433729074241401	WECASS 72	43.624750	-74.404139
431522073543501	WECASS 75	43.256150	-73.909983
433555074042001	WECASS 76	43.598808	-74.072475
441127073491501	WECASS 77	44.190850	-73.821111
441349073441001	WECASS 78	44.230281	-73.736294
442137073291101	WECASS 79	44.360419	-73.486561

Table F continued

NWIS ID	Descriptive Text	Latitude	Longitude
435238073530101	WECASS 8	43.877425	-73.883811
432242074563101	WECASS 80	43.378578	-74.942011
440846074533101	WECASS 8002	44.146183	-74.892156
440910074533001	WECASS 8003	44.153025	-74.891894
440849074571101	WECASS 8009	44.147125	-74.953297
440931074540101	WECASS 8011	44.158617	-74.900389
441340074583501	WECASS 8015	44.227981	-74.976522
431705074114501	WECASS 81	43.284828	-74.195978
441237073392501	WECASS 82	44.210511	-73.656947
442443073340101	WECASS 83	44.412175	-73.567075
435306073435801	WECASS 84	43.885103	-73.733011
435253073435201	WECASS 84A, Unnamed	43.881553	-73.731292
440908074272601	WECASS 86	44.152497	-74.457333
442839073324801	WECASS 87	44.477578	-73.546708
441613073370701	WECASS 9	44.270403	-73.618889
441331074502801	WECASS 9002	44.225533	-74.841178
441252074494001	WECASS 9005	44.214531	-74.827814
441311074493001	WECASS 9006	44.219928	-74.825044
441216074491701	WECASS 9007	44.204617	-74.821586
441137074492001	WECASS 9008	44.193814	-74.822369
441158074504501	WECASS 9009	44.199611	-74.845881
441242074471201	WECASS 9013	44.211850	-74.786764
441135074492401	WECASS 9660	44.193222	-74.823444
441141074491901	WECASS 9662	44.194889	-74.822194
441146074491501	WECASS 9663	44.196139	-74.821056
441149074490701	WECASS 9664	44.197083	-74.818611
441152074485801	WECASS 9665	44.197944	-74.816278
441155074485201	WECASS 9666	44.198861	-74.814611
441200074484501	WECASS 9667	44.200139	-74.812667
431926074005901	WECASS 97	43.324000	-74.016539

Appendix G. Example Model Projections at Two Data-Intensive Sites

Model projections for Archer Creek (Figure G-1) indicated that under the scenario of decreases in SO_4^{2-} and NO_3^- deposition to pre-industrial values, annual volume weighted concentrations of SO_4^{2-} and NO_3^- decreased 47% and 51% by 2200, compared to the values in 2015, in response to 100% reduction scenarios, respectively. Model-simulated SO_4^{2-} and NO_3^- concentrations increased 8.3% and 7.1% in response to the 15% deposition increase scenario. Model-simulated ANC and soil % BS concentrations increased 31% and 22% in 2200 in Archer Creek, respectively, compared to the values in 2015, in response to the scenario of a 100% reduction in deposition of SO_4^{2-} and NO_3^- . Values decreased 6.5% and 5.8%, respectively, in response to the 15% increase scenario. The magnitudes of increases in stream ANC were relatively small compared to the decreases in strong acid anions in Archer Creek. Sulfate + NO_3^- decreased $-54 \mu\text{eq L}^{-1}$, whereas ANC only increased $28 \mu\text{eq L}^{-1}$ from 2015 to 2200 under the 100% reduction scenario. This response can be partially explained by the high estimated base cation weathering rate at the site and the historical leaching of base cations (e.g. Ca^{2+}) from soil exchangeable sites with increases in SO_4^{2-} and NO_3^- concentrations in streams.

Buck Creek, an acid sensitive watershed that receives similar deposition as Archer Creek (deposition ratio compared to Archer Creek is 1.09), was found to be more responsive to the changes in atmospheric deposition than Archer Creek (Figure G-2). Model projections indicated that under the same scenario of decreases in atmospheric deposition of SO_4^{2-} and NO_3^- to pre-industrial values, annual volume weighted concentration of SO_4^{2-} and NO_3^- decreased 67% and 68% for Buck Creek while they only decreased 47% and 51% for Archer Creek in 2200 compared to the values in 2015. Model projected ANC and soil % BS increased 71% and 67% for Buck Creek in 2200 compared to the values in 2015 in response to the scenario of a 100% reduction in deposition of SO_4^{2-} and NO_3^- (Increased 31% and 22% for Archer Creek). Acid-sensitive streams like Buck Creek have a limited capacity to neutralize inputs of strong acid anions and show a significant decrease in the modeled stream ANC in response to historical acidic deposition. These streams generally have low ANC ($<50 \mu\text{eq L}^{-1}$) and, in turn, are more responsive to decreases in acidic deposition. Although substantial recovery generally occurs under the scenario of

100% reduction in SO_4^{2-} and NO_3^- deposition for Archer Creek and Buck Creek, model-simulated ANC values in 2200 remained below the pre-industrial level. This limited recovery can be attributed to the depletion of available base cations from soil exchange sites and desorption of S that previously accumulated in soils due to historical acidification and increases in the leaching of naturally occurring organic acids from soils and wetlands to streams.

Figure G-1. Model Simulated Annual Volume-Weighted Concentrations of SO_4^{2-} , NO_3^- , and ANC and Soil Base Saturation for Archer Creek during the Period 1850–2200

Model projections are shown for different future atmospheric deposition scenarios (i.e., business as usual, possible future and 100% reduction) based on control of SO_4^{2-} and NO_3^- deposition.

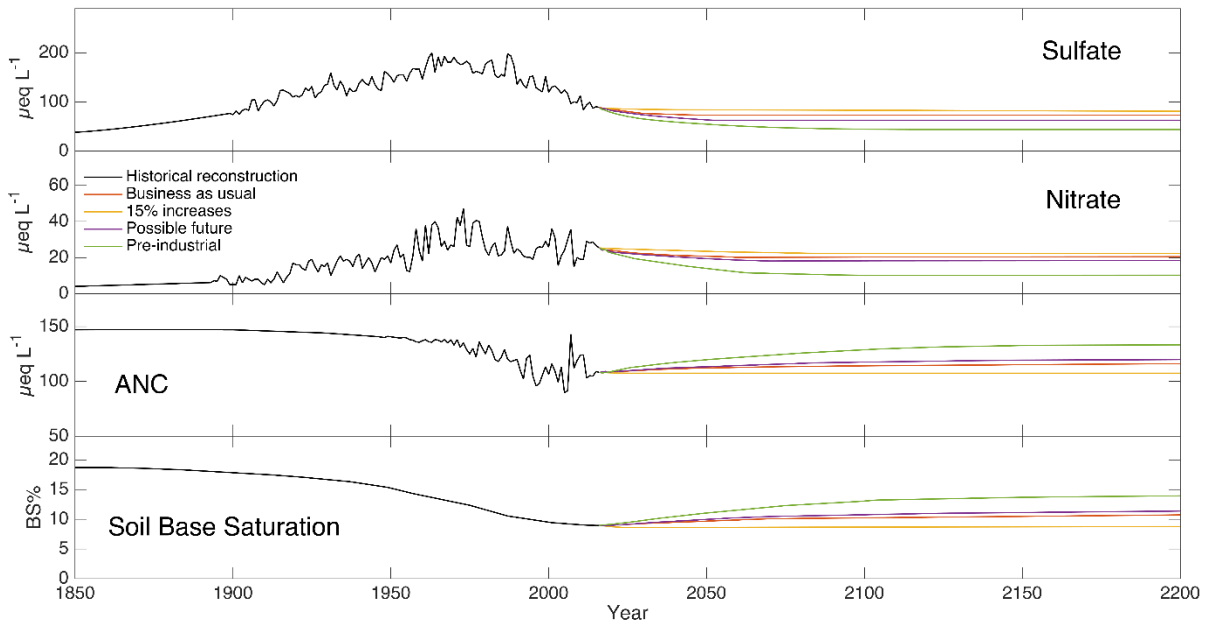
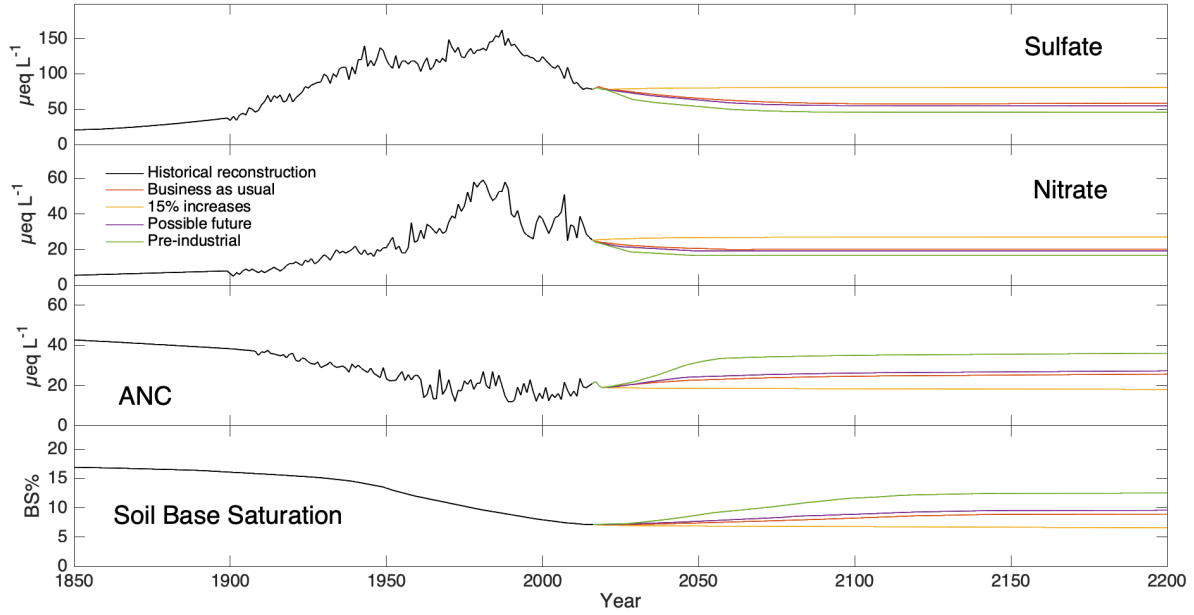


Figure G-2. Model Simulated Annual Volume-Weighted Concentrations of SO_4^{2-} , NO_3^- , and ANC and Soil Base Saturation for Buck Creek during the Period 1850–2200

Model projections are shown for different future atmospheric deposition scenarios (i.e., business as usual, possible future and 100% reduction) based on control of SO_4^{2-} and NO_3^- deposition.



Appendix H. Statistical Model Development for Predicting Target Loads

Table H-1. Candidate statistical models for predicting TLs

TL ANC=20 µeq L⁻¹, year 2050				
	Selected Variables			AIC
CurrentANC	CurrentDep	lon		114.3230
CurrentANC	CurrentDep	lon	depth_rz	114.3967
CurrentANC	CurrentDep	lon	elev	114.5052
CurrentANC	Lon			114.5533
CurrentANC	CurrentDep	lat	lon	114.8104

TL ANC=20 µeq L⁻¹, year 2150				
	Selected Variables			AIC
CurrentANC	lon	sand	silt	113.0934
CurrentANC	lon	silt		113.1904
CurrentANC	lat	lon	silt	113.2307
CurrentANC	CurrentDep	lon	silt	113.7219
CurrentANC	lat	sand	silt	113.8676

TL Site-Specific ANC, year 2050				
	Selected Variables			AIC
CurrentANC	lat	elev	decmix	142.4892
CurrentANC	CurrentDep	lat	decmix	142.5351
CurrentANC	elev	con42	decmix	142.7472
CurrentANC	lat	decmix	silt	142.9223
CurrentANC	lat	decmix	sand	143.0837

TL Site-Specific ANC, year 2150				
	Selected Variables			AIC
CurrentBCS	CurrentDep	lat		170.6213
CurrentBCS	lat	elev		170.6389
CurrentBCS	elev			171.0512
CurrentBCS	CurrentDep	lat	soilph1to1	171.2707
CurrentBCS	lat	elev	soilph1to1	171.4959

Table H-2. Predictor Variable Selection

Predictor Variable	Predictor Count Among All TL models
CurrentANC	15
lat	11
lon	9
CurrentDep	8
elev	6
silt	6
CurrentBCS	5
decmix	5
sand	3
soilph1to1	2
con42	1
depth_rz	1

Table H-3. Descriptive Statistics for TL Models

Least Squares Linear Regression of TL ANC = 20 µeq L⁻¹, Year 2050

Predictor					
Variables	Coefficient	Std Error	T	P	VIF
Constant	2470.74	904.687	2.73	0.0195	0.0
CurrentANC	0.63503	0.17399	3.65	0.0038	2.2
lat	-16.3645	16.5136	-0.99	0.3430	1.6
lon	23.2326	10.4201	2.23	0.0476	1.5
R ²	0.8097	Mean Square Error (MSE)		89.1497	
Adjusted R ²	0.7577	Standard Deviation		9.44191	

Cases Included = 15

Least Squares Linear Regression of TL ANC = 20 µeq L⁻¹, Year 2150

Predictor					
Variables	Coefficient	Std Error	T	P	VIF
Constant	2634.44	902.656	2.92	0.0140	0.0
CurrentANC	0.90116	0.17360	5.19	0.0003	2.2
lat	-22.8361	16.4766	-1.39	0.1932	1.6
lon	21.5263	10.3967	2.07	0.0627	1.5
R ²	0.8722	Mean Square Error (MSE)		88.7499	
Adjusted R ²	0.8374	Standard Deviation		9.42072	

Cases Included 15

Least Squares Linear Regression of TL Site-Specific ANC, Year 2050

Predictor

Variables	Coefficient	Std Error	T	P	VIF
Constant	-1025.86	814.650	-1.26	0.2260	0.0
CurrentANC	0.15175	0.02861	5.30	0.0001	1.1
lat	8.72561	11.3326	0.77	0.4525	1.2
lon	-8.71516	6.51936	-1.34	0.2000	1.2
R ²	0.6582	Mean Square Error (MSE)		74.5074	
Adjusted R ²	0.5941	Standard Deviation		8.63177	

Cases Included 20

Least Squares Linear Regression of TL Site-Specific ANC, Year 2150

Predictor

Variables	Coefficient	Std Error	T	P	VIF
Constant	-1615.34	1130.41	-1.43	0.1701	0.0
CurrentANC	0.11502	0.02906	3.96	0.0009	1.0
lat	26.7708	15.5933	1.72	0.1032	1.2
lon	-6.20635	9.05315	-0.69	0.5017	1.2
R ²	0.5308	Mean Square Error (MSE)		143.972	
Adjusted R ²	0.4526	Standard Deviation		11.9988	

Cases Included 2

Endnotes

- 1 <http://nadp.slh.wisc.edu/data/sites/siteDetails.aspx?net=NTN&id=NY20>, accessed Dec. 3, 2019.
- 2 https://apa.ny.gov/About_Park/history.htm
- 3 NADP; <http://nadp.slh.wisc.edu/data/sites/siteDetails.aspx?net=NTN&id=NY20>, site NY20
- 4 <https://catalog.data.gov/national-emission-inventory>
- 5 <https://www.mrlc.gov/data>
- 6 <https://www.esf.edu/hss/em/huntington/archive.html>
- 7 PRISM model; <http://www.prism.oregonstate.edu/>; accessed Oct. 23, 2019
- 8 <http://nadp.slh.wisc.edu/committees/tdep/>
- 9 <http://nadp.slh.wisc.edu/committees/tdep/>

NYSERDA, a public benefit corporation, offers objective information and analysis, innovative programs, technical expertise, and support to help New Yorkers increase energy efficiency, save money, use renewable energy, and reduce reliance on fossil fuels. NYSERDA professionals work to protect the environment and create clean-energy jobs. NYSERDA has been developing partnerships to advance innovative energy solutions in New York State since 1975.

To learn more about NYSERDA's programs and funding opportunities, visit nyserda.ny.gov or follow us on Twitter, Facebook, YouTube, or Instagram.

**New York State
Energy Research and
Development Authority**

17 Columbia Circle
Albany, NY 12203-6399

toll free: 866-NYSERDA
local: 518-862-1090
fax: 518-862-1091

info@nyserda.ny.gov
nyserda.ny.gov



NYSERDA

State of New York

Andrew M. Cuomo, Governor

New York State Energy Research and Development Authority

Richard L. Kauffman, Chair | Doreen M. Harris, Acting President and CEO